DISSERTATION | DOCTORAL THESIS

Titel | Title

Oceanic fungal ecology and biogeochemistry

verfasst von | submitted by

Eva Breyer BSc MSc

angestrebter akademischer Grad | in partial fulfilment of the requirements for the degree of

Doctor of Philosophy (PhD)

Wien | Vienna, 2024

Studienkennzahl lt. Studienblatt | Degree programme code as it appears on the student record sheet:	UA 794 685 437
Dissertationsgebiet lt. Studienblatt | Field of study as it appears on the student record sheet:	Biologie
Betreut von | Supervisor:	Univ.-Prof. Mag. Dr. Christian Griebler Univ.-Prof. Dr. Monika Bright

Acknowledgements

I would like to express my sincere appreciation to Federico Baltar, whose steady support and guidance were instrumental in enabling me to pursue my PhD journey at the University of Vienna. His mentorship not only helped shape me into a proficient scientist but also provided invaluable emotional support throughout the thesis. Fede's willingness to assist, both academically and emotionally throughout my time as PhD-student has been indispensable. I will always be grateful for that.

Ich bin auch meiner Familie zutiefst für die ständige Ermutigung und den Glauben an mich dankbar. Mein aufrichtiger Dank gilt meiner Mutter, meinem Vater und Roland für ihre fortwährende Unterstützung, die das Fundament meiner akademischen Bestrebungen gebildet haben. Ohne ihren unerschütterlichen Glauben und ihre Liebe zu mir wäre das alles nicht möglich gewesen.

I also extend my appreciation to all the members of the Fungal & Biogeochemical Oceanography group, our dedicated lab managers and Monika Bright & Christian Griebler. Their collaboration and fellowship have enriched my research experience.

Overview of Dissertation

The following thesis is presented as a cumulative dissertation. This combines a general introduction which includes processes that drive the marine carbon cycle, the origin of marine fungi and pelagic fungi in the ocean (mycoplankton), followed by three chapters that aim to investigate the ecology and biogeochemistry of marine pelagic fungi, and a general discussion that highlights the principal findings of the mentioned chapters. Chapters 1 and 2 are manuscripts published in international scientific peer-reviewed journals, whereas Chapter 3 has been submitted to a scientific peer-reviewed journal. Chapter 1 investigates the physiology and the preferred carbon substrates of three marine pelagic fungal isolates. Chapter 2 investigates the global protein degradation by mycoplankton in the ocean. Chapter 3 investigates the biomass contribution of mycoplankton to marine microbial biomass. Finally, to maintain evenness, each chapter was modified to a general format.

Table of contents

General Introduction **3**

1. The processes that drive the marine carbon cycle 3

2. The origin of marine fungi 5

3. Pelagic fungi in the ocean (mycoplankton) 5

4. Objectives of the thesis 8

References 9

Chapter 1: Physiological Properties of Three Pelagic Fungi Isolated from the Atlantic Ocean **12**

Abstract 13

1. Introduction 14

2. Material and Methods 15

2.1. Sample Collection and Isolation of Marine Fungi 15

2.2. Sequencing of the Fungal Isolates 16

2.3. Morphological Observations with Epifluorescence Microscopy 17

2.4. Physiological Tests of Fungal Growth 18

2.5. Metabolic Activity and Assimilation of Carbon Compounds by Fungal Cultures 18

2.6. Statistical Analysis 19

3. Results and Discussion 19

3.1. Isolated Fungal Species 19

3.2. Macroscopic and Microscopic Morphology of isolated Fungal Cultures 22

3.3. Fungal Growth under changing Environmental Conditions 23

3.4. Metabolic activity (FF-Plates) 26

4. Conclusions 30

References 33

Chapter 2: Global contribution of pelagic fungi to protein degradation in the ocean **37**

1. Introduction 39

2. Material and Methods 40

3. Results and Discussion 41

3.1. Occurrence, secretory capacity and α-diversity of fungal peptidases genes and transcripts in the global ocean 41

3.2. Phylogenetic affiliation of genes and transcripts encoding fungal peptidases in the global ocean 44

3.3. Functional classification of genes and transcripts encoding fungal peptidases in the global ocean 46

3.4. Taxonomic and functional affiliation of genes and transcripts encoding fungal secretory peptidases in the global ocean....47
3.5. Unique and shared protease pools between oceanic fungi and prokaryotes....48
3.6. Global abundance and expression of the dominant fungal protease families and subfamilies in the ocean....49
4. Conclusions....51
References....53
Chapter 3: The overlooked contribution of pelagic fungi to ocean biomass....56
Abstract....57
1. Introduction....58
2. Material and Methods....59
2.1. Cultivation conditions and sample preparation of marine fungal cultures....59
2.2. Determination of carbon conversion factors of ergosterol and biovolume....60
2.3. Quantification of fungal cell dry mass by suspended microchannel resonator (SMR)....61
2.4. Environmental sample collection in the Atlantic Ocean....62
2.5. Quantification of particulate organic carbon and chlorophyll a....64
2.6. Ergosterol extraction and HPLC and LC-MS/MS analysis for fungal biomass....64
2.7. Calcofluor-White (CFW) epifluorescence microscopy for fungal biomass....66
2.8. Catalyzed reporter deposition fluorescence in situ hybridization (CARD-FISH) for fungal biomass....66
2.9. Catalyzed reporter deposition fluorescence in situ hybridization (CARD-FISH) for archaeal biomass....68
2.10. Flow cytometry and fluorescence microscopy for prokaryotic biomass....68
2.11. Contribution of microbial biomass to POC....69
2.12. Estimation of global pelagic marine fungal biomass....69
2.13. Data analysis and statistics....70
3. Results and Discussion....70
3.1. Biomass conversion factors of pelagic fungal cultures....70
3.2. Environmental characteristics and oceanic fungal biomass in the Atlantic Ocean....71
3.3. Fungal biomass is lower than bacterial but higher than archaeal biomass....74
3.4. Contribution of different microbial groups to particulate organic carbon....75
3.5. Estimation of global pelagic marine fungal biomass....77
4. Conclusions....77
References....79
General Discussion....85

1. Main Aim 85
2. Functional diversity and physiology of marine mycoplankton 85
3. The contribution of mycoplankton to marine microbial biomass 89
4. Conclusions 91
References 93
Annex 95
1. Chapter 1: Supplementary Material 95
2. Chapter 2: Supplementary Material 97
2.2. Additional online files 100
3. Chapter 3: Supplementary Material 101

Abstract (Deutsch)

Pilze sind wichtige Abbauer von organischem Material welche für die Wiedereingliederung von Nährstoffen in globale Nahrungsketten in Süßwasser und Boden verantwortlich sind. Neue Erkenntnisse heben ihre allgegenwärtige Präsenz und aktive Rolle bei dem Kohlenhydratabbau in den Weltmeeren vor. Die ökologische und biogeochemische Rolle, die pelagische Pilze im Ozean spielen, bleibt jedoch unbekannt. Durch physiologische Experimente mit drei isolierten pelagischen Pilzen haben wir ihr Wachstum unter verschiedenen Umweltbedingungen und ihre bevorzugten Kohlenstoffsubstrate untersucht, wobei eine hohe Toleranz gegenüber variierenden Salzkonzentrationen und Temperaturen sowie eine gemeinsame Stoffwechselpräferenz für die Oxidation von Aminosäuren festgestellt wurde. Zusätzlich haben wir eine globale Ozean-Multi-Omics-Analyse aller pilzaffinen Proteasen durchgeführt und einen relevanten Beitrag pelagischer Pilze zum Proteinabbau in den Ozeanen aufgedeckt. In Oberflächengewässern haben wir Dothideomycetes als wichtige Beitragende zum Proteinabbau identifiziert während dies in tieferen Gewässern von Leotiomycetes übernommen wurde. Ähnlich wie bei von Pilzen stammenden CAZymes nahmen die Abundanz, Diversität und Expression von Protease-Genen mit der Tiefe zu. Dies steht im Gegensatz zur gleichmäßigeren Verteilung prokaryotischer Proteasen und CAZymes in der ozeanischen Wassersäule und deutet auf unterschiedliche ökologische Nischen für Pilze und Prokaryoten hin. Schließlich haben wir, um die Pilzabundanz und Biomasse im offenen Ozean zu bestimmen, Calcofluor-White-Fluoreszenzmikroskopie, CARD-FISH, Ergosterol-Extraktion und Mikrofluidik-Massensensortechniken entlang einer Breitengradelänge über 11.000 km über den Atlantischen Ozean kombiniert. Global betrachtet machten Pilze 0,19-0,21 Gt C aus, was einen geringeren Beitrag als Bakterien, aber einen höheren Beitrag zum POC und eine höhere Biomasse als Archaeen im Ozean zeigt (Archaeen:Pilze:Bakterien-Biomasseverhältnis von 1:4:32). Insgesamt heben unsere Ergebnisse den signifikanten Beitrag von Pilzen zur funktionellen Diversität im offenen Ozean und zur ozeanischen mikrobiellen Biomasse vor und betonen ihre Bedeutung im marinen Kohlenstoff- und Stickstoffkreislauf sowie die Notwendigkeit ihrer Einbeziehung in biogeochemische Modelle.

Abstract

Fungi are important degraders of organic matter responsible for re-integration of nutrients into global food chains in freshwater and soil. Recent evidence highlights their ubiquitous presence and active role in carbohydrate degradation in the global oceans. However, the ecological and biogeochemical role played by pelagic fungi in the ocean remains unknown. Through physiological experiments with three isolated pelagic fungi, we explored their growth patterns under different environmental conditions and their preferred carbon substrates, revealing a high tolerance to varying salinities and temperatures, along with a shared metabolic preference for oxidizing amino acids. We also performed a global-ocean multi-omics analysis of all fungal affiliated proteases and unveiled a relevant contribution of pelagic fungi to protein degradation in the oceans. Dothideomycetes in the surface and Leotiomycetes in deeper waters were identified as key contributors to protein degradation. Similar to fungal CAZymes, protease gene abundance, diversity, and expression increased with depth. This contrasts with the more even distribution of prokaryotic proteases and CAZymes in the oceanic water column, implying distinct ecological niches for fungi and prokaryotes. Finally, to determine the fungal abundance and biomass in the open ocean, we combined Calcofluor-White staining, CARD-FISH, ergosterol extraction and microfluidic mass sensor techniques along a latitudinal transect spanning over 11,000 km across the Atlantic Ocean. Globally, fungi accounted for 0.19-0.21 Gt C, showing a lower contribution than bacteria but a higher contribution to POC and higher biomass than Archaea in the ocean (Archaea:Fungi:Bacteria biomass ratio of 1:4:32). Collectively, our findings underscore the significant contribution of fungi to open ocean functional diversity and to oceanic microbial biomass, emphasizing their importance in the marine carbon and nitrogen cycle and the necessity for their inclusion in biogeochemical models.

General Introduction

1. The processes that drive the marine carbon cycle

The ocean, as the largest carbon reservoir on Earth, plays a critical role in regulating the climate and serves as a buffer against the rise of atmospheric CO_2 levels. This pivotal function is complemented by microbes, which constitute the majority of living marine biomass and act as primary drivers behind the marine nutrient cycles (*1, 2*). Consequently, the vital roles microbes play and their activities profoundly shape the ocean's functionality, impacting diverse areas including fisheries and climate change.

At the surface, atmospheric CO_2 is fixed by phytoplankton ('primary production'), which ultimately sinks through deeper water layers as particulate organic carbon (POC) where it undergoes continuous remineralization by heterotrophic microbes, resulting in a reduction in both quantity and quality, a process defined as the biological carbon pump (BCP) (Fig. 0-1) (*3, 4*).

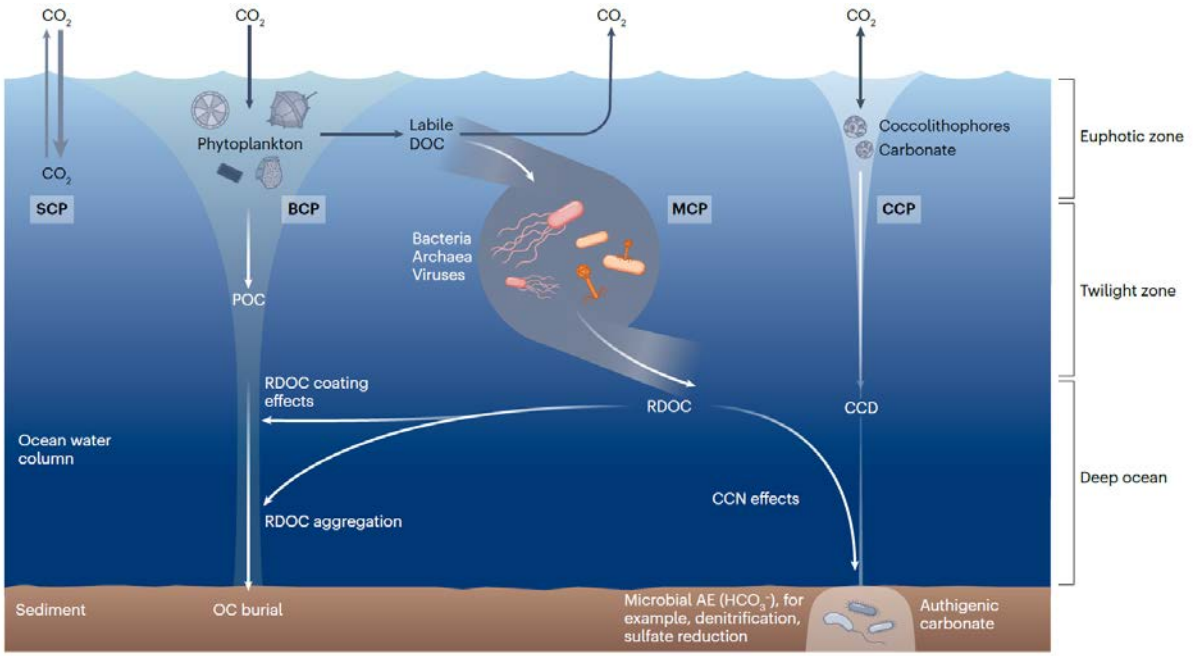

Figure 0-1. The processes that drive the marine carbon cycle. Solubility carbon pump (SCP), biological carbon pump (BCP), microbial carbon pump (MCP), carbonate counter pump (CCP), refractory DOC (RDOC), carbonate compensation depth (CCD), carbonate condensation nucleus (CCN), organic carbon (OC), alkalinity enhancement (AE). Figure derived from Jiao *et al.* (*4*).

Approximately 10-30% of the carbon derived from primary production descends beneath the euphotic layer, while only about 4% reaches the ocean seafloor (*5*). There, it can be sequestered for millennia, serving as a long-term reservoir for atmospheric-derived carbon. However, around 90% of the total marine organic carbon pool in the water column is made up by dissolved organic carbon (DOC) that is mostly released during sloppy feeding or cell lysis of phytoplankton (*6, 7*). This 'lost' carbon (DOC) is consumed by heterotrophic microbes in the 'microbial loop' and re-introduced back into the classical food chain (Fig. 0-2) (*8, 9*).

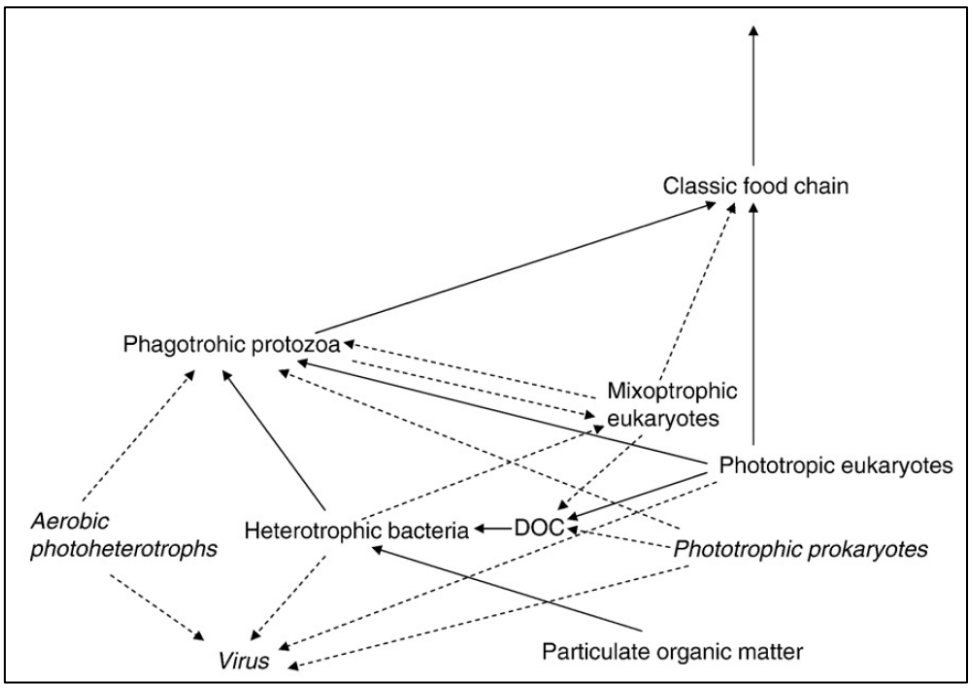

Figure 0-2. The marine microbial loop as originally described by Azam *et al.* (*8*) (solid arrows) with later additions (dashed arrows) from Fenchel (*9*) . Figure derived from Fenchel (*9*).

Moreover, heterotrophic microbes play a crucial role in converting labile dissolved organic carbon into semi-labile and ultimately refractory DOC (RDOC), a process referred to as the 'microbial carbon pump' (MCP) (Fig. 0-1) (*4, 10*), offering yet another potential for long-term storage of carbon. Two other important processes in the marine carbon cycle are the solubility carbon pump (SCP) and the carbonate counter pump (CCP): the SCP is a physico-chemical process in which increased atmospheric CO_2 concentration reduces sea-water pH. The CCP further reduces seawater pH due to the export of phytoplankton- and zooplankton-derived calcium carbonate that leads to the release of CO_2 into the surrounding waters (Fig. 0-1) (*11*).

2. The origin of marine fungi

Previous research on pelagic marine microbes typically focused on bacteria, archaea, and protists, often overlooking fungi in open ocean environments, thus hindering the accurate quantification of their role in global marine biogeochemical cycles (*12*). In contrast, terrestrial and freshwater fungi (e.g., found in lakes and rivers), play a crucial role as primary recyclers of dead organic matter. This process releases CO2 into the atmosphere while simultaneously enriching the environment with essential nutrients that are readily available to other organisms (*12-15*).

While much of our understanding of fungal ecology derived from studies conducted in terrestrial ecosystems, it is essential to consider that fungi's evolutionary origins and early diversification took place in aquatic environments (*16, 17*). Initially, fungi formed symbiotic relationships with ancestors of modern plants to colonize terrestrial habitats (*16*), leading to a remarkable diversification estimated to encompass 2.2 to 3.8 million species (*18*). A subset of these fungi later returned to marine ecosystems (*19*), where they, alongside native species, constitute today's marine fungal community (*12*). This re-entry, combined with fungi's impressive adaptability to prolonged dormancy, challenges our understanding of what defines a 'true' marine fungus (*20*). According to recent criteria, a marine fungus must exhibit consistent recovery from marine environments and meet one of the following conditions: (1) demonstrate growth or sporulation on marine substrates, (2) form symbiotic relationships with marine organisms, or (3) exhibit evolutionary or metabolic activity in marine environments (*20*). Presently, the estimated species richness of oceanic fungi stands at 10,000 (*21*), with only around 2,040 species formally described as of March 2024 (www.marine.fungi.org).

3. Pelagic fungi in the ocean (mycoplankton)

The limited research on fungi in pelagic oceans could be a result of the prevailing belief that they are surpassed by other microorganisms thriving in the ocean's diluted environment whereas fungal spores were assumed to be inactive residue from terrestrial runoff (*12*). As a consequence, the first studies of marine fungi mainly focused on culture-dependent methods of fungi derived from sediments, large macrophytes and submerged wood (*22, 23*). Only in the last decade, marine pelagic fungi ('mycoplankton') gained greater scientific attention (*12, 24*) due to their ubiquitous presence in global marine metagenomes (*25*) and their active role in degrading carbohydrates (*26-28*). This aligns with findings from a prior investigation conducted in the coastal waters off Chile, which proposed that pelagic fungi were actively

engaged in the degradation of proteinaceous compounds, as evidenced by elevated fungal-derived extracellular enzymatic activities within the water column (*29*). These researchers hypothesized that approximately 30% of the locally photosynthetically fixed carbon might have undergone remineralization by fungi, indicating a significant contribution of fungal enzymatic activities to organic matter cycling (*29*).

Concerning the specific community composition, in general, the open ocean seems to be dominated by Dikarya (Ascomycota and Basidiomycta) with abundant fungal classes such as Eurotiomycetes, Dothideomycetes, Sordariomycetes, Leotiomycetes, Saccharomycetes, Pezizomycetes, Agaricomycetes, Exobasidiomycetes, Malasseziomycetes and Microbotryomycetes (*12*). However, close to coastal areas fungi belonging to the division of Chytridiomycota become periodically abundant due to their important role as phytoplankton parasites in the marine 'mycoloop' (Fig. 0-3) (*30*). Within this ecosystem, parasitic Chytridiomycota serve as a vital trophic bridge via the 'fungal shunt' by dispersing zoospores that are readily consumed by larger zooplankton (Fig. 0-3) (*30-33*).

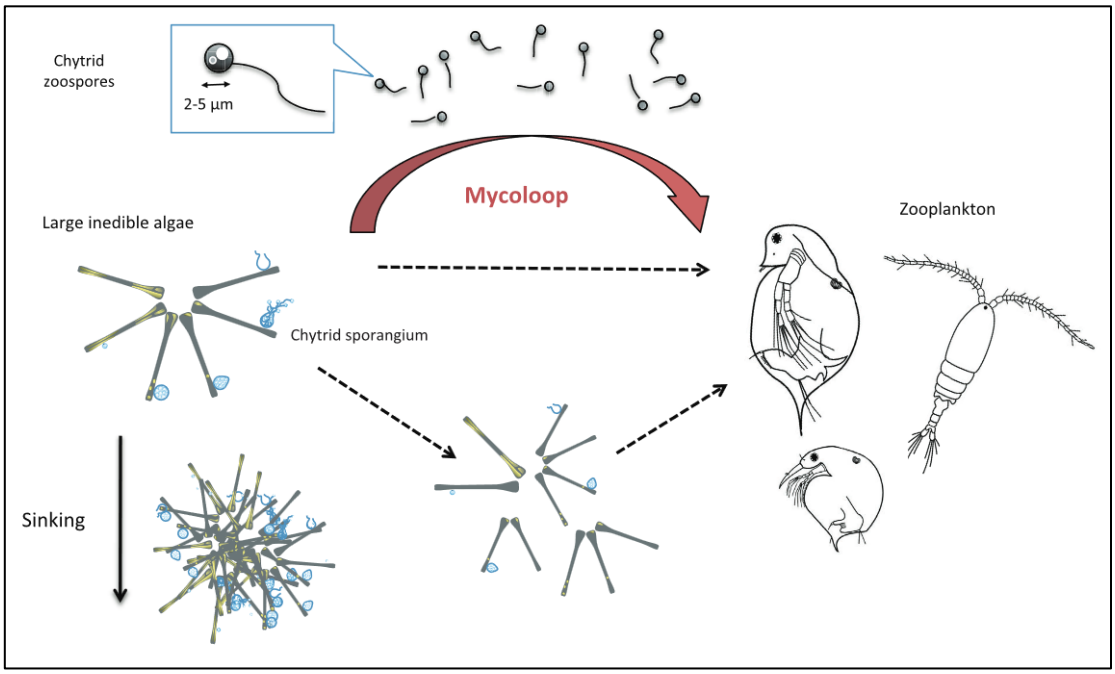

Figure 0-3. Diagram of the mycoloop. Parasitic Chytridiomycota (Chytrids) infect large inedible phytoplankton and produce zoospores which can be readily eaten by zooplankton. Figure derived from Kagami *et al.* (*30*).

Despite this growing interest and evidence, basic information about fungi in the open ocean, such as their response to different environmental conditions as a result of climate

change, their role in degrading proteins (that constitute >50% of marine biomass) and basic measurements such as quantifying their biomass, is still lacking. This knowledge gap hinders our understanding of the ecological role of fungi in our oceans, their roles in marine biogeochemical cycles and their potential responses to future global environmental changes.

4. Objectives of the thesis

The general objective of the thesis addresses a fundamental issue in marine microbiology and marine biogeochemistry, i.e., the ecology and the functional roles of oceanic fungi (mycobiome) in relation to other pelagic microbes considered to be important players in marine nutrient cycles.

In Chapter 1 (Physiological Properties of Three Pelagic Fungi Isolated from the Atlantic Ocean), we specifically addressed the question on how individual fungal isolates respond to changes in environmental conditions, which are likely to happen in future global ocean warming scenarios. (i.e., change in salinity and temperature). Additionally, as evident from recent global metatranscriptomic analyses of fungal CAZymes (*26*), marine pelagic have a high potential of degrading carbohydrates (labile and refractory) in the water column. Hence, employing a culture-dependent approach, we examined under laboratory-controlled conditions, the species-specific growth and utilization patterns of fungi when exposed to various carbon substrates.

In Chapter 2 (Global contribution of pelagic fungi to protein degradation in the ocean), we extended the previous knowledge on global pelagic fungal carbohydrate degradation (*26*) to global fungal protein degradation, bearing in mind that proteins make up more than half of living and detrital biomass. Specifically, we performed a global-ocean multi-omics analysis of fungal-affiliated peptidases in different depths and compared it to that of prokaryotes.

In Chapter 3 (The overlooked contribution of pelagic fungi to ocean biomass), we determined for the first time the contribution of marine pelagic fungi to microbial biomass in the oceans. By developing novel culture-based biomass conversion factors, we quantified pelagic fungal biomass according to three different methods in parallel along a 11,000 km latitudinal transect in the Atlantic Ocean from the surface to bathypelagic depths (2000 m). To put fungal biomass into a global context, we quantified its contribution to POC in the water column and compared it to other more studied microbial groups in the ocean such as archaea and bacteria.

References

1. P. G. Falkowski, T. Fenchel, E. F. Delong, The microbial engines that drive Earth's biogeochemical cycles. *Science* **320**, 1034-1039 (2008).
2. Y. M. Bar-On, R. Milo, The Biomass Composition of the Oceans: A Blueprint of Our Blue Planet. *Cell* **179**, 1451-1454 (2019).
3. D. A. Siegel, T. DeVries, I. Cetinić, K. M. Bisson, Quantifying the Ocean's Biological Pump and Its Carbon Cycle Impacts on Global Scales. *Ann. Rev. Mar. Sci.* **15**, 329-356 (2023).
4. N. Jiao *et al.*, The microbial carbon pump and climate change. *Nat. Rev. Microbiol*. (2024).
5. J. J. Middelburg, in *Marine Carbon Biogeochemistry*. (Springer, Switzerland, 2019), pp. 57-75.
6. H. Ogawa, E. Tanoue, Dissolved Organic Matter in Oceanic Waters. *J. Oceanogr.* **59**, 129-147 (2003).
7. G. E. Fogg, The ecological significance of extracellular products of phytoplankton photosynthesis. *Bot. Mar.* **26**, 3-14 (1983).
8. F. Azam *et al.*, The ecological role of water-column microbes in the sea. *Mar. Ecol. Prog. Ser.* **10**, 257-263 (1983).
9. T. Fenchel, The microbial loop – 25 years later. *J. Exp. Mar. Bio. Ecol.* **366**, 99-103 (2008).
10. N. Jiao *et al.*, Microbial production of recalcitrant dissolved organic matter: long-term carbon storage in the global ocean. *Nat. Rev. Microbiol.* **8**, 593-599 (2010).
11. I. Salter *et al.*, Carbonate counter pump stimulated by natural iron fertilization in the Polar Frontal Zone. *Nat. Geosci.* **7**, 885-889 (2014).
12. E. Breyer, F. Baltar, The largely neglected ecological role of oceanic pelagic fungi. *Trends Ecol. Evol.* **38**, 870-888 (2023).
13. H.-P. Grossart *et al.*, Fungi in aquatic ecosystems. *Nat. Rev. Microbiol.* **17**, 339-354 (2019).
14. M. J. Carlile, S. C. Watkinson, G. W. Gooday, *The fungi*. (Academic Press, 2001).
15. J. Dighton, in *Environmental and microbial relationships,* D. I. S., K. C. P., Eds. (Springer, 2007), vol. 4, pp. 287.
16. D. S. Heckman *et al.*, Molecular evidence for the early colonization of land by fungi and plants. *Science* **293**, 1129-1133 (2001).

17. M. L. Berbee *et al.*, Genomic and fossil windows into the secret lives of the most ancient fungi. *Nat. Rev. Microbiol.* **18**, 717-730 (2020).
18. D. L. Hawksworth, R. Lücking, Fungal diversity revisited: 2.2 to 3.8 million species. *Microbiol. Spectr.* **5**, 10 (2017).
19. J. W. Spatafora, B. Volkmann-Kohlmeyer, J. Kohlmeyer, Independent terrestrial origins of the Halosphaeriales (marine Ascomycota). *Am. J. Bot.* **85**, 1569-1580 (1998).
20. K.-L. Pang *et al.*, 'Marine fungi'and 'marine-derived fungi'in natural product chemistry research: toward a new consensual definition. *Fungal Biol. Rev.* **30**, 163-175 (2016).
21. E. G. Jones, Are there more marine fungi to be described? *Bot. Mar.* **54**, 343-354 (2011).
22. A. Amend *et al.*, Fungi in the Marine Environment: Open Questions and Unsolved Problems. *MBio* **10**, e01189-01118 (2019).
23. T. A. Richards, M. D. Jones, G. Leonard, D. Bass, Marine fungi: their ecology and molecular diversity. *Annu. Rev. Mar. Sci.* **4**, 495-522 (2012).
24. X. Peng *et al.*, Planktonic Marine Fungi: A Review. *JGR Biogeosciences* **129**, e2023JG007887 (2024).
25. S. E. Morales, A. Biswas, G. J. Herndl, F. Baltar, Global structuring of phylogenetic and functional diversity of pelagic fungi by depth and temperature. *Front. Mar. Sci.* **6**, 131 (2019).
26. F. Baltar, Z. Zhao, G. J. Herndl, Potential and expression of carbohydrate utilization by marine fungi in the global ocean. *Microbiome* **9**, 1-10 (2021).
27. N. Chrismas, M. Cunliffe, Depth-dependent mycoplankton glycoside hydrolase gene activity in the open ocean—evidence from the Tara Oceans eukaryote metatranscriptomes. *ISME J.* **14**, 2361-2365 (2020).
28. W. D. Orsi *et al.*, Carbon assimilating fungi from surface ocean to subseafloor revealed by coupled phylogenetic and stable isotope analysis. *ISME J.* **16**, 1245-1261 (2021).
29. M. H. Gutiérrez, S. Pantoja, E. Tejos, R. A. Quinones, The role of fungi in processing marine organic matter in the upwelling ecosystem off Chile. *Mar. Biol.* **158**, 205-219 (2011).
30. M. Kagami, T. Miki, G. Takimoto, Mycoloop: chytrids in aquatic food webs. *Front. Microbiol.* **5**, 166 (2014).
31. M. Kagami, A. de Bruin, B. W. Ibelings, E. Van Donk, Parasitic chytrids: their effects on phytoplankton communities and food-web dynamics. *Hydrobiologia* **578**, 113-129 (2007).

32. I. Klawonn *et al.*, Characterizing the “fungal shunt”: Parasitic fungi on diatoms affect carbon flow and bacterial communities in aquatic microbial food webs. *Proc. Natl. Acad. Sci. U.S.A* **118**, e2102225118 (2021).
33. M. H. Gutiérrez, A. M. Jara, S. Pantoja, Fungal parasites infect marine diatoms in the upwelling ecosystem of the Humboldt current system off central Chile. *Environ. Microbiol.* **18**, 1646-1653 (2016).

Chapter 1: Physiological Properties of Three Pelagic Fungi Isolated from the Atlantic Ocean

Eva Breyer[1*], Salvador Espada-Hinojosa[1], Magdalena Reitbauer[1], Samantha C. Karunarathna[2] and Federico Baltar[1*]

[1] Department of Functional and Evolutionary Ecology, University of Vienna, 1030 Vienna, Austria

[2] Center for Yunnan Plateau Biological Resources Protection and Utilization, Yunnan Engineering Research Center of Fruit Wine, College of Biological Resource and Food Engineering, Qujing Normal University, Qujing 655011, China

* Correspondence: eva.breyer@univie.ac.at, federico.baltar@univie.ac.at

Published in *Journal of Fungi*

Abstract

Oceanic fungi are widely understudied compared to their terrestrial counterparts. However, they have been shown to be important degraders of organic matter in the global pelagic oceans. By examining the physiological characteristics of fungi isolated from the pelagic waters of the ocean it is possible to infer specific functions of each species in the biogeochemical processes that occur in the marine ecosystem. In this study, we isolated three pelagic fungi from different stations and depths across a transect in the Atlantic Ocean. We identified two yeasts [(*Scheffersomyces spartinae* (Debaryomycetaceae, Saccharomycetes, Ascomycota) and *Rhodotorula sphaerocarpa* (Sporidiobolaceae, Microbotryomycetes, Basidiomycota)], and the hyphae-morphotype fungus *Sarocladium kiliense* (Hypocreales, Sordariomycetes, Ascomycota), and conducted physiological experiments to investigate their preferred carbon uptake as well as their growth patterns under different environmental conditions. Despite their taxonomic and morphological differences, all species exhibited a high tolerance towards a wide range of salinities (0–40 g/l) and temperatures (5–35 °C). Furthermore, a shared metabolic preference for oxidizing amino acids was found among all fungal isolates. Collectively, this study provides relevant information on the physiological properties of oceanic pelagic fungi, revealing a high tolerance towards salinity and temperature changes, ultimately contributing to understanding their ecology and distribution in the oceanic water column.

Keywords: ecological role, fungal isolates, marine fungi, metabolism, morphology, FF MicroPlate

1. Introduction

Fungi are ubiquitous in terrestrial, freshwater and marine habitats (*1*). Despite their global importance, most previous mycological research focused on either terrestrial (*2, 3*), freshwater (*4, 5*), or sediment-derived fungi (*6, 7*) outpointing the high undiscovered potential of oceanic pelagic fungi in terms of diversity and secondary metabolite production (*8, 9*). Additionally, many marine-derived fungi also occur in terrestrial and freshwater ecosystems. This emphasizes the remarkable adaptive capabilities of fungi but also generates the question of how many already described terrestrial species inhabit marine environments (*8*).

With these exceptional adaptive abilities, it is not surprising that, according to metagenomic analyses, fungi are present in all oceans, dominated by Dikarya (*10*). Globally, marine fungi have also been isolated from different substrates and regions, including extreme habitats such as the deep sea (*6*), hypersaline anoxic basins (*7*), hydrothermal vents (*11*) and arctic sea ice and water (*12*).

Marine fungi exhibit a range of life strategies, which is attributed to their extensive presence in diverse environments. These strategies may involve distinct approaches for obtaining nutrients and energy, coping with environmental pressures, or adapting to different ecological niches. As saprophytes (e.g., *Malassezia* and *Cladosporium*), they are decomposing recalcitrant substrates, ultimately re-integrating them back into the food chain and hence making them accessible to other organisms (*13, 14*). Certain parasitic fungi from the Chytridiomycota group, such as *Rhizophydium* and *Chytridium* (*15-17*), are common parasites on marine diatoms. These fungi produce zoospores that are readily available to zooplankton, a process known as the ‘mycoloop’ (*4*). Recent research suggests that marine fungi dominate microbial biomass on bathypelagic marine snow (*18*). In addition, pelagic fungi, particularly in the classes of Dothideomyctes, Eurotiomyctes, and Leotiomycetes, express a diverse range of CAZymes (*19*) and proteases (*20*) that degrade organic matter in the global oceans, indicating their active contribution to the cycling of major elements that make up marine biomass, both at global (*19, 20*) and local scales (*21*).

Given their global distribution (*10*), active participation in the marine C-cycle (*19*) and N-cycle (*20*) and important role in marine food web dynamics (*4*), oceanic fungi are considered as being crucial participants in global marine biogeochemical processes (*8*).

According to Jones, et al. (*22*), due to next generation sequencing (NGS), lots of sequences have been detected, arising from fungal species that have never been observed in cultures. This leads to a gap of knowledge between the uncultured ‘dark fungi’ and well-documented species descriptions (*1, 23, 24*). Taking into account their important role as

secondary metabolite producer and their relevant contribution to the remineralization of organic matter in the oceans, there is an urgent need for identifying and physiologically characterizing marine fungal isolates.

To deal with the aforementioned issues, we took the following steps: isolating three fungi from the marine pelagic environment, identifying them, and examining their morphology, growth physiology, and carbon substrate uptake by using FF Micro-Plates™. With this information, we aimed to expand our understanding of the distribution, the physiology and the ecological properties of pelagic fungi in the ocean.

2. Material and Methods

2.1. Sample Collection and Isolation of Marine Fungi

Pelagic fungi were collected during the ANTOM-1 Cruise in 2020/21 and during the Poseidon Cruise (2019) on board the RV Sarmiento de Gamboa (Fig. 1-1, Table 1-1).

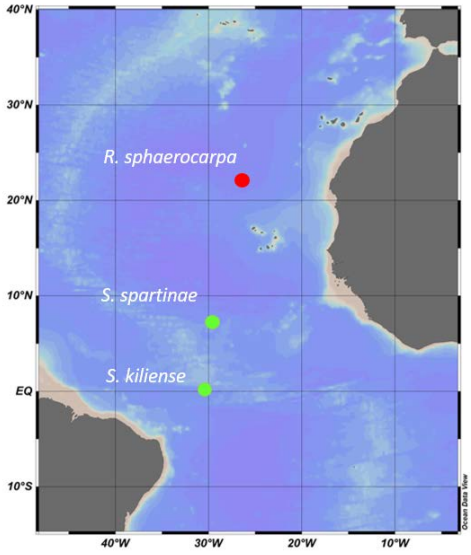

Figure 1-1. The three sampling stations where the fungi were isolated during the ANTOM-1 Cruise in 2020/21 (green dots) and the Poseidon Cruise in 2019 (red dot).

Seawater samples were collected with a CTD rosette equipped with 12-liter Niskin bottles. The sampling depth ranged from 5 to 2000 m during the ANTOM-1 Cruise and from 5 to 6197 m during the Poseidon Cruise. When collecting the fungal isolate during the Poseidon Cruise, unfiltered seawater from the respective sampling depth was pipetted directly onto the solid agar media plate (media concentration see below). To collect fungal isolates during the

ANTOM-1 Cruise, around 500 mL of seawater per sampling depth were filtered onto a combusted GF/F filter. Afterwards, the filter was inoculated on a solid agar media plate containing (g/l): 1 g glucose, 1 g peptone, 1 g yeast extract, 1 g starch, 20 g artificial sea salts, 15 g agar and 0.5 g chloramphenicol. The agar plates were incubated at environmental temperatures and checked for growth on a daily basis. Once individual colonies started to emerge, they were separated onto distinct plates, and subsequently replated until a single species was completely isolated.

Table 1-1. Fungal species isolated during the ANTOM-1 and Poseidon Cruise.

ID	Species	Cruise	Depth	Temperature	Salinity	Location
ANTOM-1 Isolate 13	*Scheffersomyces spartinae*	ANTOM-1	5 m	27 °C	34.9	Latitude: 7.343 Longitude: -29.581
ANTOM-1 Isolate 15	*Sarocladium kiliense*	ANTOM-1	45 m	26 °C	36	Latitude: 0.137 Longitude: -30.501
Poseidon isolate	*Rhodotorula sphaerocarpa*	Poseidon	93 m	20 °C	35	Latitude: 22.220 Longitude: -26.633

2.2. Sequencing of the Fungal Isolates

To identify the species, fresh agar plates were prepared from all isolates and then allowed to grow at room temperature. The solid agar media contained (g/l): 20 g agar, 10 g glucose, 5 g peptone, 3 g yeast extract, 3 g malt extract, 35 g artificial sea salts and 0.5 g chloramphenicol. Afterwards, the cultures were sent to the Westerdijk Fungal Biodiversity Institute Identification Service (Utrecht, Netherlands, https://wi.knaw.nl, accessed on: 15 March 2023) for species identification. There, after arrival, the strains were cultivated on malt extract agar (MEA) and dichloran 18% glycerol agar (DG18). The DNA was extracted from MEA after an incubation period of 3 days in the dark at 25 ˚C using the Qiagen DNeasy Ultraclean™ Microbial DNA Isolation Kit. For all strains, fragments containing the Internal Transcribed Spacer 1 and 2 regions including the 5.8S rDNA (ITS) and the large subunit region D1 and D2 (LSU) were amplified and sequenced. The primers used for the ITS region were: LS266 (GCATTCCCAAACAACTCGACTC) and V9G (TTACGTCCCTGCCCTTTGTA) and for the LSU region LR0R (ACCCGCTGAACTTAAGC) and LR5 (TCCTGAGGGAAACTTCG). Furthermore, in the case of *Sarocladium kiliense*, a partial fragment of the actin gene (Act) was amplified and sequenced. The primers used were Act512F (ATGTGCAAGGCCGGTTTCGC) and Act-783R (TACGAG-TCCTTCTGGCCCAT). The PCR fragments were sequenced in both directions with the primers used for PCR amplification using the ABI Prism® Big DyeTM Terminator v. 3.0 Ready Reaction Cycle sequencing Kit.

Samples were analyzed on an ABI PRISM 3700 Genetic Analyzer and contigs were assembled using the forward and reverse sequences with the program SeqMan from the LaserGene package. The sequences were compared on GenBank using BLAST and in the in-house sequence database of Westerdijk Fungal Biodiversity Institute (Table 1-1).

2.3. Morphological Observations with Epifluorescence Microscopy

For morphological observations, the fungal cultures were grown in liquid media containing (g/l): 2 g glucose, 2 g peptone, 2 g yeast extract 35 g artificial sea salts and 0.5 g chloramphenicol; the pH was set to 8. The growth of the fungal cells in liquid cultures was traced by measuring optical density (OD) which determines the absorbance of a material and is a dimensionless quantity. The optical density was measured on the inoculation day (day zero) with the UV-1800 Shimadzu Spectrophotometer (λ = 660 nm, Kyoto, Japan) followed by regular checks of the OD to track the fungal growth stages.

To investigate the morphology of the fungal strains, the isolates were sampled during the exponential phase and fixed with formaldehyde (Sigma-Aldrich, 37%, St. Louis, MO, USA) to a final concentration of 2%. To dilute the fungal culture, 250 µl of the liquid culture were mixed with 5 ml MilliQ-water in an Eppendorf tube and subsequently filtered onto GTTP filters (0.22 µm, 25 mm diameter, Merck Millipore, Burlington, MA, USA). Afterwards, the sampling tube was flushed with 5 ml MilliQ-water and filtered again. The filter was dried and mounted on a microscopic slide. Two different methods were used for staining the fungal cells: Calcofluor-White and DAPI (4′,6-diamidino-2-phenylindole, a fluorescent stain that binds strongly to the adenine- thymine-rich regions in the DNA). To perform Calcofluor-White staining, a mixture of 25 µl of Calcofluor-White (a fluorescent dye that binds non-specifically to chitin and cellulose, obtained from Sigma-Aldrich in St. Louis, MO, USA) and 25 µl of 10% KOH solution (mixed with 10% glycerol) was prepared. This mixture was then added to the filter based on concentrations previously determined to yield the optimal signal intensity. To stain fungal cells with DAPI, 50 µl of DAPI-mix [5.5 parts of Citifluor (Electron Microscopy Sciences, Hatfield, PA, USA), one part of Vectashield (Vector Laboratories, Newark, CA, USA) and 0.5 parts of phosphate-buffered saline (PBS) with DAPI solution (final concentration 2 g/ml)] were used to stain the culture. The samples were analyzed with a Zeiss Axio Imager 2 microscope using UV-light below 400 nm (1000x magnification).

2.4. Physiological Tests of Fungal Growth

To investigate the fungal growth under various environmental conditions, liquid cultures of each species were prepared in biological triplicates per treatment (see below culture conditions). Samples were taken at regular intervals from the liquid cultures in order to measure the OD as an indicator of the different stages of growth (Table 1-2). Sampling was discontinued once the cultures reached the stationary phase.

Table 1-2. Estimation of the fungal growth phase according to the optical density (OD).

Growth phase	Optical density (660 nm)
Adaptation	*0.070 to 0.399*
Exponential	*0.400 to 1.199*
Stationary	*>1.200*

2.4.1. Influence of Temperature

To study the effect of temperature on fungal growth, liquid media was prepared containing (g/l): 2 g glucose, 2 g peptone, 2 g yeast extract and 35 g artificial sea salts and 0.5 g chloramphenicol; the pH was set to 8. The liquid media was distributed in triplicate bottles per species. For inoculation of the liquid media, solid fungal biomass derived from the agar plates was mixed with MilliQ-water to a final OD of approximately one. Afterwards, 1 ml of this inoculum was added to 100 ml of liquid media. Finally, the bottles were incubated at 5 °C, 23 °C (room temperature) and at 35 °C on shaker incubators (Lab Companion, Shaking Incubator model ISS-7100R, 140 rpm, Billerica, MA, USA).

2.4.2. Influence of Salinity

To study the effect of salinity on fungal growth, liquid media was prepared containing (g/l): 2 g glucose, 2 g peptone, 2 g yeast extract, 0.5 g chloramphenicol and either 0 g, 20 g, 35 g or 40 g of artificial sea salts. The liquid media was adjusted to a pH of 8. For each species, triplicate bottles were prepared and inoculated with a mix of MilliQ-water and fungal biomass as explained previously. Afterwards, the bottles were incubated at 23 °C (room temperature) on shaker incubators (Lab Companion, Shaking Incubator model ISS-7100R, 140 rpm, Billerica, MA, USA).

2.5. Metabolic Activity and Assimilation of Carbon Compounds by Fungal Cultures

FF MicroPlate™ (Biolog, Inc., Hayward, CA, USA) plates were used to investigate the species-specific carbon uptake of the fungal isolates by providing them with different carbon

sources in a 96-well plate. These can give insight into the 'Metabolic Fingerprint' of different fungal species. Carbon sources used in this study include a variety of compounds such as carbohydrates, amino acids, carboxylic acids, polymers, as well as others including alcohols, nucleotides, nucleosides, amines, and amides.

The culture inocula was prepared according to manufacturer guidelines and incubated on the 96 well plates at 23 °C in the dark. During this incubation period, the absorption was measured every day for four days at a wavelength of 490 nm and 750 nm with the Tecan M200 Infinite Pro (Männedorf, Swizerland).

Increased mitochondrial respiration activity that results from oxidation of metabolizable carbon sources can be detected by the formation of a reddish-orange color at 490 nm. This is caused by the reduction in colorless tetrazolium chloride turning into red formazan (*25*). The response in turbidity caused by the production of mycelia was measured at 750 nm. For our analysis, we used the values obtained on the fourth day of incubation, and as a result, these values are presented in the results.

2.6. Statistical Analysis

All statistical analyses were performed in R (version 3.6.1). The data was visualized with the package ggplot2 (version 3.3.5) (*26*). In order to compare the utilization of different carbon compound groups by each species, a Kruskal–Wallis test was conducted. Subsequently, a pairwise comparison was carried out using the Wilcoxon test, and the resulting p-value was adjusted for multiple comparisons using the Bonferroni correction. The p-values were calculated with the package ggpubr (version 0.4.0). The statistical tests were performed with the package rstatix (version 0.7.0) (*27*). Statistics in the text are depicted as mean ± standard deviation.

3. Results and Discussion

3.1. Isolated Fungal Species

The three different fungal isolates were identified as *Scheffersomyces spartinae*, *Sarocladium kiliense* and *Rhodotorula sphaerocarpa*, by the Westerdijk Fungal Biodiversity Institute. Additionally, we characterized all species physiologically by investigating their growth pattern under different salinities and temperatures as well as their preferred carbon substrate uptake.

The fungal ascomycetous yeast *Scheffersomyces spartinae* (Debaryomycetaceae, Saccharomycetales, Saccharomycetidae, Saccharomycetes, Saccharomycotina, Ascomycota) (Fig. 1-2A,C–F) is exclusively known from aquatic environments. In previous studies, this species was isolated from habitats including brackish waters where it was found to be in association with marsh grass (*28*). Additionally, it is recognized for its capacity to potentially produce coenzyme Q-9, which plays a role in the electron transport chain and is therefore of interest in the field of biomedicine (*29*). Furthermore, *S. spartinae* has been shown to potentially act as bio-control agent (*30, 31*).

Sarocladium kiliense (Fig. 1-3) belongs to the division of Ascomycota (Hypocreales, Hypocreomycetidae, Sordariomycetes, Pezizomycotina) and grows as hyphae-morphotype. Although this taxon has a worldwide distribution, it is frequently found in soils and has been shown to be an opportunistic pathogen in humans (*32*). It is described as being alkalotolerant, meaning that it can occur in both alkaline and acidic environments. However, it has been recently isolated from very alkaline environments with a pH of 10–12 (*33*). Additionally, *S. kiliense* has been found in the deep sea at a depth of 5070 m (*34*) and has shown its potential in mercury bioremediation (*35*).

Rhodotorula sphaerocarpa (Sporidiobolaceae, Sporidiobolales, Incertae sedis, Microbotryomycetes, Pucciniomycotina, Basidiomycota) (Fig. 1-2B,G–J) is an oleaginous (oil producing) yeast which occurs in typical pink-reddish colonies resulting from pigments that block certain wavelengths to prevent cell damage. The species has been isolated from diverse environments, including mangrove forests (*36*), hypersaline waters and salterns (*37*), and deep sea sediment (*38*).

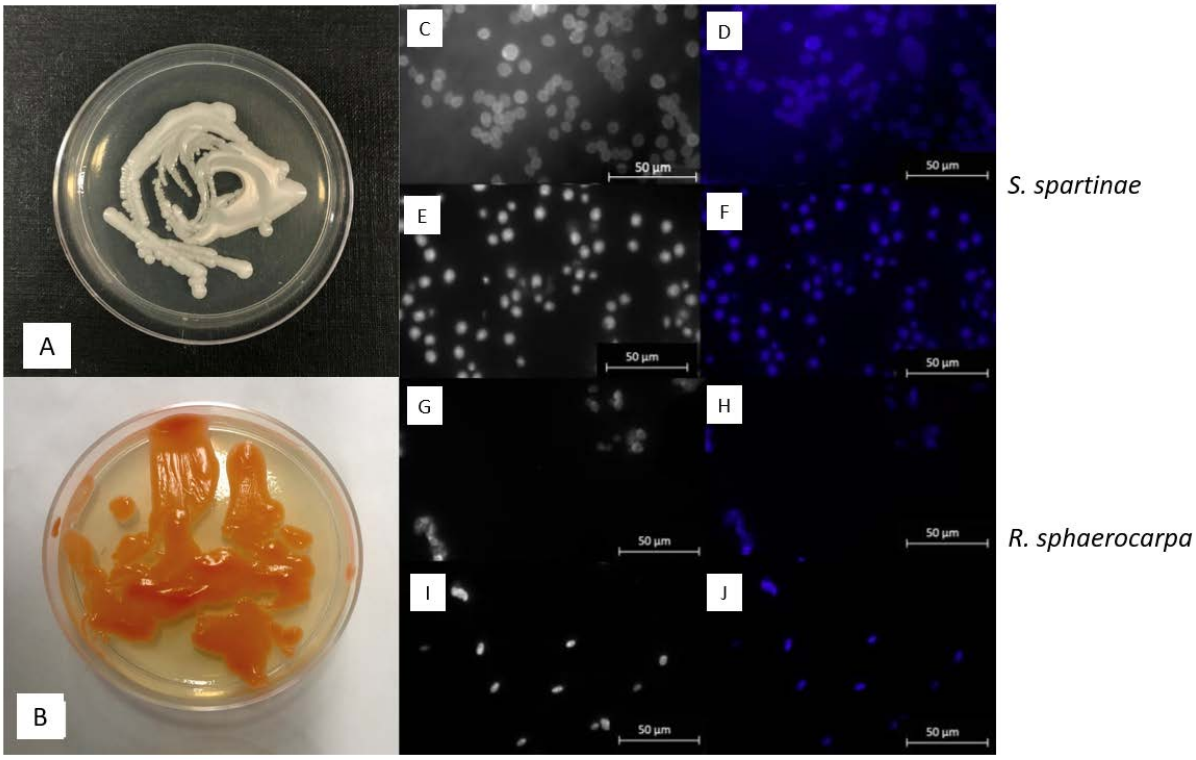

Figure 1-2. Phenotype of *Scheffersomyces spartinae* (A,C–F) and *Rhodotorula sphaerocarpa* (B,G–J). (A,B): Colonies after one week of growth; (C,D,G,H): Fungal cells stained with Calcofluor-White; (E,F,I,J): Fungal cells stained with DAPI-mix. Scale bar = 50 µm. Microscopic images were taken under UV-light below 400 nm.

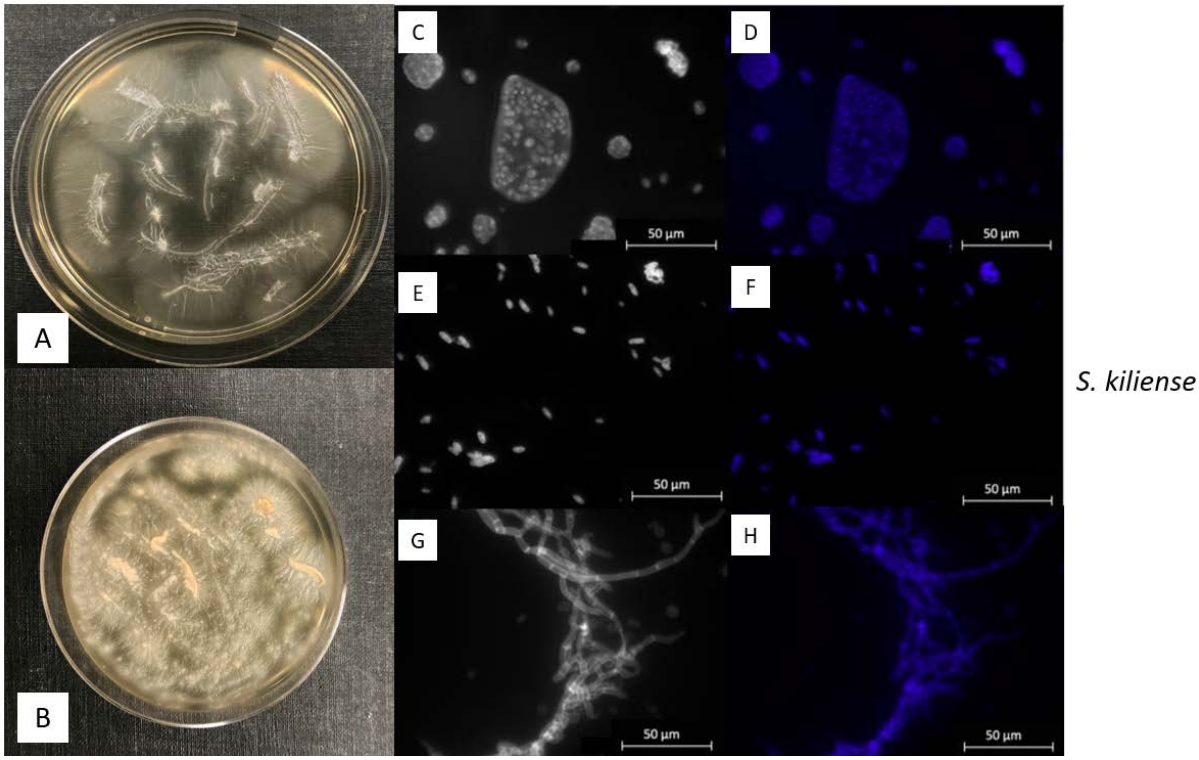

Figure 1-3. Phenotype of *Sarocladium kiliense*. (A): Colony after one week of growth; (B): Colony after four weeks of growth; (C,D): Fungal conidia stained with DAPI-mix; (E,F): Ellipsoidal Conidia stained with DAPI-mix; (G,H): Fungal hyphae stained with Calcolfuor-White. Scale bar = 50 µm. Microscopic images were taken under UV-light below 400 nm.

3.2. Macroscopic and Microscopic Morphology of isolated Fungal Cultures

After one week of incubation at room temperature, the cells of *S. spartinae* showed thin branches, some with wobbly structures and a white coloration (Fig. 1-2A,C–F). The coloration changed slightly after one month of incubation to a more yellowish tone. The shape of the cultures in general got flatter with edges being slightly more toothed. The cells of *S. spartinae* appeared to be mostly oval and ellipsoidal. They showed a rather uniform size between 1.5–2.2 × 4.1–5.3 µm (Fig. 1-2C–F). The majority of cells were observed to occur individually, although some were found to be attached, indicating asexual reproduction through budding. In general, the morphological appearance of *Scheffersomyces spartinae* in the cultures closely resembled what had been reported in previous studies (*28*).

S. kiliense exhibited a relatively rapid growth and developed flat colonies being slightly raised in the center. After one week of incubation, the colony had a white to cream appearance (Fig. 1-3A) which changed after around one month of incubation to a yellowish to light orange tone (Fig. 1-3B). Apart from the color, this taxon showed a denser growth with furry structures. In general, the most common asexual reproductive spores of *S. kiliense* are called conidia and emerge from conidiophores or hyphae. In this study, we observed conidia accumulated around the tip of hyphae (Fig. 1-3G,H). However, they also appeared dispersed (Fig. 1-3E,F) and in slimy masses (Fig. 1-3C,D). Single-celled conidia were shaped either oval or ellipsoidal with an average size between 3–5 × 2–3 µm (Fig. 1-3E,F).

The colony of *R. sphaerocarpa* showed a bright color after about one week of growth with a coral to saffron orange coloration (Fig. 1-2B). This appearance changed after approximately one month of incubation time at room temperature, after which the color changed to a lighter nuance of orange. In general, colonies of *R. sphaerocarpa* appeared shiny with a smooth structure. Like *S. spartinae*, the cells of *R. sphaerocarpa* occurred either individually or attached to each other, indicating active budding sites (Fig. 1-2G–J).

In summary, the morphological characteristics of all species are similar to reports in previous studies (*28, 39*) and confirm the species identification by parallel amplicon sequencing.

3.3. Fungal Growth under changing Environmental Conditions

3.3.1. Influence of Temperature on Fungal Growth

The lowest temperature tested in this experiment was 5 °C in which the cells of *S. spartinae* never reached the exponential phase (Fig. 1-4A). The OD values here ranged from 0.15 ± 0.01 to 0.19 ± 0.01. In contrast, *S. kiliense* entered the exponential phase on the seventh day of incubation (OD 0.45 ± 0.12), and the stationary phase on day 14 at 5 °C (Fig. 1-4B). Similarly, the liquid culture of *R. sphaerocarpa* reached the exponential phase at day 9 (OD 0.81 ± 0.07), followed by the stationary phase on day 10 (OD 1.17 ± 0.05) (Fig. 1-4C). Hence, although a general slower growth, both species show the ability to grow in colder waters. These findings are also in accordance with Nagahama (*38*) and Fan *et al.* (*34*) who isolated *R. sphaerocarpa* and *S. kiliense*, respectively, from cold deep-sea environments. However, since the lowest growth yields of all species were obtained at 5 °C compared to the other temperatures, only a weak adaptation to cold waters can be assumed. Instead, the isolated strains seemed to be more adapted to temperatures close to their in-situ conditions.

At room temperature (23 °C), *S. spartinae* reached the exponential phase on the second day of incubation with an OD of 0.41 ± 0.08. On the fourth day, the fungal biomass increased to an OD of 1.46 ± 0.03, indicating the stationary phase (Fig. 1-4A). Afterwards, the OD still increased until day 11 to a maximum OD of 1.79 ± 0.08. Additionally, *S. kiliense* reached the exponential phase at room temperature on the second day of incubation with an OD of 0.66 ± 0.01 (Fig. 1-4B). On day three, the stationary phase was reached with an OD of 1.38 ± 0.01. *Rhodotorula sphaerocarpa* showed a similar growth at room temperature: the exponential phase was already reached at day 1 (OD 0.49 ± 0.01) (Fig. 1-4C). On day 2, the value increased to an OD of 1.21 ± 0.01, revealing that the stationary phase was reached (Fig. 1-4C) and indicating the capability of quick growth of *R. sphaerocarpa* at moderate temperatures. These results provide evidence that the most favorable growth conditions for all three fungal species were those at 23 °C due to their highest growth yields under these conditions.

The third temperature investigated in this experiment was 35 °C. *Scheffersomyces spartinae* already reached the exponential phase on day one with an OD of 0.71 ± 0.01 (Fig. 1-4A). On the second day, the stationary phase was reached with an OD of 1.24 ± 0.16. *Sarocladium kiliense* reached the exponential phase at 35 °C on day two (OD 0.51 ± 0.09) (Fig. 1-4B). The values increased until the stationary phase was reached on day 7 (OD 1.13 ± 0.08), indicating that this species can grow at warmer temperatures as well although with a lower total

biomass at 35 °C in the stationary phase compared to *S. spartinae*. The fungal cells of *R. sphaerocarpa* reached the exponential phase on day one with an OD of 0.62 ± 0.01 (Fig. 1-4C). On the second day, the fungal culture entered the stationary phase (OD 1.21 ± 0.09) with an intermediate maximum growth compared to the other two species (Fig. 1-4); still indicative of good adaptations to warmer environmental conditions.

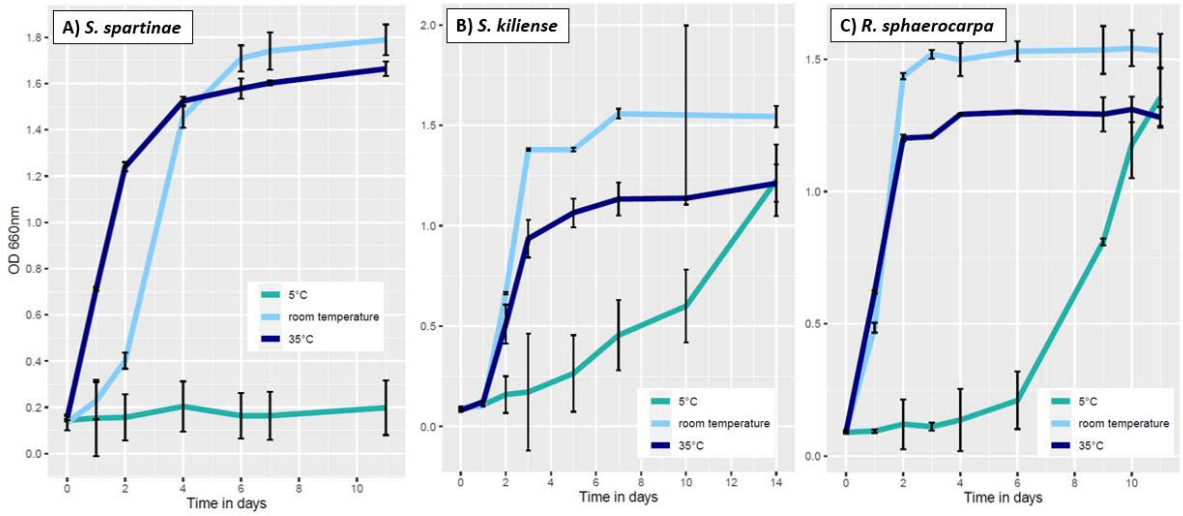

Figure 1-4: Growth curves at different temperatures (5 °C, room temperature 23 °C, 35 °C) for *Scheffersomyces spartinae* (A), *Sarocladium kiliense* (B) and *Rhodotorula sphaerocarpa* (C). Optical density (OD) refers to values at a wavelength of 660 nm. The average is shown, error bars indicate the standard deviation.

3.3.2. Influence of Salinity on Fungal Growth

The culture of *S. spartinae* incubated in the media that contained 0g/l of sea salts exhibited a steep increase in OD from 0.06 ± 0.01 to 1.41 ± 0.02 already after the first 24 hours of incubation (Fig. 1-5A). These values are quite remarkable since this species is not yet documented to occur in freshwater systems. However, our results indicate that it can also grow under non-saline conditions (Fig. 1-5A). Yet, *S. spartinae* has been isolated from brackish waters, where the salinity is usually very low (0.1–1%) caused by the mixing of fresh- and seawater (*28*). At 0 g/l sea salts, *S. kiliense* reached the exponential after one day of incubation (OD of 0.07 ± 0.00) and the stationary phase on the third day (OD of 1.35 ± 0.01) (Fig. 1-5B). *Rhodotorula sphaerocarpa* started to grow exponentially during the first day of incubation and reached the stationary phase after two days with an OD of 1.06 ± 0.01 at a salinity of 0 g/l (Fig. 1-5C). These results indicate the environmental flexibility of this species although it was previously mainly isolated from salty environments (*36, 37*) but shows here that salts are not

necessary for its successful growth. Still, compared to the other salinity treatments, *R. sphaerocarpa's* total biomass was lowest at 0 g/l.

The second salinity concentration tested was 20 g/l. At this concentration, *S. spartinae* started to grow exponentially after one day (OD 0.19 ± 0.01) and reached the stationary phase after three days (OD 1.34 ± 0.03) (Fig. 1-5A). Similarly, *S. kiliense* started to grow exponentially after one day (OD 0.08 ± 0.05) and reached the stationary phase on day three (OD of 1.29 ± 0.02) (Fig. 1-5B). Additionally, for *R. sphaerocarpa*, the exponential growth started after one day of incubation (OD 0.36 ± 0.02) whereas the stationary phase was already reached on the second day (OD 1.23 ± 0.01), showing a quicker growth at 20 g/l salinity compared to the two other species (Fig. 1-5C).

At a salinity concentration of 35 g/l, *S. spartinae* entered the exponential phase on day two with an OD of 0.40 ± 0.08 and the stationary phase on day five (OD 1.71 ± 0.05) (Fig. 1-5A). *S. kiliense* reached the exponential after one day (OD of 0.1 ± 0.00) and the stationary phase on the third day (OD of 1.37 ± 0.29) (Fig. 1-5B). *R. sphaerocarpa* started to grow exponentially after one day (OD 0.39 ± 0.02) and reached the stationary phase on the second day (OD 1.34 ± 0.01) (Fig. 1-5C). Under these conditions, *S. spartinae* and *R. sphaerocarpa* exhibited the highest total biomass compared to the other salinity treatments. These results are consistent with the observation that the salinity concentration of 35 g/l reflects the normal range of ocean salinity where the fungi were originally isolated from, which lies between 34.9 g and 36 g per liter of seawater (Table 1-1).

In the media that contained 40 g/L of sea salts, the fungal cells of *S. spartinae* entered the exponential phase after one day of growth (OD 0.24 ± 0.02), and the stationary phase was reached after around three days (OD 1.32 ± 0.03) (Fig. 1-5A). These final OD values of the stationary phase are comparable to that of the treatments of 0g/l and 20 g/l. This is not surprising, since a study conducted by Frigon and Liu (*40*) on wastewater treatment showed that *S. spartinae* could tolerate concentrations of salinities up to 120 g/l of NaCl. This emphasizes the potential wide tolerance towards different salinity conditions in this species. Under the same conditions, *S. kiliense* reached the exponential phase on day one with an OD value of 0.68 ± 0.01 and the stationary phase on the second day (OD of 1.29 ± 0.01) (Fig. 1-5 B). In general, the culture of *S. kiliense* showed a very similar growth curve at all four salinity concentrations tested (Fig. 1-5B). The fact that the fungus is not affected by changes in salinity aligns with its ubiquitous presence, as it has been found in marine environments (*34*), as well as in freshwater ecosystems such as highly alkaline lakes (*33*). This suggests that the fungus has the ability to thrive in diverse aquatic environments despite changes in salt levels (*33, 34*).

Additionally, at 40 g/l sea salts, *R. sphaerocarpa* exhibited a similar growth pattern compared to 20 g/l sea salts: i.e., after one day, the fungal culture started to grow exponentially (OD 0.25 ± 0.01) and reached the stationary phase on the second day (OD 1.23 ± 0.01) with final biomass concentrations after 6 days similar to 20 g/l sea salts (Fig. 1-5C).

In conclusion, the change of salinity did not seem to have a strong effect on the growth of oceanic fungal cultures in general. Although some species exhibited a slightly steeper or less steep growth curve compared to others at a given salinity, our experiments proved the wide tolerance of the isolated fungal cultures to different environmental salinities. Similar results have been shown before (*41*) and again highlight the potential of pelagic fungi to adapt to future global warming of the oceans accompanied by changes in salinity.

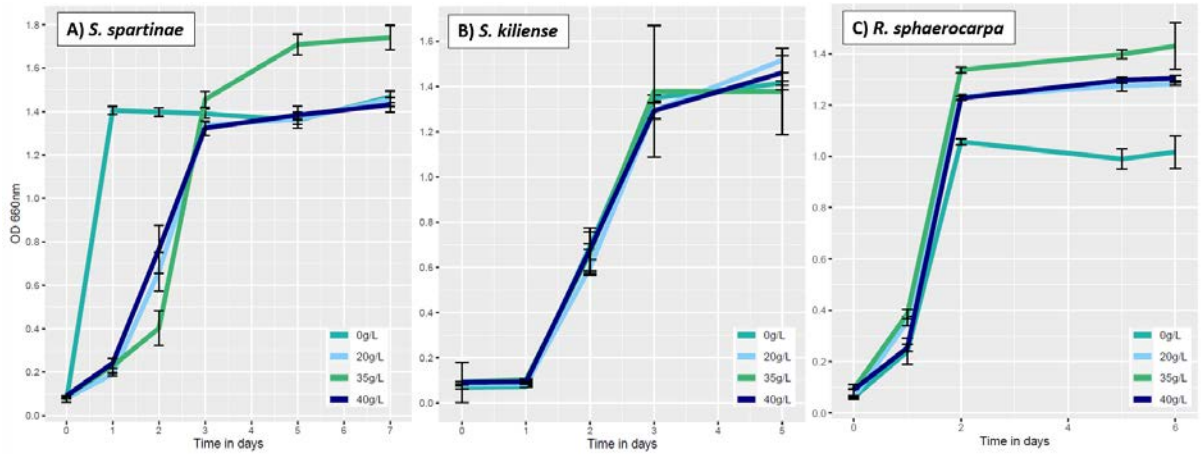

Figure 1-5. Growth curves at different salinities (0, 20, 35 and 40 g/l) for *Scheffersomyces spartinae* (A), *Sarocladium kiliense* (B) and *Rhodotorula sphaerocarpa* (C). Optical density (OD) refers to values at a wavelength of 660 nm. The average is shown, error bars indicate the standard deviation.

3.4. Metabolic activity (FF-Plates)

3.4.1. Absorption at 750 nm (Fungal Growth)

S. spartinae utilized 89 of 95 provided carbon compounds whereas *S. kiliense* and *R. sphaerocarpa* utilized all 95 provided carbon compounds (File 1-S1).

For *S. spartinae*, the three highest values were obtained for the utilization of carbon sources glycogen (1.81) (polymer), sedoheptulosan (1.74) (carbohydrate), and i-erythritol (1.56) (carbohydrate) (File 1-S1). The substrate types with the lowest fungal growth were D-trehalose (0.09) (carbohydrate), salicin (miscellaneous) (0.08) and palatinose (carbohydrate) (0.07).

The fungus *S. kiliense* showed the highest OD values for the carbon sources glycerol (miscellaneous) (OD 2.11), N-acetyl-D-glucosamine (carbohydrate) (OD 2.07) and α-D-Glucose-1-Phosphate (carbohydrate) (OD 2.04) (File 1-S1). The substrate types showing the lowest fungal growth by this species were D-melezitose (carbohydrate) (0.24), turanose (carbohydrate) (0.22) and D-psicose (carbohydrate) (0.18).

In comparison, the three substrates showing the highest growth of *R. sphaerocarpa* were L-lactic acid (carboxylic acid) (OD 1.02) followed by D-galacturonic acid (carboxylic acid) (OD 0.9) and D-cellobiose (carbohydrate) (OD 0.84) (File 1-S1). The substrates with the lowest growth were amygdalin (miscellaneous) (OD 0.12) followed by lactulose (carbohydrate), D-fructose (carbohydrate), maltose (carbohydrate), D-arabitol and D-tagatose (carbohydrates), all with an OD of 0.14. The overall growth of *Rhodotorula sphaerocarpa* on the different substrates was lower than compared to the two other species; however, it could use all the provided carbon source for its growth. Furthermore, it also preferred more complex carboxylic acids for its growth compared to more simple carbohydrates which were favoured by the other two species.

In this study we found a similar metabolic pattern between the three investigated species with highest fungal growth related mostly to carbohydrate-based substrates. Similar results were reported before (*25*), in which a saline-alkaline-tolerant fungal species was shown to metabolize more simple carbon sources. Although, at this point, research on the specific carbon substrate preferences of oceanic fungi is limited, these results give first implications about potential ecological niches in the cycling of certain carbon sources in planktonic food webs.

3.4.2. Absorption at 490 nm (Fungal Respiration)

In general, we found a tendency for the preferred utilization of amino acids (AC) followed by carboxylic acids (CA), carbohydrates (CB) and other carbon compounds (OT) whereas polymers (PY) were preferred the least (Fig. 1-6). Significant differences between the preferred utilization of amino acids, carboxylic acids and ‘other’ carbon compounds over polymers were found for *R. sphaerocarpa* (Fig. 1-6). Additionally, significant differences between the utilization of amino acids and polymers were found in *S. kiliense* and between ‘other’ carbon compounds and polymers in *S. spartinae* (Fig. 1-6). This points out that more complex compounds might take more time to metabolize compared to simple carbon substrates which are being utilized faster within the first four days of incubation. Additionally, these results are similar to those reported by Nishida *et al.* (*42*), who found that amino acids are a substantive nutritional source for fungi in general. Moreover, an experiment conducted by Shi

et al. (*43*) proved that the metabolic activity of *S. spartinae* can be enhanced by adding amino acids to the growth media.

A high variation in the consumption of carboxylic acid-compounds was found for *S. spartinae* (OD 0.93 ± 0.55) and *R. sphaerocarpa* (OD 0.66 ± 0.58) (Fig. 1-6). However, compared to the two other species, *S. kiliense* showed on average the highest total mitochondrial activity for oxidizing carboxylic acids (OD 1.47 ± 0.46) (Fig. 1-6). This is in line with a study by Fiebig (*44*), in which it was shown that aquatic fungi utilized carboxylic acids to a big extent from labile components of DOM (dissolved organic matter) and hence within the first days of incubation.

Furthermore, the results of the study indicated that *S. kiliense* had the highest metabolic activity for the utilization of carbohydrates (CB), with an average OD value of 1.75 ± 0.52. In comparison, *S. spartinae* had an average OD value of 0.51 ± 0.33 and *R. sphaerocarpa* had an average OD value of 0.5 ± 0.42 (Fig. 1-6). Similar results were shown in a previous study where species of *Sarocladium* efficiently degraded carbohydrates such as polysaccharides, pectin, and precisely *S. kiliense* exhibited high degradation rates of starch (*25*).

The substrate category of 'others' contained alcohols, nucleotides, nucleosides, amines and amides. Again, *S. kiliense* exhibited the highest metabolic activity of these substrates with an OD of 1.58 ± 0.30 (Fig. 1-6). In contrast, *S. spartinae* had an OD of 0.36 ± 0.51 and *R. sphaerocarpa* of 0.50 ± 0.42.

Lastly, in the group of polymers (PY), the metabolic activities of all species compared to the other compounds were lowest (*S. kiliense*: OD 0.94 ± 0.53; *S. spartinae*: OD 0.33 ± 0.2; *R. sphaerocarpa*: OD 0.2 ± 0.19), indicating that polymers are not oxidized to the same extent as the other substrates within the first 4 days of incubation.

Additionally, detailed analysis of the utilization of individual carbon substrates, indicated that although *S. kiliense* exhibited a higher respiratory activity compared to the two other species, there was no general pattern towards the preference of specific carbon compounds (Fig. 1-7). Instead, each of the three fungal isolates exhibited species-specific utilization patterns (Fig. 1-7), emphasizing the vast metabolic potential of oceanic fungi to degrade different carbon substrates.

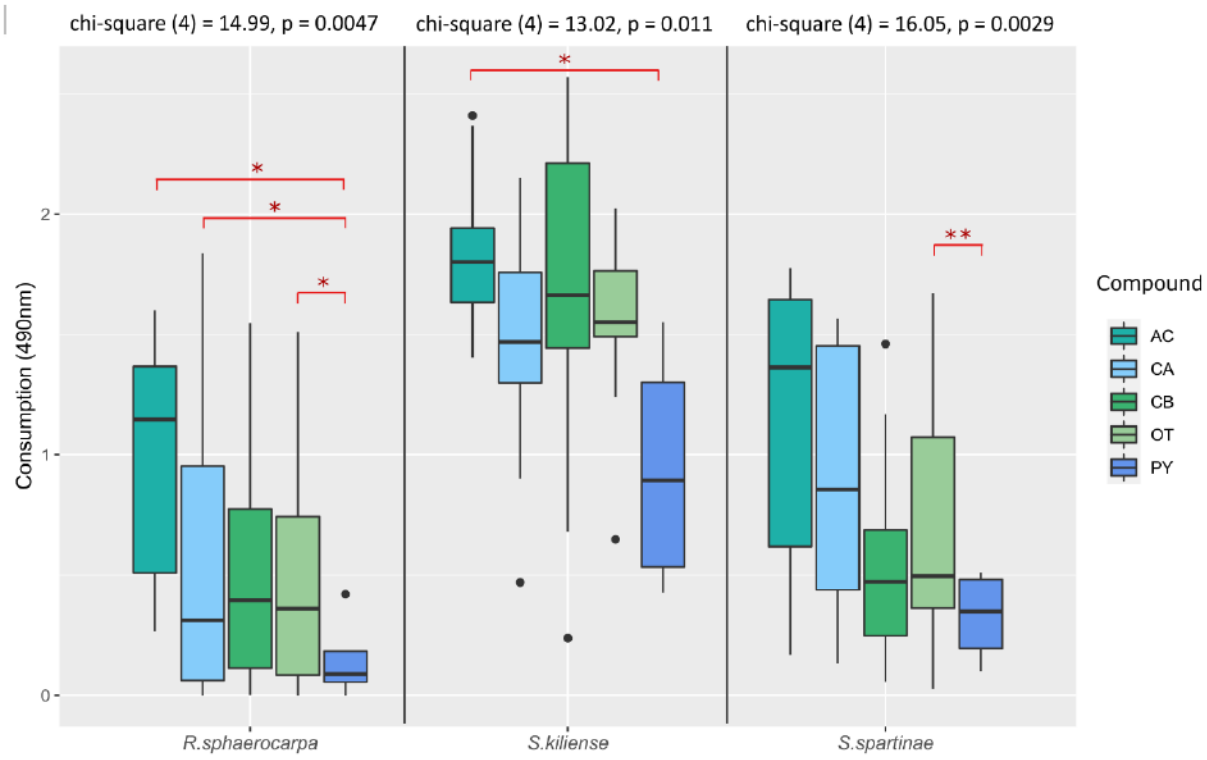

Figure 1-6. Utilization of different carbon compound groups by *Rhodotorula sphaerocarpa, Sarocladium kiliense* and *Scheffersomyces spartinae* cultures measured as absorption (OD) at a wavelength of 490 nm indicative of fungal respiration. The carbon compound groups are: AC- amino acids, CA- carboxylic acids, CB- carbohydrates, OT- others, PY- polymers. On top of each species-plot are the resulting statistics calculated with the Kruskal–Wallis test. The significance levels within each species-plot were calculated with pairwise Wilcoxon test and the p-value adjusted with Bonferroni correction (* p-value <0.05, ** p-value <0.01, dots represent outliers).

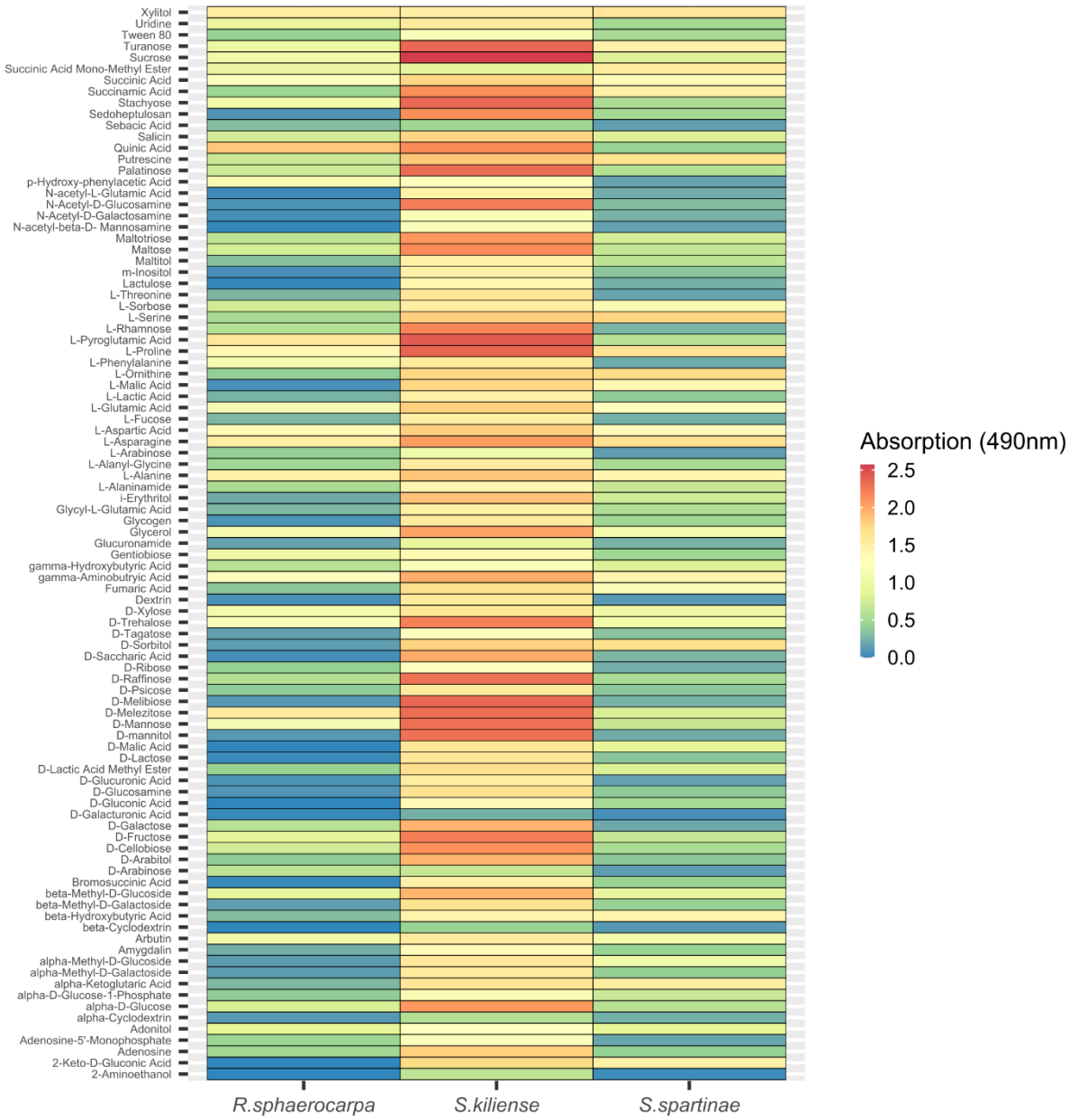

Figure 1-7. Utilization of 95 different carbon sources by *Rhodotorula sphaerocarpa*, *Sarocladium kiliense* and *Scheffersomyces spartinae* cultures measured as absorption (OD) at a wavelength of 490 nm indicative of fungal respiration.

4. Conclusions

We isolated and characterized three pelagic fungal strains from the open Atlantic Ocean belonging to three different species. Despite being phylogenetically diverse, we observed shared physiological characteristics among all of the species. Specifically, we found that all of the isolated cultures displayed their highest total biomass values during the stationary phase at 23 °C, which is the temperature closest to the in situ conditions, when compared to other

temperatures that were investigated. Yet, all species were able to grow successfully at elevated temperature (35 °C), which is especially relevant in future ocean warming scenarios. In spite of contrasting conditions at reduced temperature, two of the three species still achieved similar final biomass concentrations as in the warmest conditions tested. This suggests that these species have the potential to adapt to temperature changes in a range of 30 °C. Clearly, these results are species specific but suggest that changes in temperature through climate change could potentially have unpredictable impacts on marine fungal communities.

Furthermore, the studied species seem to be very tolerant regarding the salinity concentration of their growth medium (much wider than the salinity range generally observed in the open ocean waters), indicating a remarkable capability for pelagic oceanic fungi to thrive in a vast range of salinities. Nevertheless, *S. spartinae* and *R. sphaerocarpa* had the highest growth yields in the medium with a concentration of 35 g/l sea salts, which is closest to their in situ oceanic conditions.

The investigations at 750 nm of the FF-plates (indicative of fungal growth) showed that all fungal species showed highest growth on specific carbohydrates or carboxylic acids, which could be expected since simple and labile compounds are usually promptly degraded more easily. Similar results were found at 490 nm (indicative of fungal respiration) but in general, depending on species, substrate groups containing amino acids and carbohydrates displayed the highest metabolic activity across all the species. However, our results indicate that *S. kiliense* showed higher oxidation rates of all tested compound groups, which suggests potential differences in nutrient cycling among pelagic species.

As mentioned above, marine fungi are active players in the oceanic elemental cycles. However, our knowledge on the specific roles played by individual fungal species in the ocean is very limited. Hence, it becomes a relevant task to investigate species-specific physiological characteristics and capabilities of marine pelagic fungi to better understand the role of the individual fungal members, populations, and communities in the marine ecosystem. Research such as this is valuable for gaining insight into the physiological characteristics of marine fungi and can help enhance our understanding of their ecology and distribution in the oceanic water column.

Acknowledgements

Funding: F.B. was supported by the Austrian Science Fund (FWF) projects OCEANIDES (P34304-B), ENIGMA (TAI534), EXEBIO (P35248), and OCEANBIOPLAST (P35619-B). We thank the reviewers for the constructive comments that improved the quality of the paper.

Author Contributions

Conceptualization, E.B. and F.B.; Methodology, E.B., S.E.-H., M.R., S.C.K. and F.B.; Supervision, F.B.; Writing—original draft, E.B., M.R. and F.B.; Writing—review and editing, E.B., S.E.-H., S.C.K. and F.B.

References

1. H.-P. Grossart *et al.*, Fungi in aquatic ecosystems. *Nat. Rev. Microbiol.* **17**, 339-354 (2019).
2. W. d. Boer, L. B. Folman, R. C. Summerbell, L. Boddy, Living in a fungal world: impact of fungi on soil bacterial niche development. *FEMS Microbiol. Rev.* **29**, 795-811 (2005).
3. M. L. Berbee, T. Y. James, C. Strullu-Derrien, Early Diverging Fungi: Diversity and Impact at the Dawn of Terrestrial Life. *Annu. Rev. Microbiol.* **71**, 41-60 (2017).
4. M. Kagami, A. de Bruin, B. W. Ibelings, E. Van Donk, Parasitic chytrids: their effects on phytoplankton communities and food-web dynamics. *Hydrobiologia* **578**, 113-129 (2007).
5. C. Wurzbacher, S. Rösel, A. Rychła, H.-P. Grossart, Importance of Saprotrophic Freshwater Fungi for Pollen Degradation. *PLOS ONE* **9**, e94643 (2014).
6. G. Barone *et al.*, Benthic deep-sea fungi in submarine canyons of the Mediterranean Sea. *Prog. Oceanogr.* **168**, 57-64 (2018).
7. J. M. Bernhard *et al.*, Benthic protists and fungi of Mediterranean deep hypersaline anoxic basin redoxcline sediments. *Front. Microbiol.* **5**, (2014).
8. A. Amend *et al.*, Fungi in the Marine Environment: Open Questions and Unsolved Problems. *MBio* **10**, e01189-01118 (2019).
9. T. A. Richards, M. D. Jones, G. Leonard, D. Bass, Marine fungi: their ecology and molecular diversity. *Annu. Rev. Mar. Sci.* **4**, 495-522 (2012).
10. S. E. Morales, A. Biswas, G. J. Herndl, F. Baltar, Global structuring of phylogenetic and functional diversity of pelagic fungi by depth and temperature. *Front. Mar. Sci.* **6**, 131 (2019).
11. T. L. Calvez, G. Burgaud, S. Mahé, G. Barbier, P. Vandenkoornhuyse, Fungal Diversity in Deep-Sea Hydrothermal Ecosystems. *Appl. Environ. Microbiol.* **75**, 6415-6421 (2009).
12. B. T. Hassett *et al.*, Arctic marine fungi: biomass, functional genes, and putative ecological roles. *ISME J.* **13**, 1484-1496 (2019).
13. E. Zeghal, A. Vaksmaa, H. Vielfaure, T. Boekhout, H. Niemann, The Potential Role of Marine Fungi in Plastic Degradation – A Review. *Front. Mar. Sci.* **8**, (2021).
14. M. Cunliffe, A. Hollingsworth, C. Bain, V. Sharma, J. D. Taylor, Algal polysaccharide utilisation by saprotrophic planktonic marine fungi. *Fungal Ecol.* **30**, 135-138 (2017).

15. B. Scholz, F. C. Küpper, W. Vyverman, U. Karsten, Eukaryotic pathogens (Chytridiomycota and Oomycota) infecting marine microphytobenthic diatoms – a methodological comparison. *J. Phycol.* **50**, 1009-1019 (2014).
16. B. Hassett, R. Gradinger, Chytrids Dominate Arctic Marine Fungal Communities. *Environ. Microbiol.* **18**, 2001-2009 (2016).
17. J. D. Taylor, M. Cunliffe, Multi-year assessment of coastal planktonic fungi reveals environmental drivers of diversity and abundance. *ISME J.* **10**, 2118 (2016).
18. A. B. Bochdansky, M. A. Clouse, G. J. Herndl, Eukaryotic microbes, principally fungi and labyrinthulomycetes, dominate biomass on bathypelagic marine snow. *ISME J.* **11**, 362-373 (2017).
19. F. Baltar, Z. Zhao, G. J. Herndl, Potential and expression of carbohydrate utilization by marine fungi in the global ocean. *Microbiome* **9**, 1-10 (2021).
20. E. Breyer, Z. Zhao, G. J. Herndl, F. Baltar, Global contribution of pelagic fungi to protein degradation in the ocean. *Microbiome* **10**, 1-11 (2022).
21. M. Wang *et al.*, Metatranscriptomics and metabarcoding reveal spatiotemporal shifts in fungal communities and their activities in Chinese coastal waters. *Mol. Ecol.* **00**, 1-16 (2023).
22. E. G. Jones *et al.*, An online resource for marine fungi. *Fungal Divers.* **96**, 347-433 (2019).
23. N. N. Wijayawardene *et al.*, Ecological and Oceanographic Perspectives in Future Marine Fungal Taxonomy. *J. Fungi* **8**, 1141 (2022).
24. M. Ryberg, R. H. Nilsson, New light on names and naming of dark taxa. *MycoKeys*, 31-39 (2018).
25. C. Wang, W.-Y. Zhuang, Carbon metabolic profiling of Trichoderma strains provides insight into potential ecological niches. *Mycologia* **112**, 213-223 (2020).
26. H. Wickham, *ggplot2: elegant graphics for data analysis*. (Springer Science & Business Media, 2016).
27. A. Kassambara, Rstatix: Pipe-Friendly Framework for Basic Statistical Tests*, R package vers,* 0.7.2. (2023).
28. C. P. Kurtzman, M. Suzuki, in *The Yeasts: A Taxonomic Study*. (Elsevier, Amsterdam, The Netherlands, 2011), vol. 1, pp. 773-778.
29. C. P. Kurtzman, M. Suzuki, Phylogenetic analysis of ascomycete yeasts that form coenzyme Q-9 and the proposal of the new genera Babjeviella, Meyerozyma, Millerozyma, Priceomyces, and Scheffersomyces. *Mycoscience* **51**, 2-14 (2010).

30. X. Zou *et al.*, Yeasts from intertidal zone marine sediment demonstrate antagonistic activities against Botrytis cinerea in vitro and in strawberry fruit. *Biol. Control* **158**, 104612 (2021).
31. P. Satianpakiranakorn, P. Khunnamwong, S. Limtong, Yeast communities of secondary peat swamp forests in Thailand and their antagonistic activities against fungal pathogens cause of plant and postharvest fruit diseases. *PLOS ONE* **15**, e0230269 (2020).
32. F. Fernández-Silva, J. Capilla, E. Mayayo, D. Sutton, J. Guarro, In Vitro Evaluation of Antifungal Drug Combinations against Sarocladium (Acremonium) kiliense, an Opportunistic Emergent Fungus Resistant to Antifungal Therapies. *Antimicrob. Agents Chemother.* **58**, 1259-1260 (2014).
33. S. Bondarenko, M. Georgieva, L. Y. Kokaeva, E. Bilanenko, The first discovery of alkali-resistant fungi on the coast of chloride lake baskunchak. *Mosc. Univ. Biol. Sci. Bull.* **74**, 57-62 (2019).
34. S.-Q. Fan *et al.*, Sarocladione, a unique 5, 10: 8, 9-diseco-steroid from the deep-sea-derived fungus Sarocladium kiliense. *Org. Biomol. Chem.* **17**, 5925-5928 (2019).
35. C. L. Văcar *et al.*, Heavy metal-resistant filamentous fungi as potential mercury bioremediators. *J. Fungi* **7**, 386 (2021).
36. P. Hoondee *et al.*, Occurrence of oleaginous yeast from mangrove forest in Thailand. *World J. Microbiol. Biotechnol.* **35**, 1-17 (2019).
37. J. Zajc, P. Zalar, N. Gunde-Cimerman, in *Yeasts in Natural Ecosystems: Diversity*. (Springer, Berlin/Heidelberg, Germany, 2017), pp. 293-329.
38. T. Nagahama, in *Biodiversity and Ecophysiology of Yeasts*. (Springer, Berlin/Heidelberg, Germany, 2006), pp. 241-262.
39. C. K. Campbell, E. M. Johnson, D. W. Warnoch, *Identification of Pathogenic Fungi*. (Wiley-Blackwell, 2013).
40. M. D. Frigon, D. Liu, Effect of high salinity on yeast activated sludge reactor operation. *J. Water Sci. Technol.* **74**, 2124-2134 (2016).
41. E. G. Jones *et al.*, How do fungi survive in the sea and respond to climate change? *J. Fungi* **8**, 291 (2022).
42. I. Nishida *et al.*, Vacuolar amino acid transporters upregulated by exogenous proline and involved in cellular localization of proline in Saccharomyces cerevisiae. *J. Gen. Appl. Microbiol.* **62**, 132-139 (2016).

43. Y. Shi *et al.*, Recent advances in the biodegradation of azo dyes. *World J. Microbiol. Biotechnol.* **37**, 1-18 (2021).
44. D. M. Fiebig, in *Sediment/Water Interactions*. (Springer, Berlin/Heidelberg, Germany, 1992), pp. 311-319.

Chapter 2: Global contribution of pelagic fungi to protein degradation in the ocean

Eva Breyer[1*#], Zihao Zhao[1*#], Gerhard J. Herndl[1,2,3], Federico Baltar[1*]

[1] Department of Functional and Evolutionary Ecology, University of Vienna, Djerassiplatz 1, 1030 Vienna, Austria

[2] NIOZ, Department of Marine Microbiology and Biogeochemistry, Royal Netherlands Institute for Sea Research, Utrecht University, AB Den Burg, The Netherlands

[3] Vienna Metabolomics Center, University of Vienna, Althanstraße 14, A-1090 Vienna, Austria

* Correspondence: eva.breyer@univie.ac.at, zihao.zhao@univie.ac.at, federico.baltar@univie.ac.at

[#] Shared first co-authorship

Published in *Microbiome*

Abstract

Fungi are important degraders of organic matter responsible for re-integration of nutrients into global food chains in freshwater and soil environments. Recent evidence suggests that they are ubiquitously present in the oceanic water column where they play an active role in the degradation of carbohydrates. However, their role in processing other abundant biomolecules in the ocean in comparison to that of prokaryotes remains enigmatic. Here**,** we performed a global-ocean multi-omics analysis of all fungal affiliated peptidases (main enzymes responsible for cleaving proteins), which constitute the major fraction (>50%) of marine living and detrital biomass. We determined the abundance, expression, diversity, taxonomic affiliation and functional classification of the genes encoding all pelagic fungal peptidases from the epi- and mesopelagic layers. We found that pelagic fungi are active contributors to protein degradation and nitrogen-cycling in the global ocean. Dothideomycetes are the main fungi responsible for protease activity in the surface layers, whereas Leotiomycetes dominate in the mesopelagic realm. Gene abundance, diversity and expression increased with increasing depth, similar to fungal CAZymes. This contrasts with the total occurrence of prokaryotic peptidases and CAZymes which are more uniformly distributed in the oceanic water column, suggesting potentially different ecological niches of fungi and prokaryotes. In-depth analysis of the most widely expressed fungal protease revealed the potentially dominating role of saprotrophic nutrition in the oceans. Our findings expand the current knowledge on the role of oceanic fungi in the carbon cycle (carbohydrates) to the so far unknown global participation in nitrogen (proteins) degradation, highlighting potentially different ecological niches occupied by fungi and prokaryotes in the global ocean.

Keywords: Pelagic fungi, proteases, metagenomics, metatranscriptomics, global ocean, nitrogen cycle

1. Introduction

Microbes make up around 70% of the total marine biomass (*1*) and are involved in complex functional and phylogenetic networks with all three organismal domains of life and viruses (*2*). They harbor a set of genes responsible for driving major redox-reactions that are crucial for controlling the remineralization of organic material (*3*). Most of the research on the role of microbes in the oceanic nutrient cycling has focused on prokaryotes. Little is known on the role of pelagic fungi in the cycling of organic matter in the ocean despite fungi being recognized as key elements in remineralizing nutrients and degrading organic matter in the terrestrial and freshwater environment (*4*). However, recent studies revealed that pelagic fungi were found to dominate the microbial biomass in deep-sea marine snow (*5*) and exhibited biomass concentrations similar to that of prokaryotes during phytoplankton blooms (*6*). Moreover, by infecting inedible phytoplankton, parasitic fungi are suggested to act as trophic bridge via the fungal shunt by producing zoospores that are consumed by zooplankton, a process defined as the 'mycoloop' (*7-9*).

Recent evidence also indicates that pelagic fungi play a potentially important role in the marine carbon cycle (*10-12*). A global-ocean scale multi-omics study reported a widespread and active role of fungi in degrading carbohydrates by studying the diversity and expression of carbohydrate-active enzymes (CAZymes) phylogenetically affiliated to fungi (*12*). These authors found that the abundance and diversity of total and secretory fungal CAZymes increased with increasing depth, which contrasts the rather constant depth distribution of the abundance and diversity of prokaryotic CAZymes (*13*). This might indicate differential ecological niches and roles of pelagic fungi and prokaryotes in the degradation of carbohydrates in the ocean (*12*). Nevertheless, although carbohydrates are major components of macromolecules in marine organisms (ca. 10%), proteins constitute the major fraction (> 50%) of the organic matter making up marine planktonic cells (*14*)**.**

Thus, to obtain a more complete understanding of the role of pelagic fungi in the remineralization of organic matter, we performed a systematic investigation of the role of oceanic pelagic fungi in the degradation of proteins. We analyzed global metagenomic and metatranscriptomic data covering all major oceanic basins to reveal fungal peptidase activity in the epi- and mesopelagic waters. Also, the fungal taxa and peptidase classes responsible for protein degradation were determined. Based on the expression of CAZymes related to fungi, we hypothesized that fungi are also major contributors to the degradation of proteins in the oceanic water column. Moreover, we hypothesized that the same organisms dominating the expression of CAZymes might also dominate the expression of proteases. Finally, we

hypothesized to find evidence of shared and distinct traits involved in the degradation of organic matter between pelagic fungi and prokaryotes. Our detailed analyses of fungal proteases allowed us to infer potential lifestyle strategies of oceanic mycoplankton. Also, the comparison of our results to recent similar efforts to characterize the global distribution of fungal affiliated CAZymes (*12*), and of prokaryotic affiliated CAZymes and proteases (*13*) allowed us to decipher potential similarities and differences in the role of fungi *versus* prokaryotes in the degradation of carbohydrates and proteins.

2. Material and Methods

The sequences and occurrences in the corresponding metagenomes and metatranscriptomes of marine eukaryotic genes were downloaded from literature (*15*). For the metagenomics data, the accession number is PRJEB4352, for the metatranscriptomics data PRJEB6609. Gene occurrence in the metagenomic and metatranscriptomic dataset is available at http://www.genoscope.cns.fr/tara/ 'Tara Oceans Eukaryote Gene Catalog'. Environmental parameters were downloaded from the original paper (Carradec *et al. (15)*). A Mantel test was performed between fungal peptidase beta-diversity and environmental parameters to test the driving factors shaping fungal peptidase in marine environments. We used the presence of signal peptides as a proxy for secretory peptidase because signal peptides are short amino acid sequences in the amino terminus of proteins that direct proteins into or across membranes. Thus, the peptidase encoding genes containing signal peptide sequences can be probably translocated from the cytoplasmic to the periplasmic space as cell-associated extracellular enzymes 'in contact to the outside' or transported to the outside of the cell as cell-free extracellular enzymes.

To identify peptidase-like sequences, the 116 million eukaryotic genes were first compared against the MEROPS database (*16*) (https://www.ebi.ac.uk/merops/) using DIAMOND version.0.8.36 blast (*17*) (e-value < 1×10^{-20}). Sequences with positive hits were extracted for taxonomic identification using the lowest common ancestor algorithm adapted from DIAMOND v.0.8.36 (*17*) blast by searching against the NCBI non-redundant (NR, downloaded in March 2020) database. The top 10% hits with an e-value < 1×10^{-5} were used for taxonomic affiliation assessment (--top 10). The functional annotations at the peptidase family level were further grouped into peptidase class level according to the common designations in the MEROPS database. SignalP (*18*) (5.0) was used to detect the presence of signal peptides for fungal sequences under the eukaryotic mode. Size fractions were defined as

micro-mycobiome for samples from 0.8-5 µm (0.8-3 µm was used for samples from the mesopelagic waters as it was the only available range) and macro-mycobiome for samples from 5-2,000 µm (3-2,000 µm was used for samples from mesopelagic waters), consistent to our recent study on fungal CAZymes (*12*). Data analysis was performed using R (R version 3.6.1, www.R-project.com). *Vegan* (*19*), *rtk* (*20*) and *ggplot2* (*21*) were used for ordination, diversity calculation and visualization, respectively.

3. Results and Discussion

3.1. Occurrence, secretory capacity and α-diversity of fungal peptidases genes and transcripts in the global ocean

We examined the occurrence, diversity, functional classification, taxonomic affiliation and metabolic expression of genes encoding proteases from 445 metagenomes and 440 metatranscriptomes from 68 Tara stations of size fractions ranging from 0.8-2,000 µm, covering the epipelagic (0-200m) and mesopelagic (200-1000m) waters (see Methods). Of the 116 million non-redundant sequences of global ocean eukaryotic genes, 815,841 eukaryotic proteases sequences were retrieved. Fungi-affiliated sequences contributed 1.05% (8,637 out of 815,841) to these eukaryotic protease sequences. The abundance of fungal protease sequences ranges from 1 to 3952 in the metagenomes and from 4 to 5601 in the metatranscriptomes. Ascomycota (1 to 3681 in the metagenome, 1 to 5058 in the metatranscriptome) and Basidiomycota (1 to 269 in the metagenome, 1 to 528 in the metatranscriptome) affiliated sequences showed highest count in both metagenomics and metatranscriptomic datasets, and sequences were prodominatedly assigned to serine peptidase (1 to 1789 in the metagenome, 1 to 1083 in the metatranscriptome) and metallo peptidase (1 to 1538 in the metagenome, 1 to 2393 in the metatranscriptome). The occurrence and expression values of all eukaryotic sequences in the metagenomic and metatranscriptomic dataset were download from http://www.genoscope.cns.fr/tara/, and fungal related values used in this analysis is subtracted and supplied as supplementary material (Dataset 2-S1).

The analysis of metagenomic (MetaG) and metatranscriptomic (MetaT) data of fungal peptidases using principal coordinate analysis (PCoA) revealed that oceanic fungal communities clustered by water column depths into epipelagic (SRF, surface; MXL, mixed layer; DCM, deep chlorophyll maximum) and mesopelagic (MES) (Fig. 2-S1). In contrast, size fractionation between micro-mycobiome (0.8-5 µm) and macro-mycobiome (5-2000 µm) exhibited no clear differentiation (Fig. 2-S1). These results for pelagic fungal proteases (in both

MetaG and MetaT datasets) are consistent with the patterns observed for fungal CAZymes, which exhibited a depth-dependent clustering but no clustering based on size (*12*). A Mantel test between pelagic fungal peptidase profiles and environmental parameters showed that the fungal peptidases from the micro-fraction were significantly related to chlorophyll, phosphorus and nitrogen at the metagenomics level but not to any environmental parameters at the metatranscriptomic level (Fig. 2-S1). Analysis of the macro-fraction affiliated fungal peptidases revealed that on the metagenome level fungal peptidases were significantly related to temperature, oxygen, net primary production and iron, whereas on the metatranscriptomic level, fungal peptidases were related to phosphorus, nitrogen and iron. This suggests that pelagic fungal proteases are controlled by nutrients (particularly iron, phosphorus and nitrogen) and organic matter availability (as indicated by net primary production and chlorophyll). Similar links between nutrients and organic matter availability were reported for pelagic fungal CAZyme genes and transcripts (*12*). In contrast, the potential and expression of both peptidases and CAZymes affiliated to oceanic prokaryotes were linked to temperature, salinity and oxygen (*13*). This suggests that the cleaving of protein-rich substrates by pelagic fungi and prokaryotes are governed by different ecological factors as recently suggested for carbohydrates (*12*).

The ratio of transcripts to genes of both, total (i.e., cytosol and secreted) and secretory peptidases was generally equal or higher than 1 throughout the water column, suggesting an active expression and secretion of fungal peptidases in the epi- and mesopelagic realm and thus, an active participation in oceanic protein degradation (Fig. 2-1A, B). Interestingly, the fungal proteases (abundance and expression) were strongly related to the fungal CAZymes (Fig. 2-2). This indicates a close coupling between the degradation of carbohydrates and proteins by pelagic fungi in the oceanic water column. The abundance of both total and secretory peptidase genes and transcripts (and the percentage of secretory) was higher in the mesopelagic than in the upper water layers (SRF, MXL, DCM) (Fig. 2-1A and B). The α-diversity of fungal protease genes and transcripts was also generally higher in the mesopelagic, with a slightly higher diversity in the micro-fraction (Fig. 2-1C). This increase with depth in total and secretory fungal proteases, their diversity and expression was also observed for fungal CAZymes (*12*), again confirming the close linkage between the carbon and nitrogen cycling also in deep waters. Only secretory (but not total) prokaryotic proteases and CAZymes increase with water column depth (*13*), confirming the greater importance of secreted enzymes (both cell-associated and cell-free ones) in the degradation of organic matter with depth observed from both rate measurement (*22, 23*) and genomic approaches (*13*). These results also imply

that this increase with depth of secretory enzymes is a universal phenomenon for heterotrophs like heterotrophic bacteria and fungi in the ocean.

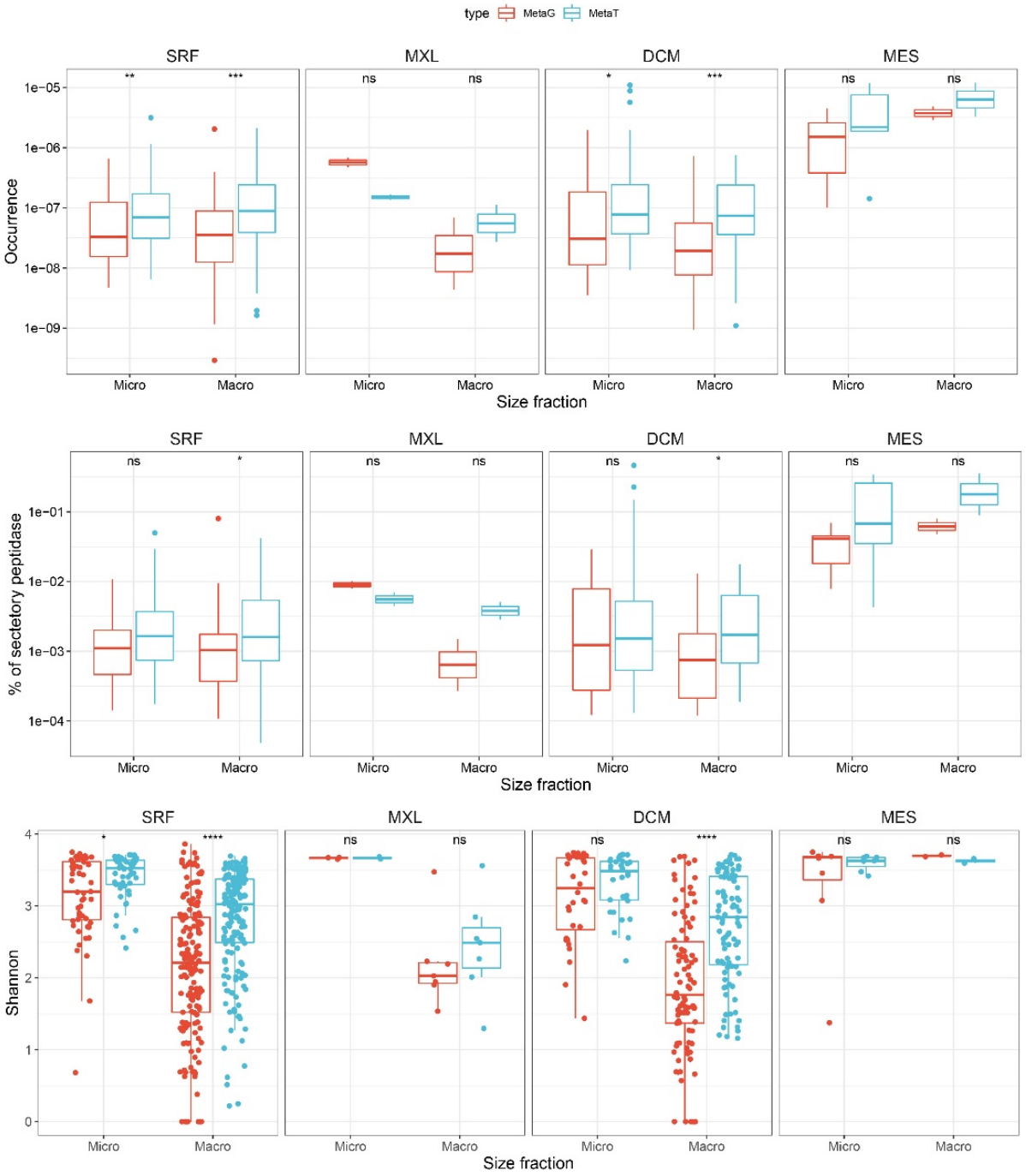

Figure 2-1. Occurrence (A), secretory capacity (B) and α-diversity (C) of genes and transcripts for fungal Peptidases. Micro, micro-mycobiome (0.8-5 μm); Macro, macro-mycobiome (5-2000 μm). Box shows median and interquartile range (IQR); whiskers show 1.5 × IQR of the lower and upper quartiles or range; outliers extend to the data range. Statistics are based on

Wilcoxon test, *P<0.05, **P<0.01, ***P<0.001, ****P<0.0001, ns, not significant. SRF, surface; MXL, mixed layer; DCM, deep chlorophyll maximum; MES, mesopelagic.

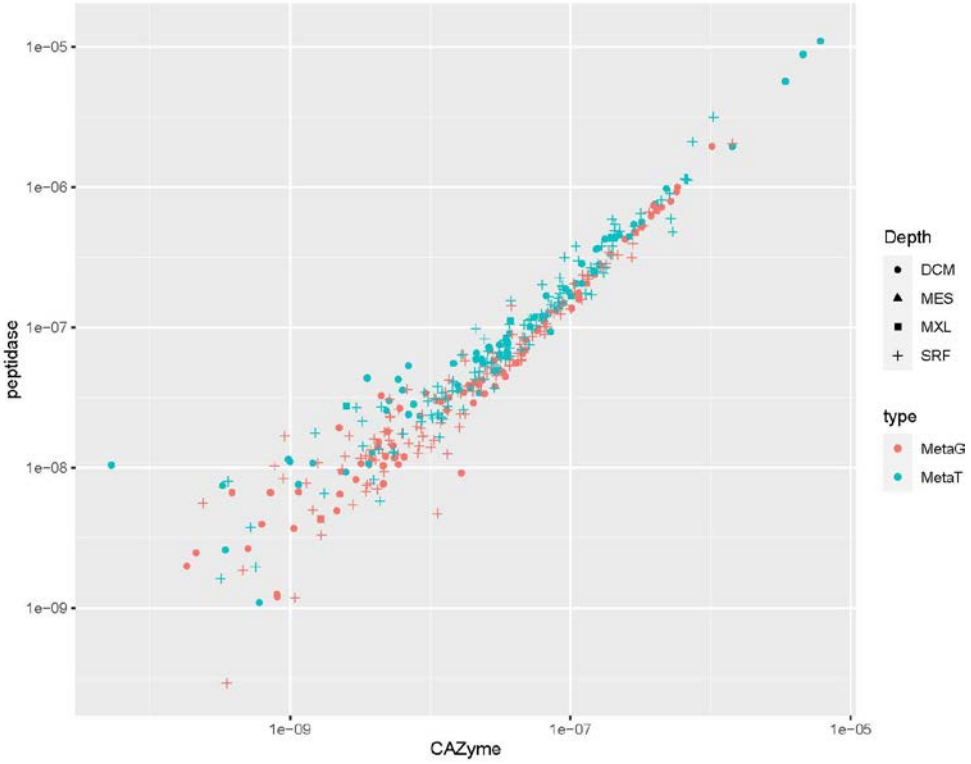

Figure 2-2. Correlation between fungal proteases genes and transcripts (from this study) with fungal CAZymes (from Zhao et al. 2020) in the global ocean epi- and mesopelagic waters. SRF, surface; MXL, mixed layer; DCM, deep chlorophyll maximum; MES, mesopelagic; MetaG, metagenomic; MetaT, metatranscriptomic.

3.2. Phylogenetic affiliation of genes and transcripts encoding fungal peptidases in the global ocean

To reveal the main responsible fungal divisions for total (cytoplasmic and secreted) fungal peptidase activity, we analyzed the taxonomic affiliation of genes and transcripts. The genomic potential and expression patterns were similar, with Ascomycota dominating in most ocean basins and depths (Fig. 2-S2). The relative abundance of peptidase genes and transcripts affiliated to Basidiomycota was higher in the Mediterranean Sea, the Indian Ocean and the Southern Ocean than in the Pacific and Atlantic. On the contrary, the mesopelagic realm was dominated by Ascomycota. Mucoromycota and Chytridiomycota played a minor role in the overall abundance of fungal proteases and transcripts. The micro- and macro-mycobiome were dominated by proteases affiliated to the same phyla. Only Mucoromycota contributed slightly

to fungal proteases in surface waters of the macro-size fraction in the South Pacific. These results are in accordance with the dominant phyla found to be responsible for the global expression of glucoside hydrolases (GH) (*11*) and of all CAZyme families (*12*) in pelagic fungi. Furthermore, our findings are consistent with a metagenomic study investigating the global phylogenetic and functional diversity of epi- and mesopelagic fungi (*10*). This implies that the major part of the CAZyme and protease activity and therefore, the degradation of proteins and carbohydrates by mycoplankton in the oceans, is dominated by only two phyla (Ascomycota and Basidiomycota). Other phyla like Chytridiomycota, however, might become sporadically abundant and important by responding to phytoplankton bloom events (*6, 24*). To gain deeper insights into the taxonomic affiliation of pelagic fungal proteases, we analyzed total (cytoplasmic and secreted) fungal peptidase genes and transcripts on fungal class level. Our results revealed that Dothideomycetes dominated the fungal protease pool in the surface layers and Leotiomycetes and Eurotiomycetes in the deep (Fig. 2-3). These classes were also found to dominate the abundance and expression of fungal CAZymes in the water column (*12*). In contrast to the fungal CAZymes dynamics (*12*), some pronounced geographical fluctuations were found in the relative abundance of classes affiliated to fungal proteases, such as a relative increase in the contribution of Eurotiomycetes of the micro-fraction of the North Atlantic Ocean and in the North Pacific Ocean and of Malasseziomycota in the Mediterranean Sea. Interestingly, although the same classes dominated the abundance and expression of proteases and CAZymes in the water column, the diversity of fungal classes affiliated to the peptidases genes and transcripts was higher than for fungal CAZymes (*12*). In summary, fungal proteases abundance and expression in all ocean basins and depths are dominated by the same fungal classes (Dothideomycetes in the surface and Leotiomycetes and Eurotiomycetes in the deep) thus, representing major players in the fungal enzymatic cleavage of proteins and carbohydrates in the ocean.

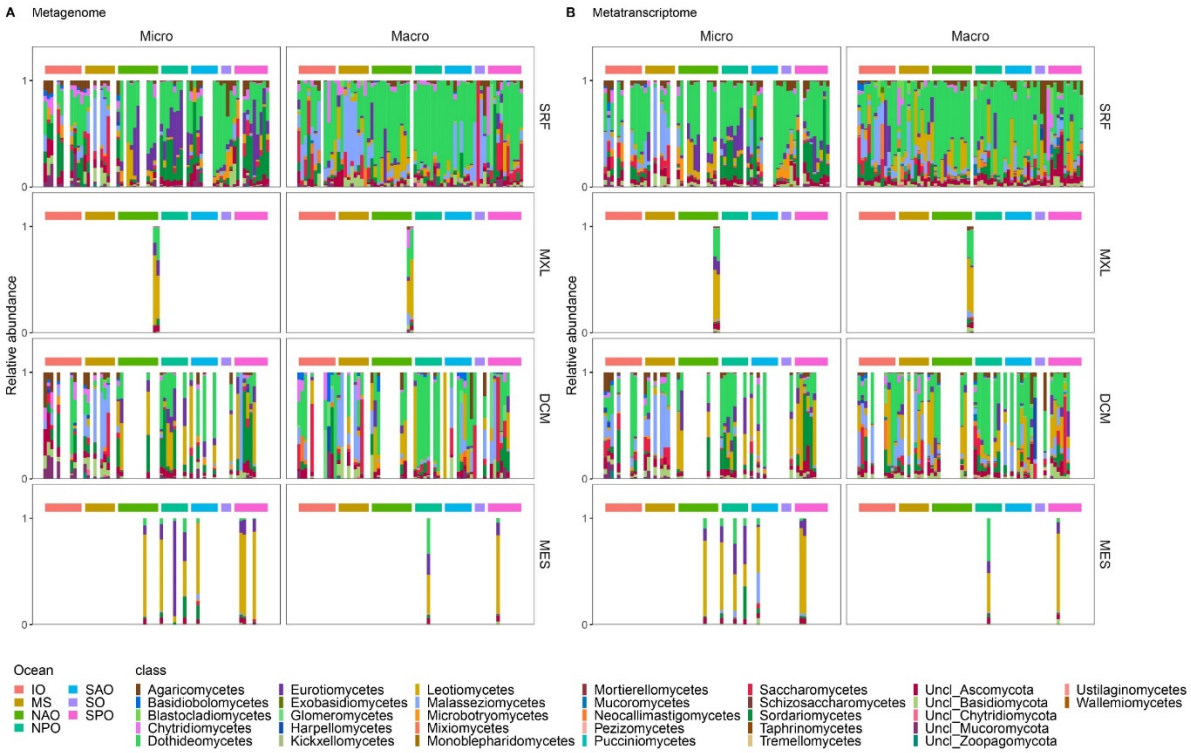

Figure 2-3. Phylogenetic affiliation of gene (A) and transcript (B) encoding fugal Peptidases at class level. Micro, micro-mycobiome (0.8-5 µm); Macro, macro-mycobiome (5-2000 µm). SRF, surface; MXL, mixed layer; DCM, deep chlorophyll maximum; MES, mesopelagic; IO, Indian Ocean; MS, Mediterranean Sea; NAO, North Atlantic Ocean; North Pacific Ocean; SAO, South Atlantic Ocean; SO, Southern Ocean; SPO, South Pacific Ocean.

3.3. Functional classification of genes and transcripts encoding fungal peptidases in the global ocean

To decipher the functional roles of fungal peptidases in the water column, we investigated the distribution of genes and transcripts of peptidase classes in different ocean basins and depths. All ocean basins, depths and size fractions were dominated by serine peptidases, followed by metallo peptidases, together contributing about 70% to the total genes and transcripts (Fig. 2-4). Similar observations were reported for the relative abundance of total prokaryotic peptidase genes and transcripts (*13*). Additionally, other families represented were cysteine peptidases, followed by aspartic peptidases and threonine peptidases, with the latter two exhibiting a higher relative contribution in the MetaG of the surface macro-mycobiome of the Mediterranean Sea, the Southern Ocean and the Indian Ocean. These regional variations in protease composition and dominance might be associated to the shift in dominance observed between Ascomycota to Basidiomycota as mentioned before for the same areas (Fig. 2-S2).

Additionally, the relative abundances of peptidase families were rather stable with depth, which contrasts the changes in the taxonomic affiliation with depth. Interestingly, the same depth pattern was reported for fungal CAZymes (*12*) and oceanic prokaryotic CAZymes and peptidases (*13*), pointing towards functional redundancy of fungi and prokaryotes in the degradation of carbohydrates and proteins in the oceanic water column.

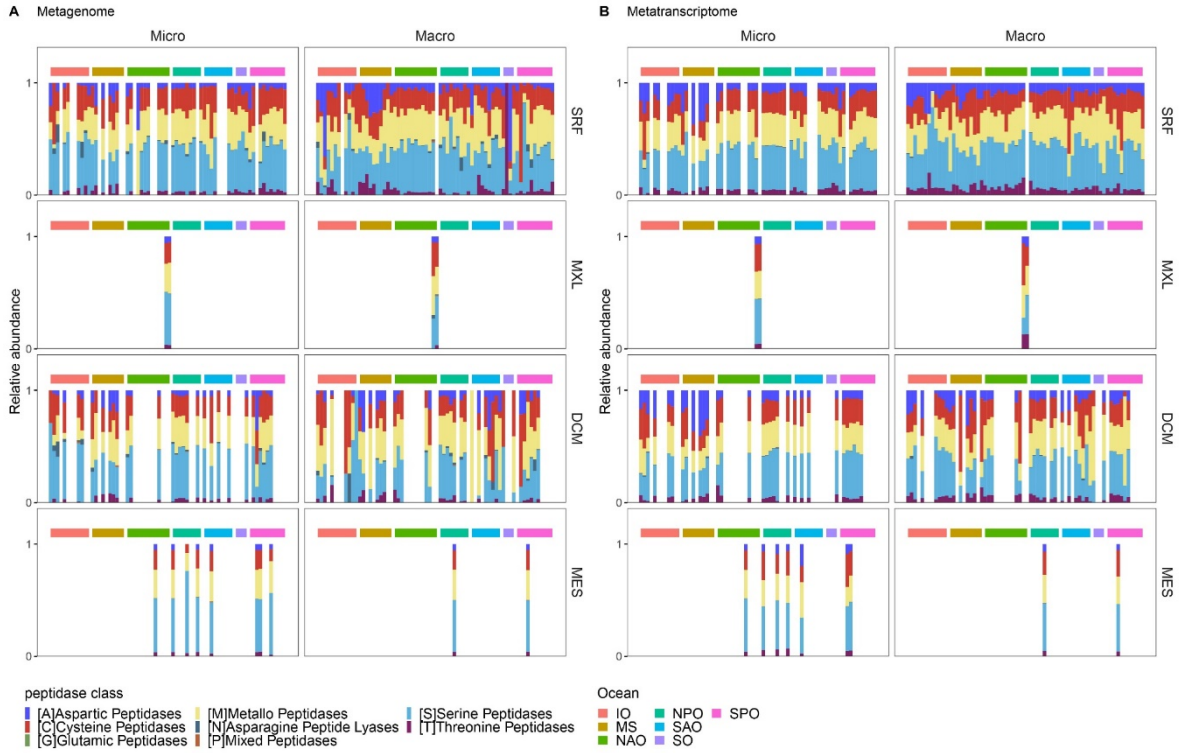

Figure 2-4. Functional classification of genes (A) and transcripts (B) encoding fungal Peptidases. Micro, micro-mycobiome (0.8-5 µm); Macro, macro-mycobiome (5-2000 µm). SRF, surface; MXL, mixed layer; DCM, deep chlorophyll maximum; MES, mesopelagic; IO, Indian Ocean; MS, Mediterranean Sea; NAO, North Atlantic Ocean; North Pacific Ocean; SAO, South Atlantic Ocean; SO, Southern Ocean; SPO, South Pacific Ocean.

3.4. Taxonomic and functional affiliation of genes and transcripts encoding fungal secretory peptidases in the global ocean

As the abundance and relative percentage of secretory proteases increased with depth as also observed for fungal CAZymes (*12*), we additionally analyzed the taxonomic and functional affiliation of fungal secretory peptidases in the water column. Overall, the pattern of secretory peptidase genes and transcripts was very similar to that of the total peptidase genes, with Ascomycota dominating global oceans and becoming even more important with increasing depths (Fig. 2-S3). Also, the taxonomic affiliation of fungal protease genes and

transcripts at the class level was dominated by the same main groups responsible for total peptidase genes and transcripts (Fig. 2-S4). Chytridiomycota do not seem to secrete peptidases, consistent with the findings on fungal secretory CAZymes (*12*). Also, the major fungal peptidase classes dominating the secretory and the total pool were basically the same, with serine and metallo peptidases being the most abundant secreted peptidase class, followed by cysteine peptidases (which slightly increased in relative abundance in the secretory relative to the total pool) (Fig. 2-S5). This is in contrast to oceanic prokaryotes, which secrete only a small fraction of cysteine peptidases (according to the metatranscriptomics and metaproteomics analysis despite representing a major fraction in the metagenome) (*13*). The contrasting composition of the secretory proteases between prokaryotes and fungi suggests different ecological strategies of these two main planktonic groups.

3.5. Unique and shared protease pools between oceanic fungi and prokaryotes

To further investigate the potentially different roles fungi and prokaryotes play in the degradation of proteins in the ocean, we determined the number of unique and shared proteases between pelagic fungi and bacteria. After categorizing all marine bacterial and fungal proteases, we found that 81 oceanic fungal protease families were shared with bacteria, 4 were unique fungal proteases and 108 were unique bacterial proteases (Table 2-S1). The four unique fungal protease families included one metallo protease, two serine proteases and one cysteine protease; specifically, tryptophanyl aminopeptidase (M77), nucleoporin 145 (S59), Ssy5 peptidase (S64) and otubain-1 (C65). Most of the existing fungal protease data are derived from *Saccharomyces cerevisiae* (Saccharomycotina) or other fungal taxa. Hence, these functional data have to be interpreted with caution. The conclusion of our analyses of these four unique fungal proteases appears, however, consistent with the available literature. Tryptophanyl aminopeptidase has been reported to originate from a common fungal ancestor and hence can only be found in the kingdom of fungi (*25*). Also, Ssy5 peptidase, involved in sensing of extracellular amino acids and in defense mechanisms against viruses, is supposed to be a fungal evolutionary innovation, which originates from Dikarya or was lost during later evolution (*26*). Thus, it is reasonable that tryptophanyl aminopeptidase and Ssy5 peptidase were exclusively found in the fungal fraction. Nucleoporin 145, which is essential for nuclear pore formation (*27*) is shared between plants, animals, SAR (stramenopiles, alveolates, Rhizaria) and fungi (*26*). Otubain-1 is a common eukaryotic isopeptidase involved in ubiquitin-based cell-signaling

mechanisms (*28*) and absent in oceanic bacteria. Also, both, Nucleoporin 145 and Otubain-1 were found to be unique to eukaryotic peptidase families (*29*).

3.6. Global abundance and expression of the dominant fungal protease families and subfamilies in the ocean

To identify the main functions involved in the fungal degradation of proteins in the ocean, we determined the abundance and expression of the main subfamilies of serine and metallo peptidases (the dominant pelagic fungal protease families) (Fig. 2-5). However, some subfamilies including 'X' in their name denote inactive peptidases, despite their occasionally widespread expression (e.g. S09X, Fig. 2-5). Nevertheless, a distinct clustering pattern was found in mesopelagic waters with a relatively high expression of a variety of subfamilies and relatively more metallo peptidases than serine peptidases compared to shallower layers. Also, some subfamilies such as glutamate carboxypeptidase (M20A), Oma1 peptidase (M48C), FtsH peptidase (M41) and D-Ala-D-Ala carboxypeptidase B (S12) were almost exclusively found to be expressed in deep waters. M20A is responsible for cleaving vitamin B9 to retrieve pteroate and L-glutamate (*30*), which might counteract the normally scarce availability of glutamate in deep waters (*31*). D-Ala-D-Ala carboxypeptidase B (S12) is involved in chitinase degradation (*32*). Transcript-based analyses (Fig. 2-5) allowed deciphering one distinct protease cluster from the Mediterranean Sea exhibiting a lower diversity of transcripts compared to other ocean basins and only expressing prolyl aminopeptidase (S33) and carboxypeptidase Y (S10) (Fig. 2-5). It is worth mentioning that S33 and S10 are the most widely expressed proteases globally. S33 has recently been suggested as a marker for saprotrophy in fungi as it is assumed to be less expressed in fungi with a pathogenic or animal-associated lifestyle (*26*). However, S33 also includes some abhydrolases, which additionally degrade other substrates like lipids. S10 is a vacuole protease (*33*) and also involved in extracellular organic matter degradation (*34*). The global dominance of and co-occurrence of S10 (plant-associated) and S33 (less expressed in fungal pathogens) might indicate that the majority of the oceanic mycobiome is dominated by saprotrophy rather than pathogeny. This assumption is further supported by the relatively high expression of the aminopeptidases M01, M24, M28 and S12, which are all indicative of saprotrophic nutrition. Additionally, subtilisin Carlsberg (S08A), a subfamily reported to be involved in nutrition and mostly secreted from the cell (*16*) was widely expressed. Since our analyses indicated that Chytridiomycota do not contribute to the secretory pool of proteases (Fig. 2-S3), this suggests fungi belonging to the subkingdom Dikarya as the main producers of S08A. This might imply that besides their role as parasites and associated processes described

as the fungal shunt and mycoloop (*7, 9*), fungi are active contributors to the organic matter cycling in the ocean and hence, play a major role in the biogeochemical cycles in the global ocean.

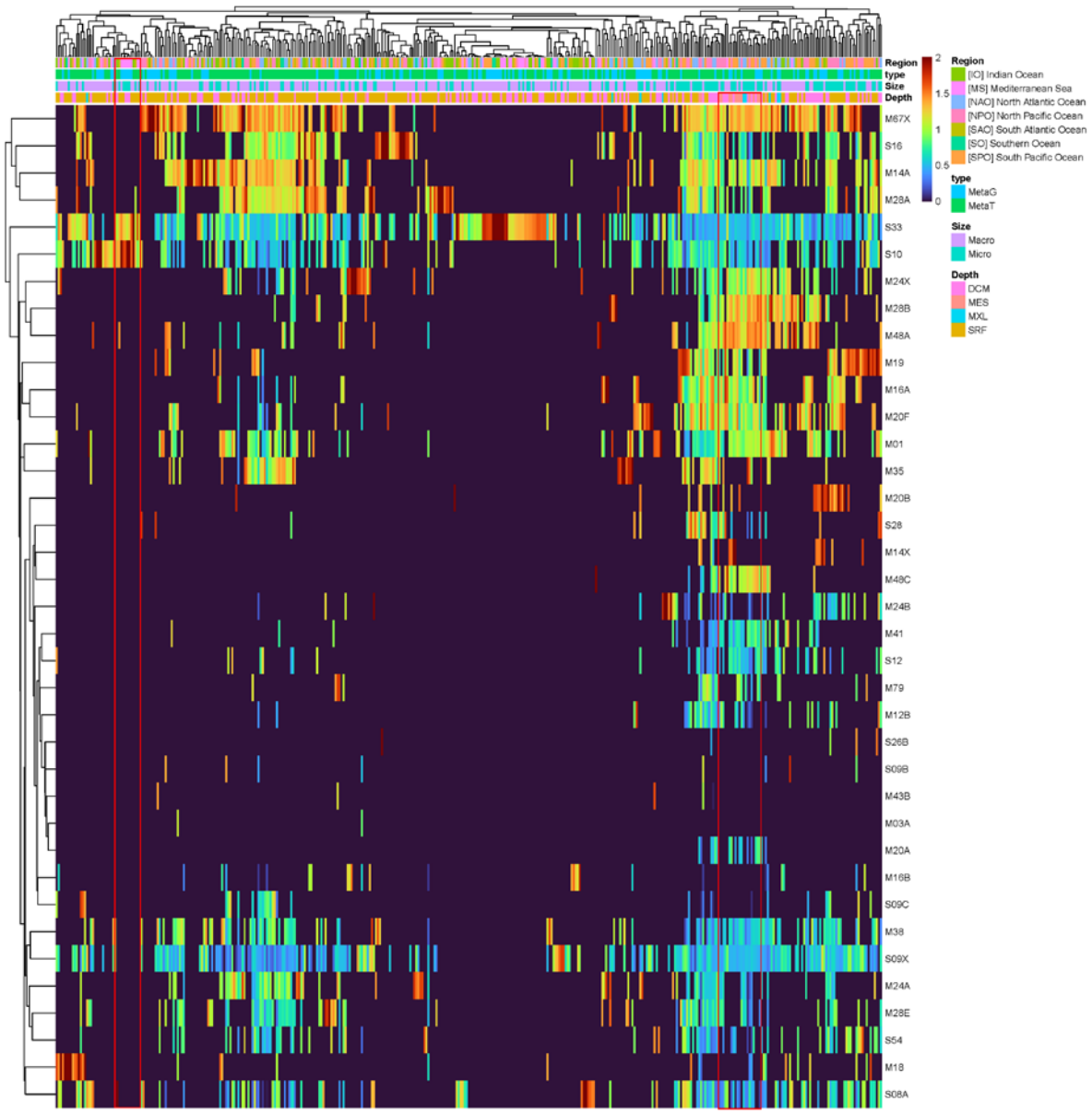

Figure 2-5. Heatmap of fungal serine and metallo subfamily Peptidase profile with abundance >1%. Red frames highlight peptidase actively expressed in the Mediterranean Sea and the mesopelagic zone. Micro, micro-mycobiome (0.8-5 µm); Macro, macro-mycobiome (5-2000 µm). SRF, surface; MXL, mixed layer; DCM, deep chlorophyll maximum; MES, mesopelagic; IO, Indian Ocean; MS, Mediterranean Sea; NAO, North Atlantic Ocean; North Pacific Ocean; SAO, South Atlantic Ocean; SO, Southern Ocean; SPO, South Pacific Ocean; MetaG, metagenomic; MetaT, metatranscriptomic.

4. Conclusions

Our findings reveal that fungi are globally active contributors to oceanic protein degradation and thus, key players in the nitrogen cycling in the water column, especially in deeper waters. This increasing abundance, diversity and expression of total and secretory fungal proteases with water column depth is consistent with the distribution pattern of fungal CAZymes (*12*) and might be related to the degradation of more refractory organic material in the dark ocean and/or the sinking of particles. In contrast, the total proteases and CAZymes of prokaryotes do not increase with depth (*13*), indicating a potentially different contribution or role of prokaryotes *versus* fungi in the deep waters (Fig. 2-2 – 2-6). The percentage of secretory fungal proteases also increased with depth, similar to fungal CAZymes (*12*) and prokaryotic proteases and CAZymes (*13*) (Fig. 2-6). This highlights the key role of secreted enzymes in the degradation of organic matter (*23*), probably indicative of a preferential particle-attached lifestyle (*13*). This also implies that the increasing fraction of secretory enzymes with depth is a conserved phenomenon across pelagic prokaryotes and fungi. However, pronounced differences were found in the composition of secretory peptidases between prokaryotes and fungi, indicating different strategies in the use of secretory peptidase between prokaryotes and fungi in the ocean. We also identified the main taxa and functions affiliated to fungal proteases, revealing Ascomycota (dominated by Dothideomycetes in epipelagic and Leotiomycetes and Eurotiomycetes in mesopelagic) and Basidiomycota as the main responsible for fungal protease expression in all depths and ocean basins. Chytridiomycota were only regionally important (probably due to their more temporal 'blooming' lifestyle). These are also the taxa dominating the fungal CAZyme pool (*12*), indicating that those are the major players in the fungal enzymatic cleavage of both, proteins and carbohydrates in the ocean. Most of the protease families used by oceanic fungi are shared with prokaryotes, although 4 unique proteases were detected in fungi. The most widely used oceanic fungal peptidases classes were serine-, followed by metallo proteases. The expression profile of protease subfamilies suggests that the majority of the pelagic fungal communities is dominated by saprotrophy rather than parasitism. The composition of the main protease classes was conserved with depth, irrespective of shifts in the taxonomic affiliation, which indicates functional redundancy in fungal communities. Interestingly, functional redundancy with depth was also reported for fungal CAZymes (*12*) and oceanic prokaryotic CAZymes and peptidases (*13*), indicating that functional redundancy might be a common trait of pelagic fungal and prokaryotic communities in the degradation of organic matter (at least for carbohydrates and proteins) in the oceanic water column. Collectively, this study highlights the active contribution of fungi in the degradation of proteins,

which are the major macromolecular compound class in living and detrital biomass in the ocean. Furthermore, our results also point towards contrasting strategies in the enzymatic degradation of organic matter by fungi and prokaryotes in the global ocean.

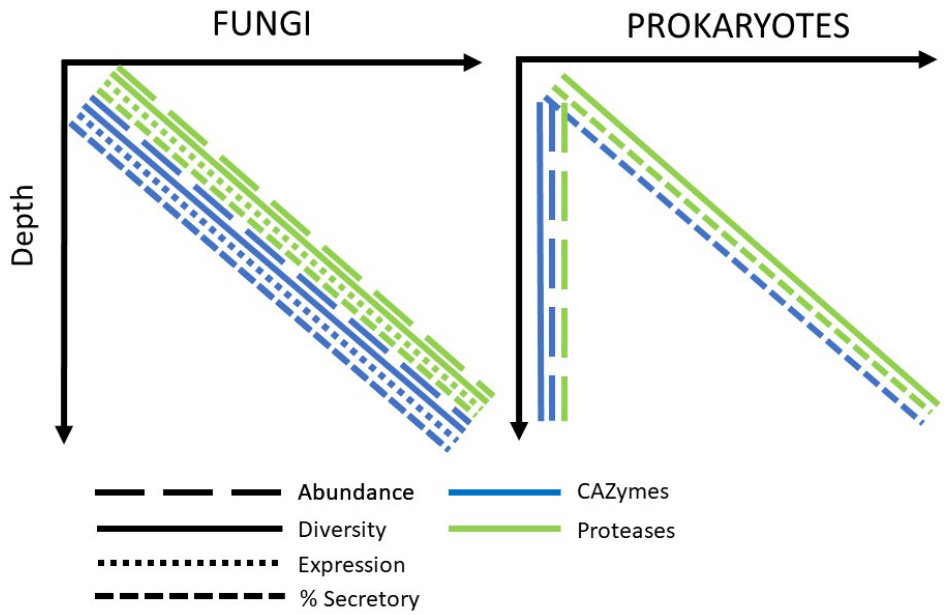

Figure 2-6. Diagram depicting the depth-related patterns in the total gene abundance, expression, diversity, and the percentage of secretory peptidases and CAZymes from pelagic fungi and prokaryotes. The pattern associated to fungal CAZymes originates from Baltar *et al. (12)*, and the prokaryotic CAZymes and peptidases are derived from Zhao *et al. (13)*. Depth-related expression of prokaryotic CAZymes and proteases are not available for comparison.

Acknowledgements

The study was supported by the Austrian Science Fund (FWF) project OCEANIDES (project number AP3430411/21), ENIGMA (project number FW764002), EXEBIO (project number AP3524811) to F.B and ARTEMIS (project number P28781-B21) to G.J.H. We thank the reviewers for the constructive comments that improved the quality of the paper.

Author Contributions

F.B. and Z.Z. conceived the project. Z.Z. performed the analysis. E.B., F.B., Z.Z. and G.J.H. interpreted the data. The manuscript was written by E.B. and F.B. All authors contributed to editing the manuscript and approved the final version.

References

1. Y. M. Bar-On, R. Phillips, R. Milo, The biomass distribution on Earth. *Proc. Natl. Acad. Sci. USA* **115**, 6506 (2018).
2. G. Lima-Mendez *et al.*, Determinants of community structure in the global plankton interactome. *Science* **348**, 1262073 (2015).
3. P. G. Falkowski, T. Fenchel, E. F. Delong, The Microbial Engines That Drive Earth's Biogeochemical Cycles. *Science* **320**, 1034-1039 (2008).
4. H.-P. Grossart *et al.*, Fungi in aquatic ecosystems. *Nat. Rev. Microbiol.* **17**, 339-354 (2019).
5. A. B. Bochdansky, M. A. Clouse, G. J. Herndl, Eukaryotic microbes, principally fungi and labyrinthulomycetes, dominate biomass on bathypelagic marine snow. *ISME J.* **11**, 362-373 (2017).
6. M. H. Gutiérrez, S. Pantoja, E. Tejos, R. A. Quiñones, The role of fungi in processing marine organic matter in the upwelling ecosystem off Chile. *Mar. Biol.* **158**, 205-219 (2011).
7. M. Kagami, A. de Bruin, B. W. Ibelings, E. Van Donk, Parasitic chytrids: their effects on phytoplankton communities and food-web dynamics. *Hydrobiologia* **578**, 113-129 (2007).
8. A. C. Cleary, J. E. Søreide, D. Freese, B. Niehoff, T. M. Gabrielsen, Feeding by Calanus glacialis in a high arctic fjord: potential seasonal importance of alternative prey. *ICES J. Mar. Sci.* **74**, 1937-1946 (2017).
9. I. Klawonn *et al.*, Characterizing the “fungal shunt”: Parasitic fungi on diatoms affect carbon flow and bacterial communities in aquatic microbial food webs. *Proc. Nat. Acad. Sci.* **118**, e2102225118 (2021).
10. S. E. Morales, A. Biswas, G. J. Herndl, F. Baltar, Global Structuring of Phylogenetic and Functional Diversity of Pelagic Fungi by Depth and Temperature. *Front. Mar. Sci.* **6**, (2019).
11. N. Chrismas, M. Cunliffe, Depth-dependent mycoplankton glycoside hydrolase gene activity in the open ocean—evidence from the Tara Oceans eukaryote metatranscriptomes. *ISME J.* **14**, 2361-2365 (2020).
12. F. Baltar, Z. Zhao, G. J. Herndl, Potential and expression of carbohydrate utilization by marine fungi in the global ocean. *Microbiome* **9**, 106 (2021).

13. Z. Zhao, F. Baltar, G. J. Herndl, Linking extracellular enzymes to phylogeny indicates a predominantly particle-associated lifestyle of deep-sea prokaryotes. *Sci. Adv.* **6**, eaaz4354 (2020).
14. J. I. Hedges *et al.*, The biochemical and elemental compositions of marine plankton: A NMR perspective. *Mar. Chem.* **78**, 47-63 (2002).
15. Q. Carradec *et al.*, A global ocean atlas of eukaryotic genes. *Nat. Commun.* **9**, 1-13 (2018).
16. N. D. Rawlings *et al.*, The MEROPS database of proteolytic enzymes, their substrates and inhibitors in 2017 and a comparison with peptidases in the PANTHER database *Nucleic Acids Res.* **46**, D642-D632 (2018).
17. B. Buchfink, C. Xie, D. H. Huson, Fast and sensitive protein alignment using DIAMOND. *Nat. Methods* **12**, 59-60 (2015).
18. J. J. A. Armenteros *et al.*, SignalP 5.0 improves signal peptide predictions using deep neural networks. *Nat. Biotechnol.* **37**, 420-423 (2019).
19. J. Oksanen *et al.*, Vegan: community ecology package. Ordination methods, diversity analysis and other functions for community and vegetation ecologists. *R package ver*, 2.3-1 (2015).
20. P. Saary, K. Forslund, P. Bork, F. Hildebrand, RTK: efficient rarefaction analysis of large datasets. *Bioinformatics* **33**, 2594-2595 (2017).
21. C. Ginestet. (Wiley Online Library, 2011).
22. F. Baltar *et al.*, High dissolved extracellular enzymatic activity in the deep central Atlantic Ocean. *Aquat. Microb. Ecol.* **58**, 287-302 (2010).
23. F. Baltar, Watch out for the “living dead”: cell-free enzymes and their fate. *Front. Microbiol.* **8**, 2438 (2018).
24. J. D. Taylor, M. Cunliffe, Multi-year assessment of coastal planktonic fungi reveals environmental drivers of diversity and abundance. *ISME J.* **10**, 2118-2128 (2016).
25. N. D. Rawlings, A. Bateman, Origins of peptidases. *Biochimie* **166**, 4-18 (2019).
26. A. Muszewska *et al.*, Fungal lifestyle reflected in serine protease repertoire. *Sci. Rep.* **7**, 9147 (2017).
27. M. P. Rout *et al.*, The Yeast Nuclear Pore Complex: Composition, Architecture, and Transport Mechanism. *J. Cell Biol.* **148**, 635-652 (2000).
28. Mariola J. Edelmann *et al.*, Structural basis and specificity of human otubain 1-mediated deubiquitination. *Biochem. J.* **418**, 379-390 (2009).

29. M. J. Page, E. Di Cera, Evolution of Peptidase Diversity. *J. Biol. Chem.* **283**, 30010-30014 (2008).
30. J. McCullough, B. Chabner, J. Bertino, Purification and properties of carboxypeptidase G1. *J. Biol. Chem.* **246**, 7207-7213 (1971).
31. C. Tamburini, J. Garcin, A. Bianchi, Role of deep-sea bacteria in organic matter mineralization and adaptation to hydrostatic pressure conditions in the NW Mediterranean Sea. *Aquat. Microb. Ecol.* **32**, 209-218 (2003).
32. T. Langner, V. Göhre, Fungal chitinases: function, regulation, and potential roles in plant/pathogen interactions. *Curr. Genet.* **62**, 243-254 (2016).
33. G. Gabriely, R. Kama, J. E. Gerst, Involvement of Specific COPI Subunits in Protein Sorting from the Late Endosome to the Vacuole in Yeast. **27**, 526-540 (2007).
34. M. Monod *et al.*, Secreted proteases from pathogenic fungi. *Int. J. Med. Microbiol.* **292**, 405-419 (2002).

Chapter 3: The overlooked contribution of pelagic fungi to ocean biomass

Eva Breyer[1*], Constanze Stix[1,] Sophie Kilker[1], Benjamin R.K. Roller[2], Fragkiski Panagou[1], Charlotte Doebke[1], Chie Amano[1], Guillem Coll Garcia[1,3], Barbara Mähnert[1], Jordi Dachs[4], Naiara Berrojalbiz[4], Maria Vila-Costa[4], Cristina Sobrino[5], Antonio Fuentes-Lema[5], Franz Berthiller[6], Martin Polz[2], Federico Baltar[1*]

[1] Fungal and Biogeochemical Oceanography Group, Department of Functional and Evolutionary Ecology, University of Vienna; Djerassiplatz 1, 1030 Vienna, Austria.

[2] Division of Microbial Ecology, Centre for Microbiology and Environmental Systems Science, University of Vienna; Djerassiplatz 1, 1030 Vienna, Austria.

[3] Environmental Microbiology Group, Mediterranean Institute for Advanced Studies (CSIC-UIB); C/ Miquel Marquès 21, 07190 Esporles, Spain.

[4] Department of Environmental Chemistry, IDAEA-CSIC; Jordi Girona 18-26, Barcelona 08034, Catalonia, Spain.

[5] Centro de Investigación Mariña da Universida de de Vigo (CIM-UVigo); 36310 Vigo, Spain.

[6] Institute of Bioanalytics and Agro-Metabolomics, Department of Agrobiotechnology (IFA-Tulln), University of Natural Resources and Life Sciences, Vienna (BOKU); Konrad Lorenz Str. 20, 3430 Tulln, Austria.

* Correspondence: eva.breyer@univie.ac.at, federico.baltar@univie.ac.at

Submitted to *Science* on 19.03.2024

Abstract

Metagenomic analysis has unveiled the widespread presence of pelagic fungi in the global ocean, yet their quantitative contribution to carbon stocks remains elusive, hindering their incorporation into biogeochemical models. Here we revealed the biomass of oceanic fungi in the open ocean water column by combining ergosterol extraction, Calcofluor-White staining, CARD-FISH, and microfluidic mass sensor techniques. We compared fungal biomass to the biomass of other more studied microbial groups in the ocean such as archaea and bacteria. Globally, fungi contributed 0.19-0.21 Gt C, less than bacteria but exceeding archaea (Archaea:Fungi:Bacteria biomass ratio of 1:4:32). Collectively, our findings reveal the important contribution of fungi to open ocean biomass and, consequently, the marine carbon cycle, emphasizing the need for their inclusion in biogeochemical models.

Keywords

mycoplankton, oceanic fungi, CARD-FISH, ergosterol, Calcofluor-White, suspended microchannel resonator

1. Introduction

The ocean constitutes about 99% of the volume in the biosphere. Oceanic microbes comprise 70-90% of the biomass of marine biota (*1, 2*), and are the main drivers of marine biogeochemical cycles (*3*). They are responsible for determining the amount of carbon fixed during photosynthesis, the subsequent release of carbon back to CO_2 through respiration, and ultimately the sequestration of carbon in the deep ocean over millennial scales. Yet, present estimates of marine microbial biomass primarily rely on bacteria, archaea, and protists. Conversely, pelagic fungal biomass has been traditionally neglected and only superficially characterized, despite their recently documented ubiquitous presence and active participation in the marine carbon and nitrogen cycles (*4-9*). Currently, only a few local coastal studies on pelagic fungal biomass are available suggesting their importance; however, we are still lacking an accurate representation of the open ocean environment. Additionally, these previous studies are based on different methods, each having their own limitations and therefore hampering a robust intercomparison of results (reviewed in (*10*)). Most available pelagic fungal biomass/abundance estimates are based on gene copy number (quantitative PCR), which gives rough estimates on true abundances/biomass (*6, 11-17*). Microscopy-based approaches have been used in a couple of studies to show that pelagic fungi significantly contributed to microbial biomass on bathypelagic marine snow particles (*18*), and revealed that highest fungal biomass coincided with coastal phytoplankton blooms (*19, 20*). Ergosterol, a membrane lipid found in fungi belonging to Ascomycota and Basidiomycota, proposed as a suitable proxy for assessing marine fungal biomass given its prevalence as a dominant sterol in pelagic fungi (*21*), has been applied to studies in Arctic seawater (*22*) and in coastal areas in the South China Sea (*14*). Previous fungal biomass estimations for oceanic pelagic fungi have also been influenced by different carbon/biomass conversion factors primarily derived from terrestrial or freshwater fungi, yielding a broad biomass range (0.01 µg C/l to 35 mg C/l) (*10*), highlighting the need for specific carbon conversion factors tailored to the marine pelagic fungi's expected physiological adaptations (*23*). In a recent attempt to create a global marine biomass inventory from all living organisms, fungal biomass was indirectly estimated based on the limited number of available studies to be around 0.3 Gt C (*1, 24*). Notably, among all the biomass of organisms/groups estimated in the ocean, fungi accounted for the highest uncertainty, ranging >2 orders of magnitude (*24*), indicating the need for a direct estimate of fungal biomass in the ocean. Given the limitations associated with the mentioned sampling locations and methods, there is an urgent need for large-scale sampling across diverse biogeographical provinces in

the open ocean, coupled with the application of various methods to address potential biases and ensure a precise quantification of the contribution of pelagic fungi to microbial biomass.

To fill this critical gap, we sampled fungal biomass on a >11,000 km long latitudinal transect crossing the Atlantic Ocean from 40N to 50S, and covering five different Longhurst marine biogeographical provinces characterized by a wide range of contrasting environmental conditions. We developed novel biomass conversion factors of ergosterol to carbon, cell biovolume to carbon and cell dry mass specifically for marine pelagic fungi, and estimated fungal biomass via three different methods in parallel [ergosterol extraction, Calcofluor-White (CFW) staining and Catalyzed Reporter Deposition-Fluorescence In Situ Hybridization (CARD-FISH)], based on five pelagic fungal isolates. Due to the recently discovered importance of fungi in the dark ocean (*7, 8, 25*), we collected samples from surface down to the bathypelagic, providing the first direct estimates of fungal biomass in the deep ocean. To put our results into a global context, we compared pelagic fungal biomass estimates to well-studied microbial groups like Archaea and Bacteria and assessed their contributions to particulate organic carbon (POC) in the oceanic water column. We hypothesized that fungal biomass would be related to POC and chlorophyll a (phytoplankton biomass) and be a significant contributor to oceanic living biomass and POC. After applying method-specific conversion factors, we expected similar results from different quantification methods. Collectively, this study demonstrates that fungi are important contributors to the marine carbon cycle, while providing an estimation of their contribution to carbon stocks much needed for their inclusion in biogeochemical models.

2. Material and Methods

2.1. Cultivation conditions and sample preparation of marine fungal cultures

Four pelagic marine fungal cultures, isolated from Atlantic and Antarctic open ocean waters (*38*), were used to calculate biomass conversion factors and cell dry mass (4 yeasts, one filamentous) i.e., *Metschnikowia australis*, *Rhodotorula sphaerocarpa*, *Sakaguchia dacryoidea*, *Rhodotorula mucilaginosa* and *Blastobotrys parvus*. To quantify species- and growth stage specific biovolume to carbon and ergosterol to carbon conversion factors, the cultures were grown in biological triplicates in liquid media ([g/l]: 2 g glucose, 2 g peptone, 2 g yeast extract, 2 g malt extract, 35 g artificial sea salts, 0.5 g chloramphenicol). The liquid cultures were incubated on a shaker incubator (Jeio Tech ISS-7100, 140 rpm) in the dark at

room temperature. Afterwards, growth stages were sampled according to daily measured optical densities (UV-1800 Shimadzu Spectrophotometer, ʎ = 660 nm).

For the quantification of ergosterol and particulate organic carbon (POC) the cultures were filtered in the adaptation, exponential and stationary growth stage, on pre-combusted glass microfiber filters (Whatman, GF/F, 47 mm, 0.7 µm pore size). Filters were stored frozen in pre-combusted aluminium foil at -20 °C until analysis. Half of each filter was used to quantify POC, the other half was used for ergosterol quantification. To account for potential DOC adsorption of the culture medium to the filter in the POC determinations, two GF/F filter were used on top of each other during filtration, where the concentration of POC resulting from the filter placed below was subtracted from the POC concentrations of the filter placed above.

To calculate fungal cell biovolume and abundances, the fungal biomass of all yeasts was further quantified by Calcofluor-White (CFW) fluorescence microscopy. Therefore, 100, 25 and 10 µl of 2% glutaraldehyde-fixed cultures in the adaptation, exponential and stationary growth phase, respectively, were filtered on polycarbonate filters (Millipore, GTTP, 25 mm, 0.2 µm pore size) using support filters below (Millipore, HAWP02500, 25 mm, 0.47 µm pore size, nitrocellulose). Filters were stored in Eppendorf tubes at -20 °C until analysis.

We also estimated fungal biomass by determining the cell dry biomass using a suspended microchannel resonator (SMR), which is a microfluidic mass sensor able to measure single-cell biomass estimates for individual cells via Archimedes' principle (*39*). *R. sphaerocarpa*, *R. mucilaginosa* and *S. dacryoidea* were additionally grown in 0.22 µm filtered liquid media and sampled in the exponential, early-, mid- and late stationary stage (see media concentrations and cultivation conditions above). *M. australis* (yeast) and *B. parvus* (filamentous) could not be determined by SMR as they either surpassed the maximum cell size that can pass through the 8x8 µm orifice at the entrance of the sensor or clumps of cells stuck together and blocked the entrance of the sensor. Samples were fixed with formaldehyde to a final concentration of 4% and stored at 4 °C in the dark until analysis.

2.2. Determination of carbon conversion factors of ergosterol and biovolume

For converting fungal biovolume and ergosterol concentration into biomass carbon, carbon conversion factors based on all the marine pelagic fungal cultures were calculated. For that we used the concentration of POC and ergosterol quantified in triplicates per species and growth stage. For each growth stage and species, the average concentration of ergosterol [mg

ergosterol/l] was compared with the average concentration of POC [mg C/l]. The overall ergosterol to POC conversion factor was expressed in mg ergosterol/g carbon.

Fungal biovolume to carbon conversion factors (based on CFW staining) were also determined for each species in all growth stages. The averages of the triplicate samples were used to calculate the fungal abundance [cells/l] and the fungal biovolume [μm^3/cell], which was quantified assuming a prolate spheroid, a sphere or a cylindrical shape. The amount of carbon per cell was calculated by dividing the concentration of POC by fungal abundance. Afterwards, this value was divided by the cell biovolume. The final value was expressed in pg C/μm^3. To avoid bias from potentially already existing or non-growing fungal cells cultured on solid agar media, the conversion factor of the adaptation phase was not applied to environmental samples. Instead, an average conversion factors of all species in the exponential and stationary phase were used to calculate carbon conversion factors. This likely better reflects the natural growing conditions of marine fungi in the ocean.

2.3. Quantification of fungal cell dry mass by suspended microchannel resonator (SMR)

Dry mass was determined mass for fixed cells using the LifeScale mass sensor and software (Affinity Biosensors). We resuspended cells from each sample in two different fluids of known density (*39, 40*) to obtain paired buoyant mass measurements. The two fluids of known density were prepared from a 10x phosphate buffered saline (PBS) stock (Fisher Bioscientific, certified density of 1.07 g/ml) and diluted to make either 1x PBS in ultrapure water (pure H_2O density 0.997 g/ml) or 1x PBS in deuterated water (99% D_2O certified density 1.107 g/ml) by adding 1 part 10x PBS into 9 parts H_2O or D_2O. These mixtures have final densities of either: 1x PBS in H_2O =1.0043 g/ml or 1x PBS in D_2O = 1.1033. The median buoyant mass was determined from measuring a large number of cells in each fluid (N = 947-21884 cells per sample, see Table 3-S1) and we calculated dry mass using these measurements and the known fluid densities using equations from (*39*). The LifeScale measurements were validated by measuring NIST standard polystyrene beads of various sizes with certified diameters and densities in 1x PBS in ultrapure water with a known density. This allows us to calculate the expected buoyant mass for any given bead size. We regress the observed median buoyant mass of each bead size against the expected buoyant mass for several bead sizes (Fig. S1) and find a slope indistinguishable from 1 (1.0049, 95% CI 0.9955 - 1.0144) and an intercept indistinguishable from zero (-14.1177, 95% CI -35.3934 - 7.1579), thus validating the accuracy of measurements between a buoyant mass from approximately 20 fg to 6 pg. The median

buoyant mass of fungal cells of all 3 species fell within the range of our calibrated dataset (*R. mucilaginosa* = 0.6-2.3 pg, *R. sphaerocarpa* = 8.7-1.8 pg, *S. dacryoidea* = 2.3-5.3 pg). There was no statistically significant difference between species-specific cell dry mass at different time points. Hence, we calculated the abundance-based conversion factor using SMR by taking the average of all measurements in the exponential and stationary growth stage based on all species.

2.4. Environmental sample collection in the Atlantic Ocean

The environmental samples were collected in December/January 2021 during the ANTOM-1 cruise from Vigo (Spain) to Punta Arenas (Chile) on board of the R.V. Sarmiento de Gamboa. The transect comprised a total of 24 stations crossing both hemispheres across the Atlantic Ocean (Fig. 3-1). A Sea-Bird SBE 9 CTD (conductivity, temperature, depth) rosette, equipped with 24 12-liter Niskin bottles, was used to collect seawater from the epipelagic (0-200 m), mesopelagic (200-1000 m) and bathypelagic (2000 m) realms. In the epipelagic, we specifically sampled surface waters (5 m) and the deep chlorophyll maximum (DCM) layer (ranging from 18-140 m). At all stations and sampling depths (86 samples in total), environmental parameters including temperature, salinity and oxygen were determined, and samples for fungal biomass and POC were collected. Additionally, chlorophyll a was quantified at the surface and in the DCM layer in different size fractions (0.2–2 µm, 2–20 µm, >20 µm). Furthermore, to put the fungal biomass into context with other microbial groups, 62 samples were collected for prokaryote biomass and 23 samples for archaeal biomass, randomly distributed across the transect (Table 3-S5).

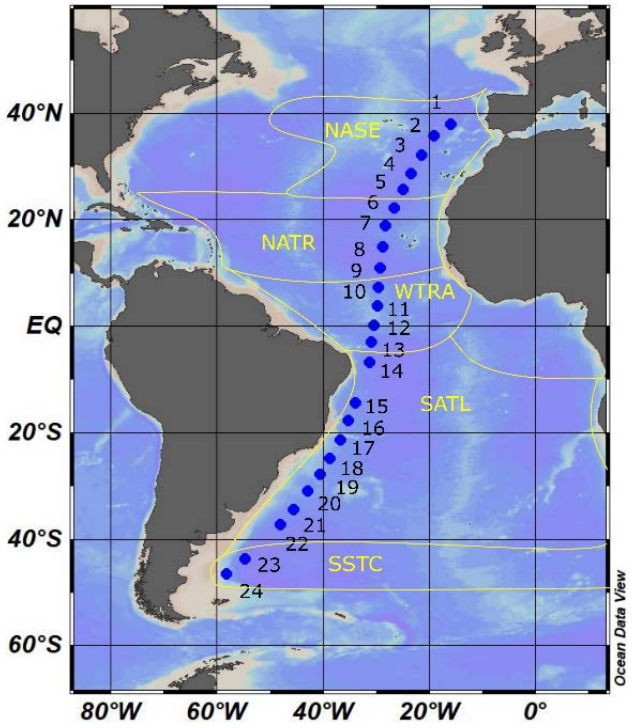

Figure 3-1. Map of sampling stations during the ANTOM-1 Cruise. Environmental data were collected at 24 cruise stations crossing five Longhurst biogeographical provinces: North Atlantic Subtropical Gyral Province East (NASE), North Atlantic Tropical Gyral Province (NATR), Western Tropical Atlantic Province (WTRA), South Atlantic Gyral Province (SATL), South Subtropical Convergence Province (SSTC). The map was generated with Ocean Data View (ODV). The Longhurst biogeographical provinces are indicated with yellow lines.

For ergosterol-based fungal biomass quantification and POC quantification, 10 l of seawater were collected in acid-cleaned carboys and filtered onto pre-combusted glass microfiber filters (Whatman, GF/F, 47 mm, 0.7 µm pore size). The filters were folded and stored in pre-combusted aluminum foil and kept at -20 °C. Half of each filter was used for ergosterol extraction while the other half was used for POC quantification (as described for fungal cultures above). Additionally, nine samples including from epi-, meso-, and bathypelagic were collected to quantify potential DOC adsorption to the filter (*41*), resulting in average values (ca. 10% of total POC) subtracted from final POC concentrations.

For fungal biomass quantification with CFW staining and CARD-FISH microscopy, 2x 50-100 ml of seawater were collected in acid-cleaned polycarbonate bottles and fixed with formaldehyde to a final concentration of 4%. Afterwards, the seawater was filtered onto polycarbonate filters (Millipore, GTTP, 25 mm, 0.22 µm pore size) using support filters below (Millipore, HAWP02500, 25 mm, 0.47 µm pore size, nitrocellulose). The polycarbonate filters

were stored in Eppendorf tubes at -20 °C. The same filter collected for fungal CARD-FISH was also used to quantify archaeal biomass (also by CARD-FISH, see below) and used for enumeration of prokaryotic cells by DAPI (4',6-diamidino-2-phenylindol) counts. Additional samples for prokaryotic abundances were collected and analyzed by flow cytometry (see below).

Seawater samples for chlorophyll a analysis were taken directly from the Niskin bottle to further filtration. For each sample, 250 ml were gently filtered under dim light in triplicate through a size fraction cascade system with 20, 2 and 0.22 µm size pore 47-mm Filter-Lab polycarbonate filters, and immediately stored at -20 °C until further analysis.

2.5. Quantification of particulate organic carbon and chlorophyll a

POC was quantified according to the JGOFS (Joint Global Ocean Flux study) protocol (*42*). Briefly, the filters were thawed and dried for 24 h in a desiccator with silica gel and then fumigated with concentrated HCl (37%) in a desiccator for 24 h to remove inorganic carbon. Finally, filters were dried again in a desiccator with silica gel. The POC was measured with a CHNS elemental analyzer (vario microcube, elementar) in 2 technical replicates per sample.
For chlorophyll a extraction, the filters were kept at 4 °C overnight in acetone 90% and then, chlorophyll a concentration (µg/l) was estimated following the acidification method (*43*) employing a Turner A10 fluorimeter calibrated with a pure chlorophyll a standard solution (SIGMA C5753-1mg).

2.6. Ergosterol extraction and HPLC and LC-MS/MS analysis for fungal biomass

Ergosterol was extracted from fungal cultures and seawater samples according to the protocol of (*44*) that we had recently adapted/modified for marine pelagic fungal biomass (*45*). Briefly, the filters were incubated in 3 ml of chloroform:methanol (2:1, *v/v*) (chloroform: Alfa Aesar, ≥99.5% HPLC grade; methanol: Sigma Aldrich, ≥99.9% HPLC grade) in combusted glass screw-top tubes in the dark at room temperature for 24 h. The extracts were transferred into sterile plastic polypropylene tubes. Afterwards, 660 µl of MilliQ-water (MQ; methanol:MQ = 3:2) were added to each sample and mixed thoroughly. The polypropylene tubes were placed into a centrifuge for 3 minutes at 3214 rcf (Eppendorf centrifuge 5810 R). The two phases were separated, and the lipid-containing organic solvent chloroform phase was left evaporating to dryness. The extraction was repeated twice on the same filter and both extracts were combined. Finally, the dry extracts were re-suspended in ultra-pure methanol

(Sigma Aldrich, ≥95.0% HPLC grade) and stored in the dark at -20 °C until LC-MS/MS or HPLC analysis.

The ergosterol extracts from the fungal cultures were measured according to a protocol by (*46*) with an injection volume of 400 µl. The Agilent 1260 Infinity Bioinert HPLC system included a programmable autosampler, a quaternary pump, a column oven and an UV detector. An Agilent Zorbax SB-Aq Analytical Guard Column precolumn (4.6 x 12.5 mm; 5 µm pore size) and an Agilent Zorbax Eclipse AAA Rapid resolution main column (4.6 x 150 mm; 3.5 µm pore size) were used. The separation of ergosterol was done by using a gradient of 100% methanol for 15 minutes and the detector was set to a wavelength of 282 nm. Ergosterol standards in methanol (Sigma Aldrich, ≥ 95.0% HPLC grade) were prepared in the following concentrations: blank, 13 nM, 64 nM, 320 nM, 1.6 µM, 8 µM, 40 µM, 200 µM, 1 mM. 1/x weighted linear calibrations were performed using peak areas, resulting in linearity over the whole calibration range (r^2 >0.999). Measurements of the standards yield a lower detection limit between 13 and 64 nM.

The ergosterol extracts from the seawater samples were measured on an Agilent (Waldbronn, Germany) 1290 UHPLC system coupled to a Sciex (Framingham, MA, USA) QTrap 6500+ mass spectrometer. A Phenomenex (Aschaffenburg, Germany) Gemini C18 column (150 x 4.6 mm, 5 µm particle size) was used for separation. Isocratic elution at 35 °C was performed using acidified acetonitrile, containing 0.1% formic acid, as mobile phase. A flow rate of 2.5 ml/min was chosen and 20 µl were injected. The eluent was sent to the APCI source between 3.0 to 4.5 min, while the whole run took 5 mins. The obtained retention time for ergosterol was 3.80 min. A heated nebulizer APCI probe was used in the Turbo V source for ionization of ergosterol in positive ion mode with the following settings: curtain gas 30 psi, nebulizer gas 40 psi, temperature 500 °C and nebulizer current 3 µA. The mass spectrometer was operated in selected reaction monitoring mode, using both the $[M+H-H_2O]^+$ (declustering potential 100 V) and the unusual $[M+H-2H_2]^+$ (declustering potential 50 V) ions as precursors (*47*). The following six transitions were monitored for 50 ms each (Q1 mass > Q3 mass (collision energy, CE)): 379.3>295.2 (20 eV), 379.3>159.1 (30 eV), 379.3>145.1 (35 eV), 379.3>69.0 (55 eV), 393.3>268.2 (30 eV), 393.3>173.1 (35 eV). Analyst version 1.6.3 was used for data acquisition and evaluation. Ergosterol standards in methanol were prepared for quantification in the following concentrations: blank, 10 nM, 100 nM, 1000 nM, 10.000 nM. 1/x weighted linear calibrations were performed using peak areas, resulting in linearity over the whole calibration range (r^2 > 0.995). Repeated measurements of the lowest standard yielded

a limit of detection of 1.5 nM (signal to noise 3/1) and a limit of quantification of 5.0 nM (signal to noise 10/1).

2.7. Calcofluor-White (CFW) epifluorescence microscopy for fungal biomass

CFW is a fluorescent dye that binds to β-1,3 and β-1,4 polysaccharides and therefore to Chitin in fungal cell walls. It is a common technique used in aquatic ecology to visualize fungal cells (*48, 49*), and has been used to quantify fungal biomass during marine phytoplankton blooms (*20*). Various concentrations of CFW were preliminary tested to achieve optimal staining results of fungal cell wall staining. Based on that, 25 µl of CFW (Sigma-Aldrich, USA) and 25 µl of KOH (10% mixed with 10% glycerin) were mixed and added on top of an ethanol-cleaned microscope slide. Afterwards, the polycarbonate filter was placed on the slide and covered again with the CFW-KOH mix and kept in the dark for 10 min. The samples were immediately analyzed with a Zeiss Axio Imager 2 microscope (1000x magnification, Carl Zeiss, Jena, Germany) using UV-light below 400 nm (DAPI, filter set 49). The fungal abundance was estimated by randomly selecting a minimum of 20 Field of Views (FOVs) (125 *x* 125 µm each). Total cell numbers were counted and each cell biovolume was quantified assuming a prolate spheroid, a sphere or a cylindrical shape.

For seawater samples, fungal abundance per liter was converted into fungal biomass (referred to 'abundance-based' fungal biomass, SMR method) by using the culture-based average cell dry mass, whereas fungal biovolume was converted into fungal biomass (referred to 'biovolume-based' fungal biomass) by applying the culture-based average biovolume to carbon conversion factor.

2.8. Catalyzed reporter deposition fluorescence in situ hybridization (CARD-FISH) for fungal biomass

To quantify fungal biomass and abundances in seawater samples, we applied a modified method of Priest *et al.* (*19*), based on Pernthaler and Amann (*50*) and Thiele *et al.* (*51*). Since the enzyme mix used to permeabilize fungal cells applied by Priest *et al.* (*19*) (Glucanex, Sigma-Aldrich, St. Louis, MO, USA) is commercially not available anymore, we had to develop/adapt a novel procedure for the permeabilization of fungal cell walls. For that, we first tried to replicate the original enzyme concentrations of Glucanex together with additional chitinase as described in (*19*). This permeabilization buffer was applied to four pelagic fungal cultures isolated during the cruise (unknown species comprising filamentous fungi and yeasts)

and to *R. mucilaginosa* cultures. For the hybridization, we used horseradish peroxidase-labelled oligonucleotide probes: the fungal PF2 probe (5'-CTCTGGCTTCACCCTATTC-3', (*52*)) and the bacterial EUB338 I probe (5'- GCT GCC TCC CGT AGG AGT-3', (*53*)) (as negative control in all samples). As an additional control, we tested the PF2 and the EUB338 I probe to a *Alteromonas mediterranea* culture (permeabilized with lysozyme according to (*54*)), to confirm the specific binding of EUB338 I probe to *Alteromonas mediterranea*, and that PF2 was not binding to that bacterium. Since a positive PF2 probe hybridization was not achieved with the replicated permeabilization buffer based on Priest *et al.* (*19*) (i.e., replicating the concentrations of the original Glucanex), we progressively increased the individual enzyme concentrations. Furthermore, lyticase (Sigma-Aldrich), not originally included in Glucanex, was included in the buffer by testing increasing concentrations until a positive hybridization of the PF2 probe to >75% of fungal cells (from our fungal cultures) was achieved with no hybridization of the PF2 probe in the *A. mediterranea* culture (positive hybridization was cross-checked with underlying DAPI staining of the DNA). The final protocol was considered successful when additionally, the bacterial cells where positively stained with the EUB338 I probe but not with the PF2 probe (detailed information of the final fungal-specific CARD-FISH protocol including the new permeabilization buffer can be found in the Table 3-S4).

Once the protocol was successful with the pelagic fungal cultures, it was applied to the filtered seawater samples to quantify pelagic fungal abundance and biomass with the PF2 probe. Simultaneously, a fungal culture was still used as positive control. Cells were counterstained with DAPI-mix [(5.5 parts Citifluor, 1 part Vectashield (Vector Laboratories), 0.5 parts PBS, DAPI final concentration 2 µg/ml)] and analyzed with a Zeiss Axio Imager 2 microscope (1000x magnification, Carl Zeiss, Jena, Germany) using UV-light below 400 nm (DAPI, filter set 49) and the FITC channel (fluorescein isothiocyanate, filter set 44) for the HRP-probe. Fungal biomass was estimated by randomly selecting a minimum of 40 FOVs (125 *x* 125 µm each) and quantified based on biovolume and abundance as mentioned above for CFW staining. A hybridization to fungal cells was considered positive only in the presence of a corresponding DAPI signal below and a simultaneous positive hybridization in the fungal culture. Additionally, and as conservative measure, cells were not considered positive fungi, if there was an overlapping signal from potential autofluorescence potentially originating from phytoplankton cells in the rhodamine channel (filter set 20 HE) (*55*). Final CARD-FISH based fungal biomass were calculated as explained for the CFW biomass estimated explained above: fungal abundance/l was converted into biomass using the culture-based average cell dry mass

('abundance-based'), and fungal biovolume was converted into fungal biomass ('biovolume-based') by applying the culture-based biovolume to C conversion factor.

2.9. Catalyzed reporter deposition fluorescence in situ hybridization (CARD-FISH) for archaeal biomass

Archaeal biomass was estimated after a modified method of Pernthaler *et al.* (*54*) with permeabilization of archaeal cells according to Woebken *et al.* (*56*) by using the general archaeal probe Arch915 (5'-GTGCTCCCCCGCCAATTCCT-3', (*57*)), the euryarchaeal probe Eury806 (5'-CACAGCGTTTACACCTAG-3',(*58*)), a mix of the two crenarchaeal probes Cren537 (5'-TGACCACTTGAGGTGCTG-3',(*58*)) and Cren554 (5'-TTAGGCCCAATAATCMTCCT-3',(*59*)), and the Non338 probe (5'-ACTCCTACGGGAGGCAGC-3', (*60*)). The Non338 probe hybridized with <0.1% of total DAPI counts. Additionally, all archaeal probes were tested on an *Alteromonas mediterranea* culture which resulted in <1% stained cells with the Arch915 probe and no stained cells with the three other probes. This is in agreement with previous investigations reporting that the Arch915 probe overestimates archaeal biomass (*31*). Filters were counterstained with DAPI-mix and analyzed with a Zeiss Axio Imager 2 microscope (as described above). The archaeal abundance was estimated by randomly selecting a minimum of 7-14 FOVs (119 *x* 119 µm each). Total cell numbers were converted into biomass carbon by using the average conversion factor of 8.4 fg C/cell (*61*).

2.10. Flow cytometry and fluorescence microscopy for prokaryotic biomass

Prokaryotic abundance was quantified by counting positive DAPI signals on minimum 10 FOVs (10.25 x 10.25 µm each) per filter (same filter as for archaeal CARD-FISH). An additional 39 samples underwent analysis via flow cytometry, following the methodology outlined elsewhere (*62*). In brief, each sample (0.4 ml) designated for the enumeration of heterotrophic non-pigmented total bacteria was fixed using a 1% buffered paraformaldehyde solution (pH 7.0) plus 0.05% glutaraldehyde, and then incubated at room temperature in darkness for 10 minutes. Subsequently, cells were stained with 4 µl of a 10 SG1 solution (Molecular Probes) for 10 minutes, with a final dilution of 1:1000 (vol/vol), and quantified using a FACSCalibur flow cytometer at a low speed (15 µl min^{-1}). Fluorescent microspheres served as an internal standard, utilizing yellow-green 0.92-µm Polysciences latex beads (10^6 ml^{-1}). Prokaryotic cells were discerned within a dot plot of side scatter versus green

fluorescence (FL1), and population concentrations were estimated utilizing CellQuest and PaintAGate software (Becton Dickinson, Palo Alto, CA).

Final values from DAPI counts and Flow Cytometry were combined, and total cell numbers converted into biomass carbon by using the average conversion factor 10 fg C/cell (*63*). Bacterial biomass was calculated by subtracting archaeal biomass (Arch915 probe) from total prokaryotic biomass.

2.11. Contribution of microbial biomass to POC

To put the fungal biomass into context we additionally compared the contribution of different microbial groups (Fungi, Archaea, Bacteria) to POC in the water column by calculating the percentage of the biomass of each microbial group in C units to the total POC (where total POC is 100%). It is worth noting that in the specific case of abundance-based fungal biomass the contribution might be slightly overestimated, given that cell dry mass includes elements other than carbon. Nevertheless, considering the C:N:P ratio of fungal biomass (250:16:1 (*64*)) carbon should constitute the majority (>93%) of the biomass. This is further supported by our results showing that biovolume-based fungal biomass is in the same range as abundance-based fungal biomass, indicating that indeed carbon made up most of the biomass.

2.12. Estimation of global pelagic marine fungal biomass

In evaluating fungal biomass across the global ocean, we first established the proportions of fungal, archaeal, and bacterial biomass in relation to the total prokaryotic biomass derived from our dataset. Subsequently, knowing that the estimated global marine prokaryotic biomass is 1.6 Gt C (encompassing both free-living and particle-attached) (*1*), we employed the previously determined relationships to compute the global marine fungal biomass. As ergosterol is absent in some fungal groups, we focused on fungal biomass concentrations derived from CARD-FISH and CFW by calculating the average fungal biomass of biovolume-based and abundance-based estimates for each method. We focused on total archaeal biomass quantified with the general Arch915 CARD-FISH probe as the combined euryarchaeal- and crenarchaeal probes might miss some cells, representing probably a higher archaeal contribution and therefore, when compared to fungi, a conservative approach.

2.13. Data analysis and statistics

All statistical analyses were performed in R (v.4.0.3) (*65*). The dplyr package (*66*) was used to calculate summary statistics which are expressed as mean ± standard error. Normal distribution of the data was tested with the Shapiro test (stats package in R). The rstatix package (*67*) was used for pair-wise Wilcoxon test between biomass in different zones and provinces and p-vales adjusted for multiple corrections according to Benjamini and Hochberg (*37*) (BH). The psych package (*68*) was used to calculate Spearman correlations of complete observations and associated statistics, p-values were corrected following the BH method and results were plotted with the corrplot package (*69*). The number of principal components was estimated with the Kfold method (missMDA package (*70*)) and confirmed by plotting the Mean Squared Error of Prediction (MESP) of the first 5 principal components. Missing values were imputed with an iterative PCA algorithm for the previously estimated number of principal components (missMDA package (*70*)). The PCA on the imputed dataset was performed with the FactoMineR package (*71*) and plotted with the factoextra (*72*) and ggplot2 (*73*) packages. Buoyant mass data from the LifeScale software were processed using custom Python scripts and further analyzed in R to calculate dry mass. All other plots were created with the ggpubr (*73*) and gggplot2 (*73*) packages in R or with Ocean Data View (*74*) (ODV, v.5.6.5.).

3. Results and Discussion

3.1. Biomass conversion factors of pelagic fungal cultures

We obtained marine specific conversion factors for fungal biomass by growing 5 oceanic fungi in the lab and using CFW staining, ergosterol extraction, and cell dry mass using a microfluidic mass sensor known as a suspended microchannel resonator (SMR) (see Material and Methods). This led to average conversion factors of 6.19 mg ergosterol/g C, 0.57 pg C/μm^3, and 7998 fg/cell (Table 3-S1 – 3-S3, Fig. 3-S1). Our results for ergosterol per biomass carbon are consistent with the one previous study (*22*), but the carbon per biovolume in our study is around 2 times lower than other studies on other marine provinces or based on terrestrial conversion factors (*18-20*). This underscores the importance of calculating environment-specific conversion factors, emphasizing the dynamic nature of fungal cell wall and the ability to adapt to different environments (*23*).

3.2. Environmental characteristics and oceanic fungal biomass in the Atlantic Ocean

We collected samples for environmental parameters and fungal biomass from the surface to 2000 m during the ANTOM-1 Cruise in 2020/2021, while crossing the Atlantic Ocean from Vigo (Spain) to Punta Arenas (Chile) (Fig. 3-1). We crossed five Longhurst provinces representing different biogeographical water characteristics [North Atlantic Subtropical Gyral Province East (NASE), North Atlantic Tropical Gyral Province (NATR), Western Tropical Atlantic Province (WTRA), South Atlantic Gyral Province (SATL), South Subtropical Convergence Province (SSTC)] characterized by a wide range of different temperatures (3-27 °C), salinity (32-37), POC (0.6-108 µg/l) and chlorophyll a concentrations (0-0.49 µg/l) (Fig. 3-2). The SSTC province exhibited a significantly lower salinity, but higher chlorophyll a concentration in the 2-20 µm size fractionation, compared to all other provinces ($p<0.05$, pairwise Wilcoxon Test). The highest values of chlorophyll a and POC were found towards the more southern stations, indicative of an increase in phytoplankton biomass and accumulation of organic matter in the shallower waters of the southern sites (Fig. 3-S2).

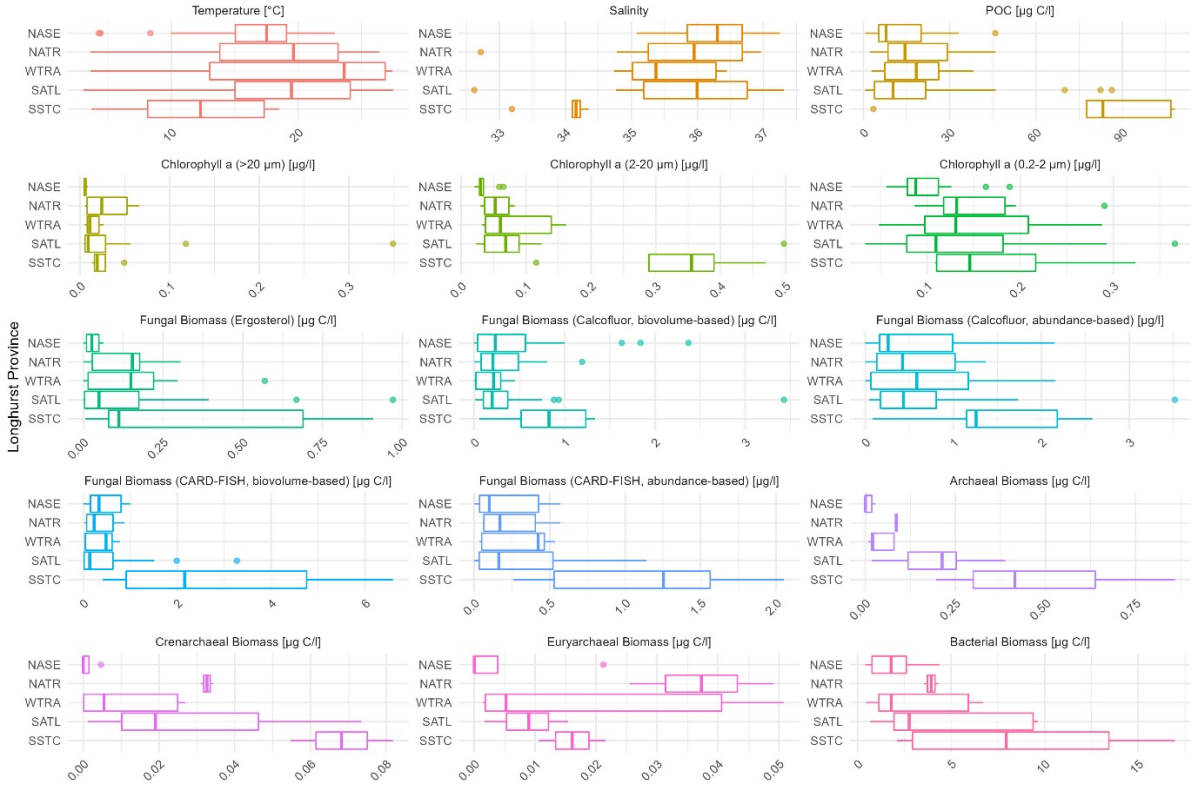

Figure 3-2. Environmental parameters and microbial biomass in different Longhurst biogeographical provinces along the sampling transect. North Atlantic Subtropical Gyral Province East (NASE), North Atlantic Tropical Gyral Province (NATR), Western Tropical Atlantic Province (WTRA), South Atlantic Gyral Province (SATL), South Subtropical

Convergence Province (SSTC). The box represents the interquartile range (IQR) containing the central 50% of the data, the line inside the box depicts the median, and whiskers extend to 1.5 times the IQR, with outliers plotted individually.

We applied the culture derived biomass conversion factors to quantify marine pelagic fungal biomass by ergosterol extraction, CFW staining and CARD-FISH. Additionally, for CFW and CARD-FISH microscopy, we compared fungal biomass estimated by cell biovolume (biovolume-based) and by cell dry mass (abundance-based) (Fig. 3-2, Fig. 3-S2)

Ergosterol was detected in most stations in surface waters (5 m depth), the deep chlorophyll maximum (DCM) layer and at 200 m depth, but only once at 375 m and at 400 m, remaining undetected in the bathypelagic. This indicates that most Dikarya-derived fungal biomass is present in the upper 200 m, with a peak in southern stations (Fig. 3-S2). The highest ergosterol-based fungal biomass of 0.97 µg C/l was found in the DCM (Fig. 3-S2), which is consistent with the average ergosterol-based fungal biomass of 1.02 µg C/l reported in Arctic coastal waters (*22*). Our maximum value is similar to the average value reported by Hassett *et al.* (*22*), likely because their sampling was restricted to six stations close to the highly productive coastal waters of Svalbard, whereas our transect covered a larger latitudinal distance crossing various climatic and trophic zones. The other study using ergosterol to quantify fungal biomass reported an average 0.11 to 0.28 mg C/l fungal biomass in coastal waters of the South China Sea (*14*). This estimate is orders of magnitude higher than what was found by Hassett *et al*. (*22*) and by us, probably due to the location of the study area in a bay in close proximity to major Chinese cities (e.g., Hong Kong, Shenzen) permanently impacted by anthropogenic influences and river discharges leading to increased abundance of microbes (*14*). Although ergosterol-based estimations are conservative (since ergosterol is absent in early diverging divisions like Chytridiomycota (*21*) known as prevalent parasites during phytoplankton blooms (*26*)), they reveal a substantial contribution of fungi to biomass in the ocean.

Based on CFW staining, we also detected fungal cells in all surface and DCM samples (8.1×10^3 – 4.4×10^5 cells/l). We calculated the CFW fungal biomass by two independent approaches: 1) by directly measuring the biovolume of the cells ('biovolume-based'), and 2) by converting the number of fungal cells into biomass applying the conversion factor derived from the SMR ('abundance-based'). The maximum biomass concentrations were 3.4 µg C/l and 3.5 µg/l estimated by fungal biovolume and fungal abundances, respectively (Fig. 3-S2). Abundance-based fungal biomass increased in surface oligotrophic waters (middle of the transect) relative to biovolume-based biomass. In contrast, biovolume-based estimates reach

their peak at northern and southern stations closer to the coast (Fig. 3-S2). The discrepancy between these two estimation methods likely arises from the prevalence of smaller cells in oligotrophic areas, while larger cells were more commonly detected in proximity to coastal areas (fungal biovolume size range: 2.07 μm^3-238 μm^3). These results indicate that purely abundance-based methods may lead to an overestimation of overall biomass, as they do not account for variations in cell sizes. Although CFW binds not only to chitin but also to cellulose, and is absent in certain fungal life stages and can be present in non-fungal species (*27, 28*), CFW and ergosterol based estimates are within the same order of magnitude, confirming the substantial contribution of fungi to ocean biomass.

We found even higher fungal biomass with our adapted CARD-FISH protocol (Table 3-S4), reaching up to 6.6 µg C/l (1.2 x 10^7 μm^3/l) for biovolume-based and 2.1 µg C/l (2.6 x 10^5 cells/l) for abundance-based estimates (Fig. 3-S2). Consistent with CFW estimates, a higher abundance-based biomass was detected in the oligotrophic (mid transect) surface waters compared to fungal biovolume-based estimates (Fig. 3-S2). All biomass quantification methods were consistently showing no statistically significant difference among different Longhurst provinces ($p>0.05$, pairwise Wilcoxon Test), a positive correlation with POC and chlorophyll a, and a negative correlation with depth (Fig. 3-3, Fig. 3-S3). Similar links between fungal and phytoplankton biomass were reported in the South China Sea (*14*) and in the coastal upwelling areas of Chile (*20*), altogether underscoring the important role of marine pelagic fungi in processing phytoplankton-derived organic matter (*4, 6-8, 29, 30*). Collectively, there is a general agreement among all approaches, confirming the substantial contribution of fungal biomass, even across a wide range of different biogeographical provinces in the open ocean.

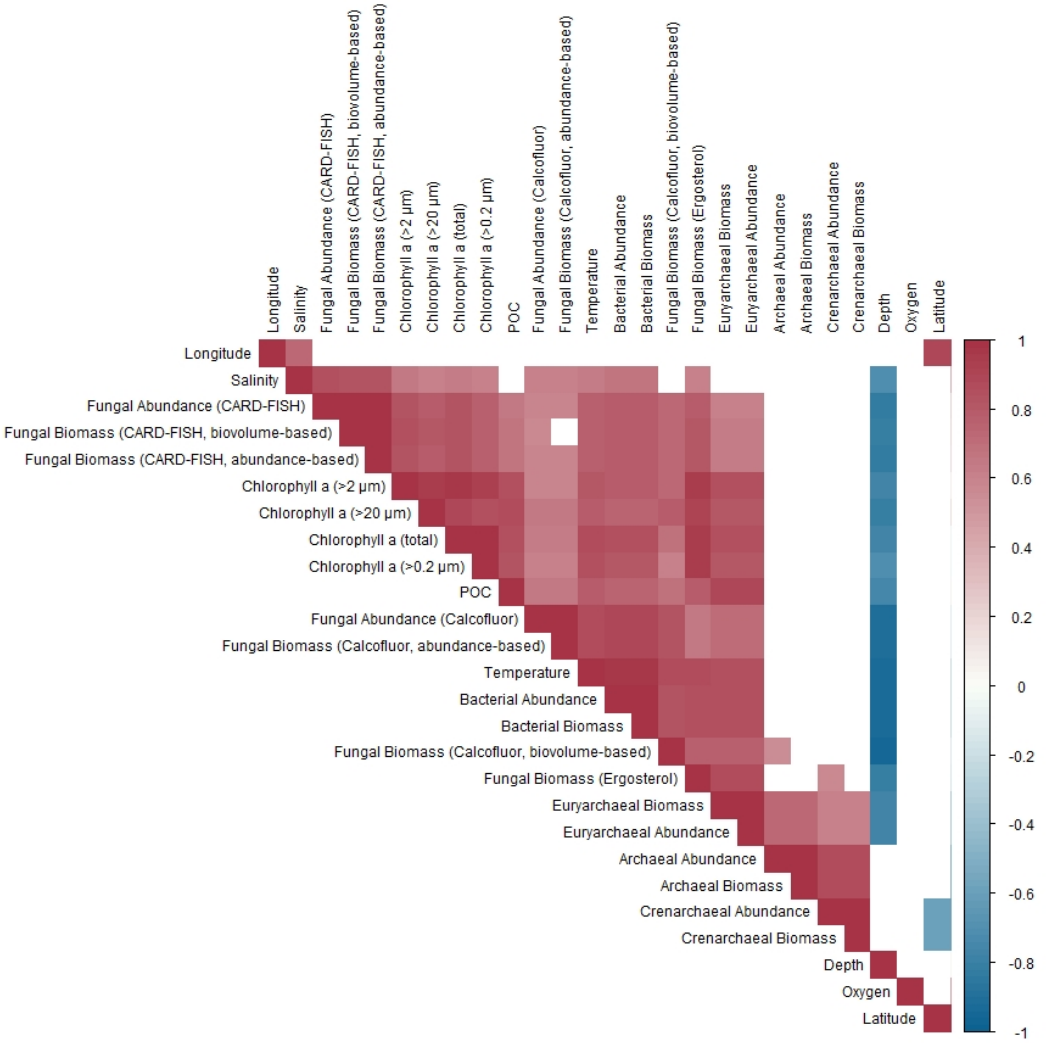

Figure 3-3. Relationship between environmental parameters and microbial biomass in the oceanic water column of the Atlantic Ocean. Spearman cross-correlation analysis of environmental parameters and microbial biomasses. Only significant (p-value <0.05) relationships are shown, red indicates positive correlation, blue indicates negative relation. P-values were adjusted for multiple comparisons according to the Benjamini & Hochberg method (*37*).

3.3. Fungal biomass is lower than bacterial but higher than archaeal biomass

The highest bacterial biomass (17 µg C/l) was found in surface waters, and significantly decreased from the epipelagic to the bathypelagic (epipelagic: 7.8 ± 1.3 µg C/l; mesopelagic: 1.8 ± 0.2 µg C/l; bathypelagic: 0.5 ± 0.1 µg C/l) ($p<0.05$, pairwise Wilcoxon Test) (Fig. 3-2). Similarly, total archaeal biomass decreased with depth, with a maximum concentration of 0.85 µg C/l in the epipelagic (epipelagic: 0.25 ± 0.08 µg C/l; mesopelagic: 0.11 ± 0.05 µg C/l; bathypelagic: 0.01 ± 0.01 µg C/l). In general, we detected more cells with the total archaeal

probe (Arch915) than with the combined results of the crenarchaeotal probe (Cren537/554) and the euryarchaeal probe (Eury806) (maximum crenarchaeal biomass in epipelagic: 0.08 µg C/l, maximum euryarchaeal biomass in epipelagic: 0.05 µg C/l) (Fig. 3-2). This is in agreement with previous investigations reporting that the Arch915 probe overestimates archaeal biomass (*31*), indicating that with this probe we likely overestimate archaeal abundances/biomass. CARD-FISH [1.3 ± 0.3 µg C/l (biovolume-based), 0.63 ± 0.1 µg C/l (abundance-based)] and CFW [CFW: 0.62 ± 0.1 µg C/l (biovolume-based), 1 ± 0.1 µg C/l (abundance-based)] based fungal biomass were higher compared to total archaeal biomass, particularly in the epipelagic ($p<0.05$, pairwise Wilcoxon Test), irrespectively if estimated by cell biovolume or cell abundances. However, ergosterol-based fungal biomass (0.23 ± 0.04 µg C/l) was not significantly different from archaeal biomass (0.25 ± 0.08 µg C/l) ($p = 0.91$, pairwise Wilcoxon Test), likely because ergosterol can underestimate fungal biomass, and the Arch915 probe overestimates archaeal biomass. Altogether, our study revealed an overall agreement between the fungal biomass estimation methods employed (Fig. 3-3 and Fig. 3-S3), indicating that the biomass of pelagic fungi is higher than that of Archaea. With Archaea acknowledged for their relevant contributions to the marine ecosystem and carbon cycle, it is crucial to provide comparable importance to pelagic fungi.

3.4. Contribution of different microbial groups to particulate organic carbon

The contribution of fungal, archaeal, and bacterial biomass to total POC generally decreased with depth (Fig. 3-4), although, this trend varied based on the microbial group (Fig. 3-4). In the epipelagic, fungal biomass estimated by ergosterol extraction, total archaeal biomass, euryarchaeal biomass and crenarchaeal biomass contributed on average approximately up to 1% to total POC (ergosterol-derived fungal biomass: 0.7 ± 0.1%; total archaeal biomass: 0.4 ± 0.1%) (Fig. 3-4). Fungal biomass estimated by CARD-FISH and CFW staining contributed on average between 1.9 and 4.2% to the total POC (Fig. 3-4). Bacterial biomass contributed the most to total POC with an average of 20% (± 3.2). Likewise, within mesopelagic waters, fungal biomass derived from ergosterol and archaeal biomass contributed an average of up to 1% to the total POC (Fig. 3-4). Fungal biomass estimates obtained through CFW staining and CARD-FISH ranged between 1.7 and 7.5% on average in terms of their contribution to total POC (Fig. 3-4). Bacterial biomass again dominated with an average contribution of 38% to total POC in the mesopelagic ocean (Fig. 3-4). Lastly, in the bathypelagic ocean, fungal biomass estimated by ergosterol and CFW microscopy as well as

archaeal biomass contributed on average less than 1% to total POC (Fig. 3-4). Fungal biomass, as determined by CARD-FISH, constituted on average 2.3% of the total POC in the bathypelagic zone, while the contribution of bacterial biomass declined, contributing approximately 28% to the total POC (Fig. 3-4).

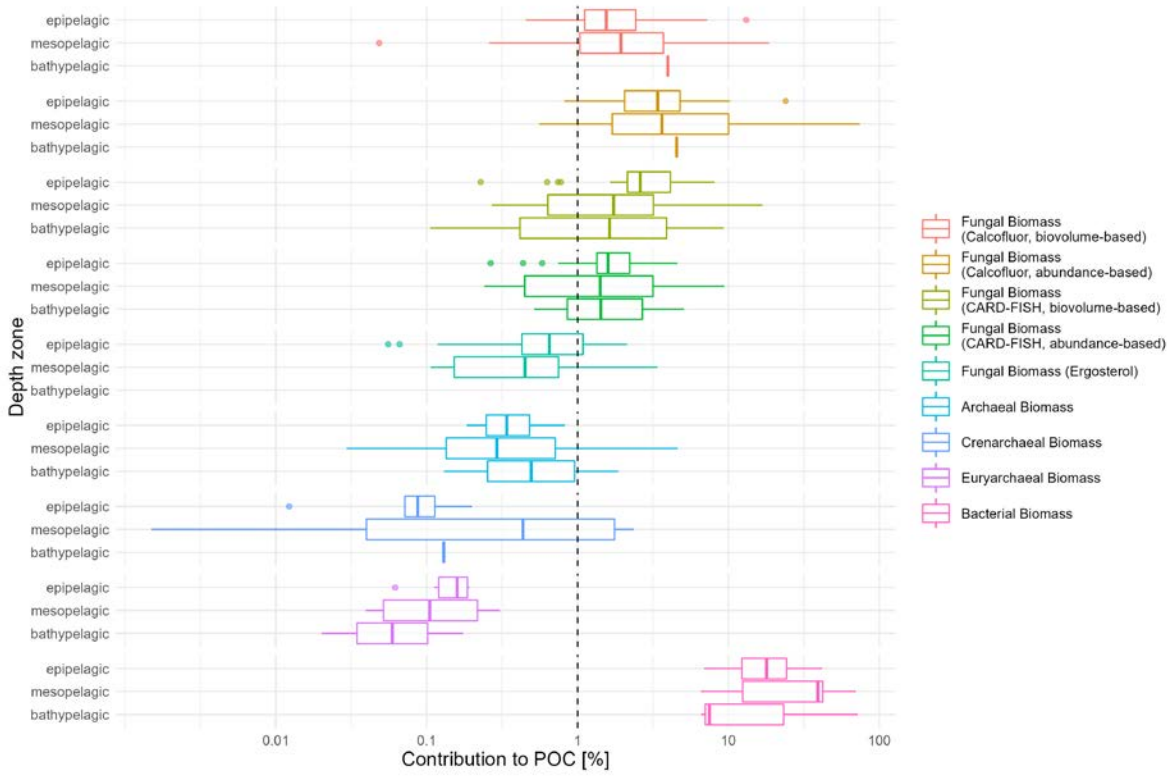

Figure 3-4. Contribution of microbial biomass to particulate organic carbon (POC) in different depth zones of the Atlantic Ocean. Epipelagic (0-200 m), mesopelagic (200-1000 m), bathypelagic (1000-4000 m). The dashed vertical line indicates 1% contribution to POC. Fungal biovolume-based biomass is derived from individual cell biovolume whereas abundance-based biomass is derived from individual cell dry mass. Note the logarithmic scale on the x-axis. The box represents the interquartile range (IQR) containing the central 50% of the data, the line inside the box depicts the median, and whiskers extend to 1.5 times the IQR, with outliers plotted individually.

The observed depth patterns in the contribution of various archaeal groups to POC align with the idea that Euryarchaeota primarily function as heterotrophs, leading to higher relative abundances near the surface (*32, 33*), whereas most Crenarchaeota are identified as ammonia-oxidizing chemoautotrophs, showing lower dependence on phytoplankton biomass and consequently appearing in higher relative abundances in the mesopelagic ocean (*32, 33*). Irrespective of depth, fungal biomass constituted a greater proportion of POC than archaeal

biomass (Fig. 3-4). This observation again underscores the significant role of marine pelagic fungal biomass in oceanic ecosystems.

3.5. Estimation of global pelagic marine fungal biomass

CFW-based fungal biomass was equivalent to 13% (± 2.4) of total prokaryotic biomass, which is remarkably consistent with the 12% (± 1.8) from the CARD-FISH-based fungal biomass, and much higher than the 3% (± 0.8) contribution of archaeal biomass. This 12-13% contribution translates into a biomass range of 0.19-0.21 Gt C of marine pelagic fungi globally. This global fungal biomass is lower than the estimated 0.3 Gt C by Bar-On *et al.* (*24*), likely because it was based on the available data at the time which was restricted to two studies based on gene copy numbers (*12, 34*), one on fungal biomass in nutrient-rich waters during a phytoplankton bloom (*20*) and one focusing only on deep-sea marine snow particles (*18*). Also, the biovolume to carbon conversion factors used in the latter two studies were not based on marine pelagic fungi. We expand the available data by covering a larger number of samples across a wide range of depths/latitudes, applying newly calculated biomass conversion factors (specifically to marine pelagic fungi) and by using three different quantification methods in parallel. Finally, considering that in our study bacterial biomass accounted for 97% (± 0.8) of the total prokaryotic biomass, we derived a biomass ratio of Archaea:Fungi:Bacteria of 1:4:32 in the water column of the global ocean.

4. Conclusions

Accurate biomass quantification is a critical measurement essential for calculating global budgets and serves as a crucial parameter in modelling major biogeochemical cycles in the ocean. Our results indicate that fungi are not only important in terms of diversity and activity as recently indicated (*4-9, 35, 36*), but also in terms of biomass and therefore relevant in the marine carbon cycle. Their relevant contribution underscores the importance of incorporating them into biogeochemical models. This study sets the base, particularly critical under the light of global changes, but future studies should expand global marine fungal biomass quantifications across diverse oceans and latitudes, further advancing our understanding of the contribution of pelagic fungi to global biomass and elemental cycles in the ocean.

Acknowledgements

This work was supported by the Austrian Science Fund (FWF) projects OCEANIDES (P34304-B), ENIGMA (TAI534), EXEBIO (P35248), and OCEANBIOPLAST (P35619-B) to F.B. ANTOM and MIQAS projects (Spanish Ministry of Science, Innovation and Universities PGC2018-096612-B-I00 and PID2021-128084OB-I00) and University of Vigo Marine Research Center (CIM) also provided funding and technical support. The unit of marine technology (UTM-CSIC) and the crew of RV Sarmiento de Gamboa is acknowledged for the support during the ANTOM-1 cruise.

Author Contributions

E.B. and F.B. conceived the project, collected the environmental samples and interpreted the data. E.B performed the experiments and analysed the data. E.B., C.S., S.K., F.P. and C.D. analysed the microscopic data. E.B., S.K., J.D., M.V-C. and N.B. collected samples for/and analysed prokaryotic cell counts. E.B., C.A., C.S. and S.K. developed the fungal CARD-FISH protocol. E.B. and C.D. quantified POC. E.B. and G.C.G. extracted ergosterol. B.R.K.R. and M.P. analysed the fungal cell dry mass. B.M. and Fr.B. quantified ergosterol. A.F-L and C.S. collected and quantified chlorophyll data. J.D., N.B. and M.V-C organized the cruise. F.B. supervised the project. The manuscript was written by E.B. and F.B. All authors contributed to editing the manuscript and approved the final version.

References

1. Y. M. Bar-On, R. Phillips, R. Milo, The biomass distribution on Earth. *Proc. Natl. Acad. Sci. U.S.A* **115**, 6506-6511 (2018).
2. R. Cavicchioli *et al.*, Scientists' warning to humanity: microorganisms and climate change. *Nat. Rev. Microbiol.* **17**, 569-586 (2019).
3. P. G. Falkowski, T. Fenchel, E. F. Delong, The microbial engines that drive Earth's biogeochemical cycles. *Science* **320**, 1034-1039 (2008).
4. M. Cunliffe, A. Hollingsworth, C. Bain, V. Sharma, J. D. Taylor, Algal polysaccharide utilisation by saprotrophic planktonic marine fungi. *Fungal Ecol.* **30**, 135-138 (2017).
5. S. E. Morales, A. Biswas, G. J. Herndl, F. Baltar, Global structuring of phylogenetic and functional diversity of pelagic fungi by depth and temperature. *Front. Mar. Sci.* **6**, 131 (2019).
6. W. D. Orsi *et al.*, Carbon assimilating fungi from surface ocean to subseafloor revealed by coupled phylogenetic and stable isotope analysis. *ISME J.* **16**, 1245-1261 (2021).
7. F. Baltar, Z. Zhao, G. J. Herndl, Potential and expression of carbohydrate utilization by marine fungi in the global ocean. *Microbiome* **9**, 1-10 (2021).
8. E. Breyer, Z. Zhao, G. J. Herndl, F. Baltar, Global contribution of pelagic fungi to protein degradation in the ocean. *Microbiome* **10**, 1-11 (2022).
9. X. Peng, D. L. Valentine, Diversity and N2O production potential of fungi in an oceanic oxygen minimum zone. *J. Fungi* **7**, 218 (2021).
10. E. Breyer, F. Baltar, The largely neglected ecological role of oceanic pelagic fungi. *Trends Ecol. Evol.* **38**, 870-888 (2023).
11. J. D. Taylor, M. Cunliffe, Multi-year assessment of coastal planktonic fungi reveals environmental drivers of diversity and abundance. *ISME J.* **10**, 2118 (2016).
12. X. Wang *et al.*, Distribution and diversity of planktonic fungi in the West Pacific Warm Pool. *Plos One* **9**, e101523 (2014).
13. Y. Wang, B. Sen, Y. He, N. Xie, G. Wang, Spatiotemporal distribution and assemblages of planktonic fungi in the coastal waters of the Bohai Sea. *Front. Microbiol.* **9**, 584 (2018).
14. Y. Wang, K. Sen, Y. He, Y. Xie, G. Wang, Impact of environmental gradients on the abundance and diversity of planktonic fungi across coastal habitats of contrasting trophic status. *Sci. Total. Environ.* **683**, 822-833 (2019).

15. K. Sen *et al.*, Spatial Patterns of Planktonic Fungi Indicate Their Potential Contributions to Biological Carbon Pump and Organic Matter Remineralization in the Water Column of South China Sea. *J. Fungi* **9**, 640 (2023).
16. Y. Duan *et al.*, Patchy distributions and distinct niche partitioning of mycoplankton populations across a nearshore to open ocean gradient. *Microbiol. Spectr.* **9**, e01470-01421 (2021).
17. K. Sen, M. Bai, B. Sen, G. Wang, Disentangling the structure and function of mycoplankton communities in the context of marine environmental heterogeneity. *Sci. Total. Environ.* **766**, 142635 (2021).
18. A. B. Bochdansky, M. A. Clouse, G. J. Herndl, Eukaryotic microbes, principally fungi and labyrinthulomycetes, dominate biomass on bathypelagic marine snow. *ISME J.* **11**, 362-373 (2017).
19. T. Priest, B. Fuchs, R. Amann, M. Reich, Diversity and biomass dynamics of unicellular marine fungi during a spring phytoplankton bloom. *Environ. Microbiol.* **23**, 448-463 (2021).
20. M. H. Gutiérrez, S. Pantoja, E. Tejos, R. A. Quinones, The role of fungi in processing marine organic matter in the upwelling ecosystem off Chile. *Mar. Biol.* **158**, 205-219 (2011).
21. M. H. Gutiérrez *et al.*, Biochemical fingerprints of marine fungi: implications for trophic and biogeochemical studies. *Aquat. Microb. Ecol.* **84**, 75-90 (2020).
22. B. T. Hassett *et al.*, Arctic marine fungi: biomass, functional genes, and putative ecological roles. *ISME J.* **13**, 1484-1496 (2019).
23. N. A. Gow, M. D. Lenardon, Architecture of the dynamic fungal cell wall. *Nat. Rev. Microbiol.* **21**, 248-259 (2022).
24. Y. M. Bar-On, R. Milo, The Biomass Composition of the Oceans: A Blueprint of Our Blue Planet. *Cell* **179**, 1451-1454 (2019).
25. E. Laiolo *et al.*, Metagenomic probing toward an atlas of the taxonomic and metabolic foundations of the global ocean genome. *Front. Sci.* **1**, (2024).
26. M. Kagami, T. Miki, G. Takimoto, Mycoloop: chytrids in aquatic food webs. *Front. Microbiol.* **5**, 166 (2014).
27. M. S. Fuller, I. Barshad, Chitin and Cellulose in the cell walls of Rhizidiomyces sp. *Am. J. Bot.* **47**, 105-109 (1960).
28. C. A. Durkin, T. Mock, E. V. Armbrust, Chitin in diatoms and its association with the cell wall. *Eukaryot. Cell* **8**, 1038-1050 (2009).

29. M. Kagami, A. de Bruin, B. W. Ibelings, E. Van Donk, Parasitic chytrids: their effects on phytoplankton communities and food-web dynamics. *Hydrobiologia* **578**, 113-129 (2007).
30. I. Klawonn *et al.*, Characterizing the "fungal shunt": Parasitic fungi on diatoms affect carbon flow and bacterial communities in aquatic microbial food webs. *Proc. Natl. Acad. Sci. U.S.A* **118**, e2102225118 (2021).
31. A. Pernthaler, C. M. Preston, J. Pernthaler, E. F. DeLong, R. Amann, Comparison of Fluorescently Labeled Oligonucleotide and Polynucleotide Probes for the Detection of Pelagic Marine Bacteria and Archaea. *Appl. Environ. Microbiol.* **68**, 661-667 (2002).
32. M. B. Karner, E. F. DeLong, D. M. Karl, Archaeal dominance in the mesopelagic zone of the Pacific Ocean. *Nature* **409**, 507-510 (2001).
33. A. E. Santoro, R. A. Richter, C. L. Dupont, Planktonic Marine Archaea. *Annu. Rev. Mar. Sci.* **11**, 131-158 (2019).
34. M. C. Pernice *et al.*, Large variability of bathypelagic microbial eukaryotic communities across the world's oceans. *ISME J.* **10**, 945-958 (2016).
35. A. Amend *et al.*, Fungi in the Marine Environment: Open Questions and Unsolved Problems. *MBio* **10**, e01189-01118 (2019).
36. X. Peng *et al.*, Planktonic Marine Fungi: A Review. *JGR Biogeosciences* **129**, e2023JG007887 (2024).
37. Y. Benjamini, Y. Hochberg, Controlling the False Discovery Rate: A Practical and Powerful Approach to Multiple Testing. *J. R. Stat. Soc. Series B.* **57**, 289-300 (1995).
38. K. Salazar Alekseyeva, G. J. Herndl, F. Baltar, Extracellular enzymatic activities of oceanic pelagic fungal strains and the influence of temperature. *J. Fungi* **8**, 571 (2022).
39. N. Cermak *et al.*, Direct single-cell biomass estimates for marine bacteria via Archimedes' principle. *ISME J.* **11**, 825-828 (2017).
40. F. Feijó Delgado *et al.*, Intracellular Water Exchange for Measuring the Dry Mass, Water Mass and Changes in Chemical Composition of Living Cells. *PLOS ONE* **8**, e67590 (2013).
41. S. B. Moran, M. A. Charette, S. M. Pike, C. A. Wicklund, Differences in seawater particulate organic carbon concentration in samples collected using small- and large-volume methods: the importance of DOC adsorption to the filter blank. *Mar. Chem.* **67**, 33-42 (1999).

42. UNESCO, Protocols for the Joint Global Ocean Flux Study (JGOFS) Core Measurement. *Intergovernmental Oceanographic Commission, Manual and Guides* **29**, 169 (1994).
43. M. Estrada, in *Libro blanco de métodos y técnicas de trabajo oceanográfico en la Expedición MALASPINA*. (2012), pp. 399-405.
44. E. G. Bligh, W. J. Dyer, A rapid method of total lipid extraction and purification. *Can. J. Biochem. Physiol.* **37**, 911-917 (1959).
45. K. Salazar Alekseyeva *et al.*, Adapting an ergosterol extraction method with marine yeasts for the quantification of oceanic fungal biomass. *J. Fungi* **7**, 690 (2021).
46. V. Gulis, F. Bärlocher, in *Methods in Stream Ecology,* F. R. Hauer, G. A. Lamberti, Eds. (Academic Press, Cambridge, 2017), pp. 177-192.
47. L. Ory *et al.*, Detection of ergosterol using liquid chromatography/electrospray ionization mass spectrometry: Investigation of unusual in-source reactions. *Rapid Commun. Mass Spectrom.* **34**, e8780 (2020).
48. S. Rasconi, M. Jobard, L. Jouve, T. Sime-Ngando, Use of Calcofluor White for Detection, Identification, and Quantification of Phytoplanktonic Fungal Parasites. *Appl. Environ. Microbiol.* **75**, 2545-2553 (2009).
49. I. Klawonn *et al.*, Fungal parasitism on diatoms alters formation and bio–physical properties of sinking aggregates. *Commun. Biol.* **6**, 206 (2023).
50. A. Pernthaler, R. Amann, Simultaneous Fluorescence In Situ Hybridization of mRNA and rRNA in Environmental Bacteria. *Appl. Environ. Microbiol.* **70**, 5426-5433 (2004).
51. S. Thiele, B. M. Fuchs, R. I. Amann, in *Treatise on Water Science,* P. Wilderer, Ed. (Elsevier, Oxford, 2011), pp. 171-189.
52. V. A. Kempf, K. Trebesius, I. B. Autenrieth, Fluorescent in situ hybridization allows rapid identification of microorganisms in blood cultures. *J. clin. microbiol.* **38**, 830-838 (2000).
53. R. I. Amann *et al.*, Combination of 16 rRNA-targeted oligonucleotide probes with flow cytometry for analyzing mixed microbial populations. *Appl. Environ. Microbiol.* **56**, 1919-1925 (1990).
54. A. Pernthaler, J. Pernthaler, R. Amann, Fluorescence in situ hybridization and catalyzed reporter deposition for the identification of marine bacteria. *Appl. Environ. Microbiol.* **68**, 3094-3101 (2002).
55. E. Breyer *et al.*, Autofluorescence is a Common Trait in Different Oceanic Fungi. *J. Fungi* **7**, 709 (2021).

56. D. Woebken, B. M. Fuchs, M. M. M. Kuypers, R. Amann, Potential interactions of particle-associated anammox bacterial with bacterial and archaeal partners in the Nambian Upwelling System. *Appl. Environ. Microbiol.* **73**, 4648-4657 (2007).
57. D. A. Stahl, R. Amman, *Development and application of nucleic acid probes in bacterial systematics*. (Wiley & Sons Ltd, Chichester, 1991).
58. E. Teira, T. Reinthaler, A. Pernthaler, J. Pernthaler, G. J. Herndl, Combining catalyzed reporter deposition-fluorescence in situ hybridization and microautoradiography to detect substrate utilization by Bacteria and Archaea in the deep ocean. *Appl. Environ. Microbiol.* **70**, 44411-44414 (2004).
59. R. Massana, A. E. Murray, C. M. Preston, E. F. DeLong, Vertical distribution and phylogenetic characterization of marine planktonic *Archaea* in the Santa Barbara Channel. *Appl. Environ. Microbiol.* **63**, 50-56 (1997).
60. G. Wallner, R. Amann, W. Beisker, Optimizing fluorescent in situ hybridization with rRNA-targeted oligonucleotide probes for flow cytometric identification of microorganisms. *Cytometry* **14**, 136-143 (1993).
61. G. J. Herndl *et al.*, Contribution of *Archaea* to total prokaryotic production in the deep Atlantic Ocean. *Appl. Environ. Microbiol.* **71**, 2303-2309 (2005).
62. T. Falcioni, S. Papa, J. M. Gasol, Evaluating the flow-fytometric nucleic acid double-staining protocol in realistic rituations of planktonic bacterial death. *Appl. Environ. Microbiol.* **74**, 1767-1779 (2008).
63. H. Ducklow, in *Microbial ecology of the oceans.,* D. L. Kirchman, Ed. (Wiley-Liss, New York, 2000), pp. 85-120.
64. J. Zhang, J. J. Elser, Carbon:Nitrogen:Phosphorus Stoichiometry in Fungi: A Meta-Analysis. *Front. Microbiol.* **8**, 1281 (2017).
65. R Core Team, R: A language and environment for statistical computing [Internet]. Vienna, Austria. (2020).
66. H. Wickham, R. François, L. Henry, K. Müller, Dplyr: A grammar of data manipulation. (2022).
67. A. Kassambara, Rstatix: Pipe-Friendly Framework for Basic Statistical Tests*, R package vers,* 0.7.2. (2023).
68. W. Revelle, psych: Procedures for Psychological, Psychometric, and Personality Research. 2024.
69. T. Wit, V. Simko, R package 'corrplot': Visualization of a Correlation Matrix. (2021).

70. J. Josse, F. Husson, missMDA: A Package for Handling Missing Values in Multivariate Data Analysis. *J. Stat. Software* **70**, 1-31 (2016).
71. S. Le, J. Josse, F. Husson, FactoMineR: An R Package for Multivariate Analysis. *J. Stat. Software* **25**, 1-18 (2008).
72. A. Kassambara, F. Mundt, factoextra: Extract and Visualize the Results of Multivariate Data Analyses. (2020).
73. H. Wickham, *ggplot2: elegant graphics for data analysis*. (Springer Science & Business Media, 2016).
74. R. Schlitzer, Ocean Data View. (2023).

General Discussion

1. Main Aim

The primary aim of this thesis was to investigate the ecology and biogeochemistry of oceanic fungi. Particularly, employing both culture-dependent and -independent methodologies, our objective was to elucidate their physiological characteristics and their role in organic matter degradation and microbial biomass dynamics within the ocean. First, we conducted experiments using three phylogenetically diverse pelagic fungal isolates to assess their carbon substrate preferences and growth responses under various environmental conditions, such as salinity and temperature (Chapter 1). Furthermore, we presented novel findings on global marine pelagic fungal protein degradation by linking fungal protease genes with transcripts and comparing them to protein degradation of prokaryotes (Chapter 2). Lastly, we conducted the first direct quantification of oceanic fungal biomass using three distinct methods simultaneously across a large oceanic transect covering a wide range of environmental conditions. We compared these biomass estimations with other essential marine microbes, including bacteria and archaea, and provided global estimates for mycoplankton biomass (Chapter 3). The following sections will synthesize the results of the three previous chapters and put them into a global context.

2. Functional diversity and physiology of marine mycoplankton

Given their role as main degraders/recyclers of organic matter in terrestrial environments, aquatic fungi are expected to play similar roles due to their parasitic and/or saprotrophic lifestyles (*1-3*). Besides their role as parasites in the marine mycoloop (*4*), saprotrophic fungi are also expected to significantly contribute to oceanic carbon cycling by decomposing phytoplankton-derived organic matter (*3, 5*). This is supported by previous studies that linked oceanic fungi to blooms of marine phytoplankton (*6-8*), showing that their degradation activities intensified during periods of elevated phytoplankton biomass (*6*). Moreover, recently marine mycoplankton was linked to the production of N_2O in oxygen minimum zones (*9*), underscoring their potential critical role in ocean biogeochemistry (*3*).

This leads us to the following questions: What is known about the degradation of other important elements (i.e., nitrogen)? How does this relate to other main water column decomposers (prokaryotes), and what does this tell us about marine biogeochemical cycles? What information can we gain from *in vitro* experiments, where we can directly manipulate the

environment of marine pelagic fungal cultures (e.g. different substrate types, changes salinity and temperature)?

The advancement of high throughput sequencing techniques has been instrumental in highlighting the distribution of mycoplankton (*3, 10*). However, direct links between their phylogenetic and functional diversity remain limited. Recently, for the first time, the global functional potential of oceanic fungi was characterized through the integration of metagenomics and global ocean sampling schemes (TARA Oceans project) (*10*). This characterization revealed the ubiquitous presence of mycoplankton in the water column, with a core metabolism contributing to various biogeochemical cycles, including carbohydrate, amino acid, and lipid metabolism (*10*). Additionally, a metagenomic study in the South China Sea highlighted amino acid, carbohydrate, and energy metabolism, among others, as core functions of marine mycoplankton (*11*). Similar results were reported before for marine subsurface fungi (*12*). Notably, depth stratification in fungal functions within the water column (*10*) resembled patterns observed for prokaryotic functions (*13*), with distinct differences between epipelagic and mesopelagic waters (*10*). These differences encompassed shifts in UV protection, dietary changes to carbohydrate limitation, and utilization of alternative energy sources. Furthermore, a latitudinal gradient in fungal functional diversity linked to temperature variations suggests potential impacts of climate change on mycoplankton functions (*10*).

Metagenomic analyses offer valuable insights into the potential functional capabilities of microbial communities, including fungi, but may not fully capture their actual ecological roles. In contrast, metatranscriptomics (the study of gene expression profiles) provide a more direct view of microbial activity. In oceanic environments, metatranscriptomic studies have revealed significant fungal involvement in subsurface nutrient dynamics (*12*) and carbon cycling (*14-16*). Specifically, recent research on pelagic fungi have demonstrated the active expression of fungal genes related to carbohydrate degradation in the water column (Fig. 4-1) (*14-16*). Depth-related analyses indicate a stratification in fungal CAZyme activity, with higher expression and diversity observed in the mesopelagic waters compared to the epipelagic zone (*14*). This is contrary to the distribution pattern reported for pelagic prokaryotic CAZymes (*3, 17*). Similar, in mesopelagic waters, the ratio of secretory to total fungal CAZymes was comparatively higher than in epipelagic waters (*14*). Overall, fungal carbohydrate degradation was dominated by Dothideomycetes (followed by Malasseziomycetes) in the epipelagic and by Leotiomycetes (followed by Eurotiomycetes) in the mesopelagic (*14*), whereas Chytridiomycota were only regionally relevant (Fig. 4-1) (*14*). This aligns with findings from DNA stable isotope probing (DNA-SIP) studies (*8, 16*), indicating specific fungal taxa like

Cladosporium and *Malassezia* (both Ascomycota) as significant contributors to phytoplankton-derived carbohydrate degradation in oceanic environments. Globally, fungal CAZyme functions exhibited a consistent diversity across depths and oceanic regions, dominated by glycoside hydrolases (GH), glycosyl transferases (GT) and auxiliary activities (AA) (*3, 14*). In contrast, pelagic prokaryotes had a significant proportion of carbohydrate esterases (CE) and carbohydrate-binding modules (CBM), which are not prevalent in pelagic fungi (Fig. 4-1) (*3, 14, 17*).

Consistently with fungal CAZymes, by applying the same approach to marine pelagic fungal proteases (responsible for the degradation of proteins), we found in this Thesis increased abundance, expression, diversity, and percentage of secretory proteases with increasing depth (Fig. 2-1). In contrasts, a previous study reported that the distribution of prokaryotic proteases showed no depth-related changes (*17*). Additionally, we found a strong correlation between fungal CAZymes and proteases (Fig. 2-2), suggesting a close coupling of fungal carbohydrate and protein degradation in the ocean (*3*). Interestingly, similar to fungal carbohydrate degradation, Dothideomycetes (followed by Malasseziomycetes) prevailed in epipelagic waters, while Leotiomycetes (followed by Eurotiomycetes) dominated in mesopelagic waters (Fig. 2-3, Fig. 4-1). The most widely used fungal peptidase subfamilies were serine and metallo peptidases (Fig. 2-4, Fig. 4-1) as reported before for pelagic prokaryotes (*17*). However, while mycoplankton constantly secreted cysteine peptidases (Fig. 2-S5, Fig. 4-1) they are hardly secreted by prokaryotes (*17*). This disparity in secretory protease composition between pelagic prokaryotes and fungi might indicate different ecological strategies (*3, 14*). Additionally, based on the most widely expressed fungal proteases globally, the majority of pelagic fungal communities exhibited dominance in saprotrophy rather than parasitism (Fig. 2-5), therefore playing a major role in oceanic biogeochemical cycles by recycling dead organic matter (*3*). Moreover, although there was no change in the expression of protease and CAZyme (*14*) classes with depth, a shift in community composition, as reported similarly for prokaryotic CAZymes and peptidases (*17*), implies functional redundancy in both carbohydrate and protein degradation (Fig. 4-1) (*3*).

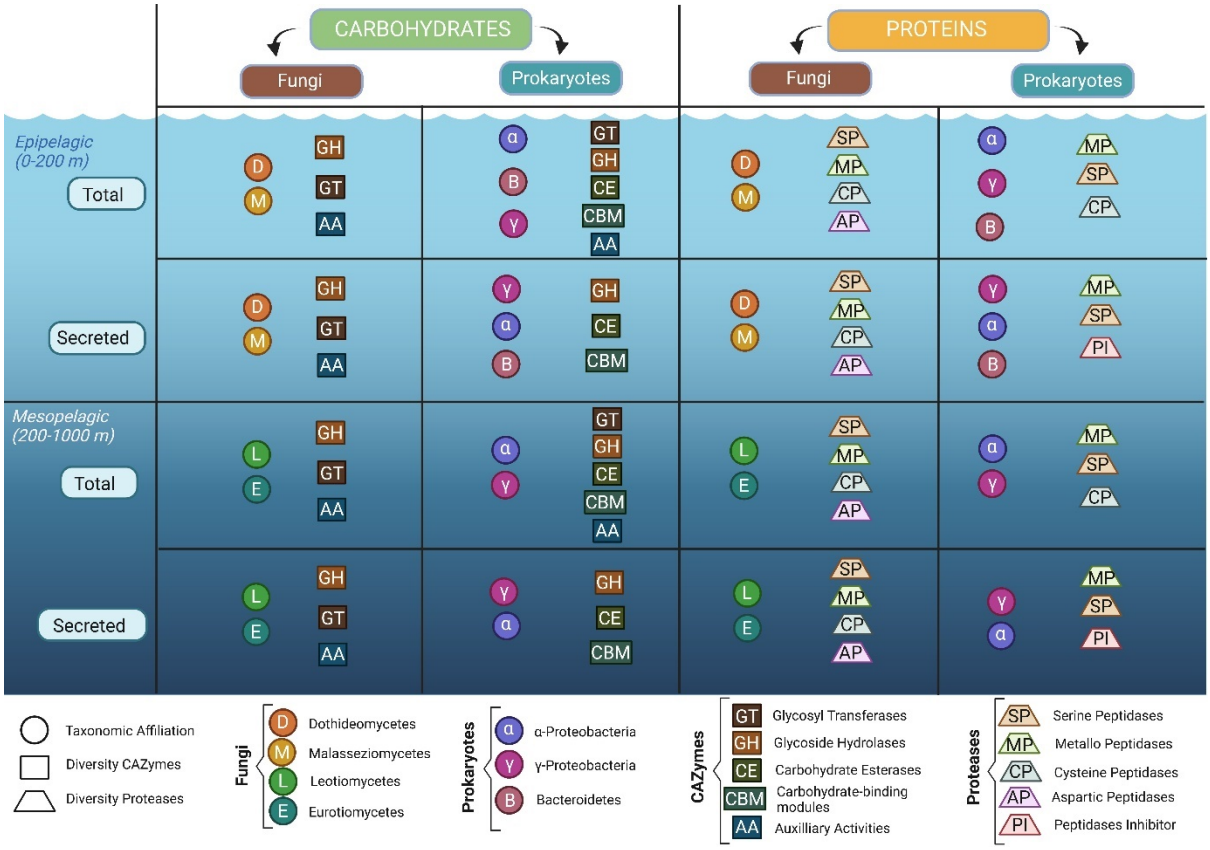

Figure 4-1. Functional diversity and taxonomic affiliation of carbohydrate and protein utilization by oceanic fungi and prokaryotes in the epipelagic and mesopelagic water column, for the total (i.e., cytosol plus secreted) and secreted fractions. Figure derived from Breyer & Baltar (*3*).

However, while the study of global metagenomes or metatranscriptomes provides insights into the diversity and functions of natural communities it may be difficult to infer actual physiological functions or metabolic activities, especially on species level, without experimental validation. Moreover, while studying temporal physiological changes through -omics techniques can be time-consuming, it is easier to directly observe the temporal dynamics of individual species responding to controlled environmental changes. Additionally, oceanic fungi are less studied than their terrestrial counterparts or marine fungi attached to solid substrates (e.g., wood, plastic), underscoring the urgent need to investigate potential physiological adaptations of fungi to pelagic marine environments, especially in the light of future ongoing climate change (*3, 5*).

Through the manipulation of salinity concentrations across three phylogenetically diverse oceanic fungi, we observed a striking adaptability to varying salt concentrations (Fig. 1-5). This contrasts with terrestrial or freshwater fungi, which in general are known to grow

better at lower salinities (*18*). Generally, the live in marine habitats requires a wide adaptability to different salt concentrations considering the extensive salt ranges in coastal areas (e.g. mangroves) or between tropical and polar regions. Previous research has also shown that higher salt concentration improved the production of antimicrobial metabolites derived from marine fungi, which was not the case for terrestrial fungi (*19*). Yet, while most of the studied fungi were isolated from marine sediments, wooden substrates, or sponges (*19*), the successful cultivation of all three pelagic fungi isolated here under a 40-fold change in salinity suggests a likely impact on the diversity of secondary metabolites produced. Considering that metabolomic studies on marine pelagic fungi are scarce, there is a high potential to discover new secondary metabolites derived from marine pelagic cultures grown under varying salinities (*3*). Furthermore, we found a high potential of pelagic fungal cultures to adapt to a wide range of temperature (± 30 °C), with 2 out of 3 studied species demonstrating resilience to both elevated and reduced temperature (Fig. 1-4). A previous study has shown that temperature had a strong substrate-dependent effect on marine fungal extracellular enzyme production, indicating that global warming could potentially impact their role in oceanic biogeochemical cycles (*20*).

Additionally, although all three fungal isolates exhibited a shared preference for oxidizing amino acids (Fig. 1-6), the detailed fungal utilization pattern of the 95 different carbon sources showed species-specific preferences for individual substrates (Fig. 1-7). In general, S.*kiliense* exhibited a distinct oxidation pattern (Absorption at 490 nm) compared to the two other species with higher total oxidation values (Fig. 1-7). Similar, maximal fungal growth (absorption at 750 nm) of *S.kiliense* was higher compared to *R.spherocarpa* and S.*spartinae* (File 1-S1). The species-specific utilization pattern of different carbon sources highlights the potential for degrading a high diversity of substrates in the open ocean. Considering the lower quality of organic matter in deeper waters, the increasing expression, diversity, and proportion of secreted CAZymes and peptidases in the mesopelagic, along with the wide-ranging capability observed in culture-based experiments to utilize different carbon sources, suggest a potentially important role for marine pelagic fungi in the breakdown and recycling of low-quality organic matter in the dark ocean.

3. The contribution of mycoplankton to marine microbial biomass

Although traditionally neglected, recent studies started to unravel the important role of oceanic fungi in marine biogeochemical cycles (*3, 5, 10, 14*). However, current research on

fungal abundance and biomass is still severely limited (*3*). Yet, fungal biomass can surpass prokaryotic biomass during phytoplankton blooms (*6*), and fungi can dominate microbial biomass on bathypelagic marine snow (*21*). Global estimates suggest the ocean holds approximately 6 Gt of carbon from marine biota, with pelagic fungi estimated to account for 0.3 Gt (*22*). Yet, these estimates carry a notable uncertainty due to DNA quantification reliance (*22*). Compiled data indicates oceanic fungal biomass ranges widely, from 0.01 µg C to 35 mg C per L, with abundances varying by four orders of magnitude (10^2 - 10^5 cells per L) (*3*). This uncertainty arises from limited studies and differing biomass conversion factors used (*3*). Most studies focus on coastal regions, leaving a data gap in global oligotrophic oceans, which comprise about 70% of Earth's surface. Additionally, previous studies applied different independent techniques, including qPCR, fluorescence microscopy, and chemical bioindicators like ergosterol, each with its drawbacks (*3*). Until now, a direct quantitative contribution of fungal abundance and biomass in the open ocean has been elusive, precluding an estimation of their contribution to carbon stocks, which hampers their inclusion in biogeochemical models (*3*).

Here, we combined ergosterol extraction, CFW staining, CARD-FISH, and microfluidic mass sensor techniques along a latitudinal transect spanning over 11,000 km across the open (Atlantic) Ocean water column, allowing us to unveil their overlooked contribution to ocean biomass. Additionally, we applied newly developed biomass conversion factors specifically to marine pelagic fungi. Our study revealed an overall good agreement among these different techniques to estimate fungal biomass, while also indicating fungi as relevant contributors to open ocean microbial biomass. We found continuous presence of pelagic fungi in surface waters of the Atlantic Ocean (Fig. 3-S2). Despite being a conservative biomarker for fungal biomass, ergosterol was detected at most stations from the surface until 200 m depth with maximum fungal biomass of 0.97 µg C/l. By applying CFW, we detected even higher biomass (up to 3.5 µg C/l) in epipelagic waters whereas highest fungal biomass (up to 6.6 µg C/l) was detected after applying fungal-specific CARD-FISH. Furthermore, fungal biomass was positively correlated to phytoplankton biomass (in all size fractions) (Fig. 3-3), further supporting their important parasitic and saprotrophic role during phytoplankton blooms. Surprisingly, when comparing to other microbes considered as important participants in the marine microbial loop (i.e., archaea and bacteria), we found that although bacterial biomass was dominating (max. 17 µg C/l), fungal biomass outcompeted archaeal biomass (archaeal biomass: max. 0.85 µg C/l) (Fig. 3-2). Specifically, the contribution of fungal biomass to POC in the epipelagic was on average 0.7 to 4.2% and on average 1.7 to 7.5% in mesopelagic

waters (dependent on the method employed) (Fig. 3-4). In contrast, the contribution of archaeal biomass to POC in epi- and mesopelagic waters was below 1% (Fig. 3-4). This highlights the importance of the so far neglected contribution of mycoplankton to oceanic microbial biomass and therefore emphasizes the need to include oceanic fungi in future models of biogeochemical cycles.

4. Conclusions

Pelagic fungi, often overlooked in oceanic research, are prevalent throughout the water column. The main phyla responsible for degrading carbohydrates and proteins belong to Asco- and Basidiomycota (Fig. 4-1) (*3*). However, early diverging lineages, such as Chytridiomycota, can become locally important, especially due to their parasitic role during marine phytoplankton blooms (*3*). Marine pelagic fungi exhibit diverse functions, actively participating in vitamin, complex carbon, and fatty acid metabolism (*10*). Their genomic potential aligns closely with expressed enzymes involved in degradation and recycling of organic matter. Mesopelagic fungi exhibited higher gene diversity, abundance, and expression of CAZymes and proteases compared to the epipelagic, suggesting differing enzymatic strategies compared prokaryotes (*3*). Although Archaea are recognized members of the microbial loop, oceanic fungi exhibited higher total biomass concentrations throughout the water column. Considering their ubiquitous presence, their active participation in the cycling of organic matter, and their important contribution to marine microbial biomass, it is important to include oceanic fungi as active members of the 'microbial loop' (Fig. 4-2) (*3*). Recognizing the ecological role of pelagic fungi is vital, particularly in the light of climate change and ocean warming. Their integration into ecological and biogeochemical models is essential for a complete understanding of their impact on marine ecosystems and nutrient cycling and crucial for accurate predictions of future oceanic environments.

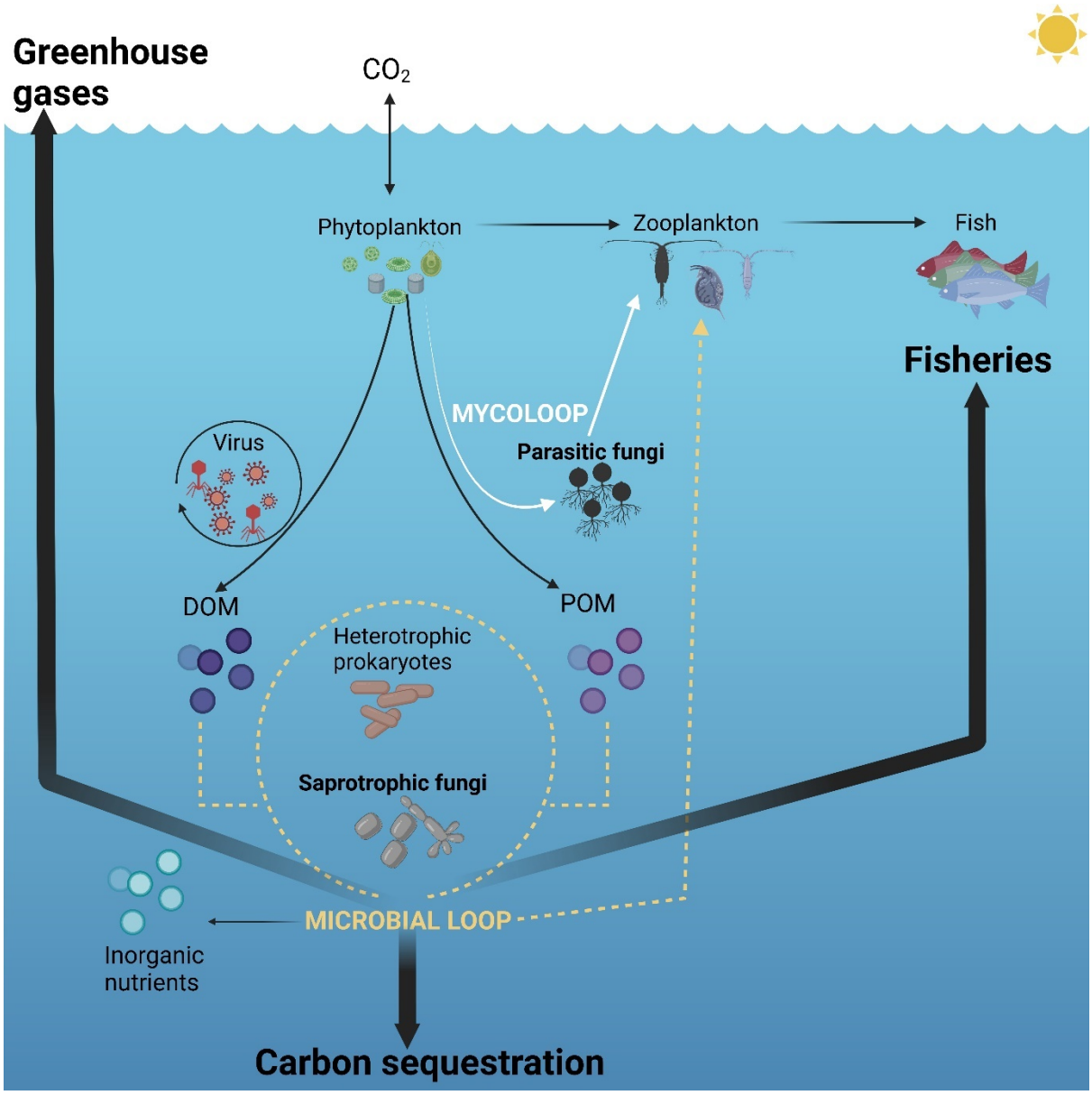

Figure 4-2. Schematic, simplified representation of the oceanic trophic chain and the associated carbon fluxes. Figure derived from Breyer & Baltar (*3*).

References

1. H.-P. Grossart *et al.*, Fungi in aquatic ecosystems. *Nat. Rev. Microbiol.* **17**, 339-354 (2019).
2. A. Amend *et al.*, Fungi in the Marine Environment: Open Questions and Unsolved Problems. *MBio* **10**, e01189-01118 (2019).
3. E. Breyer, F. Baltar, The largely neglected ecological role of oceanic pelagic fungi. *Trends Ecol. Evol.* **38**, 870-888 (2023).
4. M. Kagami, T. Miki, G. Takimoto, Mycoloop: chytrids in aquatic food webs. *Front. Microbiol.* **5**, 166 (2014).
5. X. Peng *et al.*, Planktonic Marine Fungi: A Review. *JGR Biogeosciences* **129**, e2023JG007887 (2024).
6. M. H. Gutiérrez, S. Pantoja, E. Tejos, R. A. Quinones, The role of fungi in processing marine organic matter in the upwelling ecosystem off Chile. *Mar. Biol.* **158**, 205-219 (2011).
7. M. H. Gutiérrez, S. Pantoja, R. A. Quinones, R. R. Gonzalez, First record of filamentous fungi in the coastal upwelling ecosystem off central Chile/Primer registro de hongos filamentosos en el ecosistema de surgencia costero frente a Chile central. *Gayana* **74**, 66 (2010).
8. M. Cunliffe, A. Hollingsworth, C. Bain, V. Sharma, J. D. Taylor, Algal polysaccharide utilisation by saprotrophic planktonic marine fungi. *Fungal Ecol.* **30**, 135-138 (2017).
9. X. Peng, D. L. Valentine, Diversity and N2O production potential of fungi in an oceanic oxygen minimum zone. *J. Fungi* **7**, 218 (2021).
10. S. E. Morales, A. Biswas, G. J. Herndl, F. Baltar, Global structuring of phylogenetic and functional diversity of pelagic fungi by depth and temperature. *Front. Mar. Sci.* **6**, 131 (2019).
11. K. Sen, M. Bai, B. Sen, G. Wang, Disentangling the structure and function of mycoplankton communities in the context of marine environmental heterogeneity. *Sci. Total. Environ.* **766**, 142635 (2021).
12. W. D. Orsi, J. F. Biddle, V. Edgcomb, Deep sequencing of subseafloor eukaryotic rRNA reveals active fungi across marine subsurface provinces. *PloS One* **8**, e56335 (2013).
13. E. F. DeLong *et al.*, Community genomics among stratified microbial assemblages in the ocean's interior. *Science* **311**, 496-503 (2006).
14. F. Baltar, Z. Zhao, G. J. Herndl, Potential and expression of carbohydrate utilization by marine fungi in the global ocean. *Microbiome* **9**, 1-10 (2021).

15. N. Chrismas, M. Cunliffe, Depth-dependent mycoplankton glycoside hydrolase gene activity in the open ocean—evidence from the Tara Oceans eukaryote metatranscriptomes. *ISME J.* **14**, 2361-2365 (2020).
16. W. D. Orsi *et al.*, Carbon assimilating fungi from surface ocean to subseafloor revealed by coupled phylogenetic and stable isotope analysis. *ISME J.* **16**, 1245-1261 (2021).
17. Z. Zhao, F. Baltar, G. J. Herndl, Linking extracellular enzymes to phylogeny indicates a predominantly particle-associated lifestyle of deep-sea prokaryotes. *Sci. Adv.* **6**, eaaz4354 (2020).
18. E. G. Jones *et al.*, How do fungi survive in the sea and respond to climate change? *J. Fungi* **8**, 291 (2022).
19. R. Masuma, Y. Yamaguchi, M. Noumi, S. Omura, M. Namikoshi, Effect of sea water concentration on hyphal growth and antimicrobial metabolite production in marine fungi. *Mycoscience* **42**, 455-459 (2001).
20. K. Salazar Alekseyeva, G. J. Herndl, F. Baltar, Extracellular enzymatic activities of oceanic pelagic fungal strains and the influence of temperature. *J. Fungi* **8**, 571 (2022).
21. A. B. Bochdansky, M. A. Clouse, G. J. Herndl, Eukaryotic microbes, principally fungi and labyrinthulomycetes, dominate biomass on bathypelagic marine snow. *ISME J.* **11**, 362-373 (2017).
22. Y. M. Bar-On, R. Phillips, R. Milo, The biomass distribution on Earth. *Proc. Natl. Acad. Sci. U.S.A* **115**, 6506-6511 (2018).

Annex

1. Chapter 1: Supplementary Material

File 1-S1: Absorption of carbon substrates by fungal isolates at 750 nm, indicative for fungal growth.

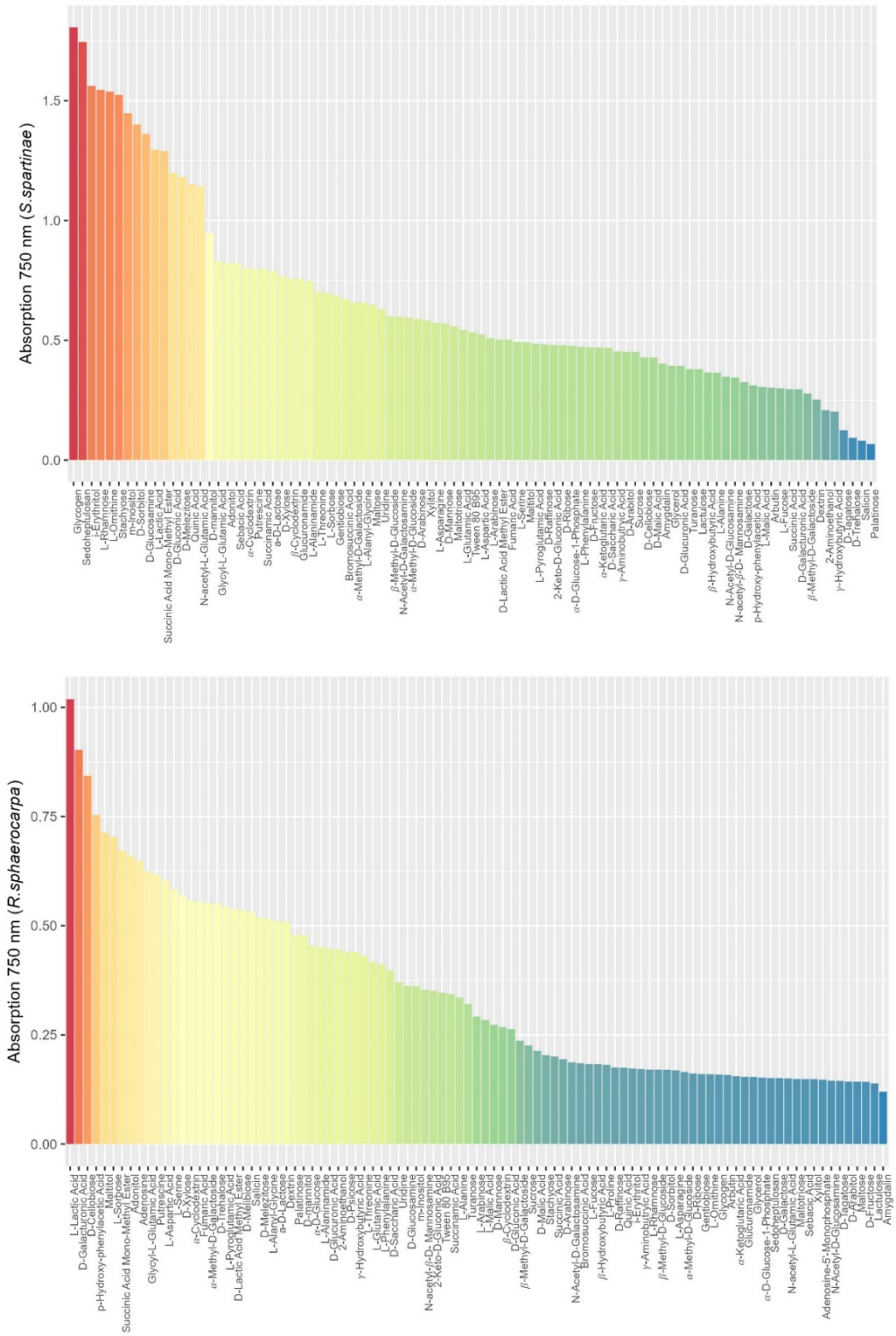

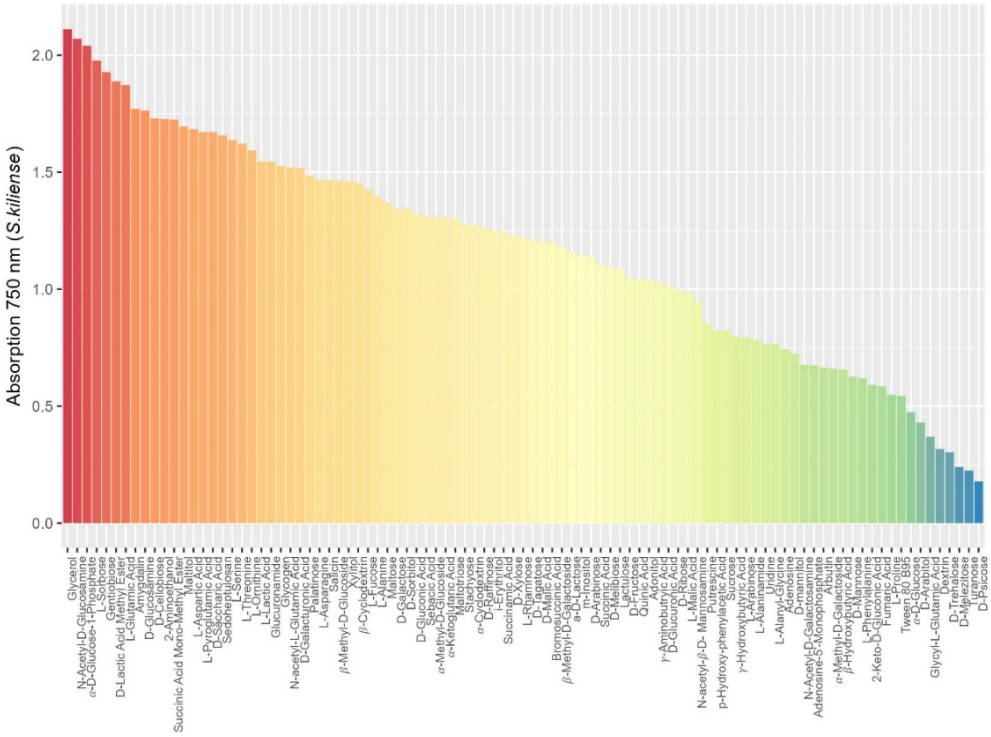
Absorption 750 nm (S.kiliense)
2.0
1.5
1.0
0.5
0.0
Glycerol
N-Acetyl-D-Glucosamine
α-D-Glucose-1-Phosphate
L-Sorbose
Gentiobiose
D-Lactic Acid Methyl Ester
L-Glutamic Acid
Amygdalin
D-Glucosamine
D-Cellobiose
2-Aminoethanol
Succinic Acid Mono-Methyl Ester
L-Aspartic Acid
L-Pyroglutamic Acid
D-Serine
Sedoheptulosan
L-Serine
L-Threonine
L-Ornithine
L-Lactic Acid
Glucuronamide
Glycogen
N-acetyl-L-Glutamic Acid
D-Galactonic Acid-γ-Lactone
Putrescine
L-Asparagine
Salicin
β1-Methyl-D-Glucoside
Xylitol
β-Cyclodextrin
L-Fucose
L-Alanine
Maltose
D-Galactose
D-Sorbitol
D-Gluconic Acid
Stachyose
α1-Methyl-D-Glucoside
α-Ketoglutaric Acid
Maltotriose
Turanose
α-Cyclodextrin
D-Raffinose
D-Fructose
Succinamic Acid
D-Xylose
L-Rhamnose
D-Tagatose
D-Malic Acid
Bromo-Succinic Acid
β1-Methyl-D-Galactoside
α-D-Lactose
m-Inositol
D-Arabitol
Succinic Acid
D-Melibiose
Lactulose
D-Fructose
Quinic Acid
Adonitol
γ-Aminobutyric Acid
D-Glucuronic Acid
Dulcitol
L-Malic Acid
N-acetyl-β-D- Mannosamine
Putrescine
p-Hydroxy-phenylacetic Acid
Sucrose
γ-Hydroxybutyric Acid
Arbutin
L-Alaninamide
Uridine
L-Alanyl-Glycine
Adenosine
D-mannitol
N-Acetyl-D-Galactosamine
Adenosine-5'-Monophosphate
Arbutin
α1-Methyl-D-Galactoside
β-Hydroxybutyric Acid
D-Mannose
L-Phenylalanine
2-Keto-D-Gluconic Acid
Fumaric Acid
L-Proline
Tween 80
α-D-Glucose
D-Arabitol
Glycyl-L-Glutamic Acid
Dextrin
D-Trehalose
D-Melezitose
D-Raffinose
D-Psicose

2. Chapter 2: Supplementary Material

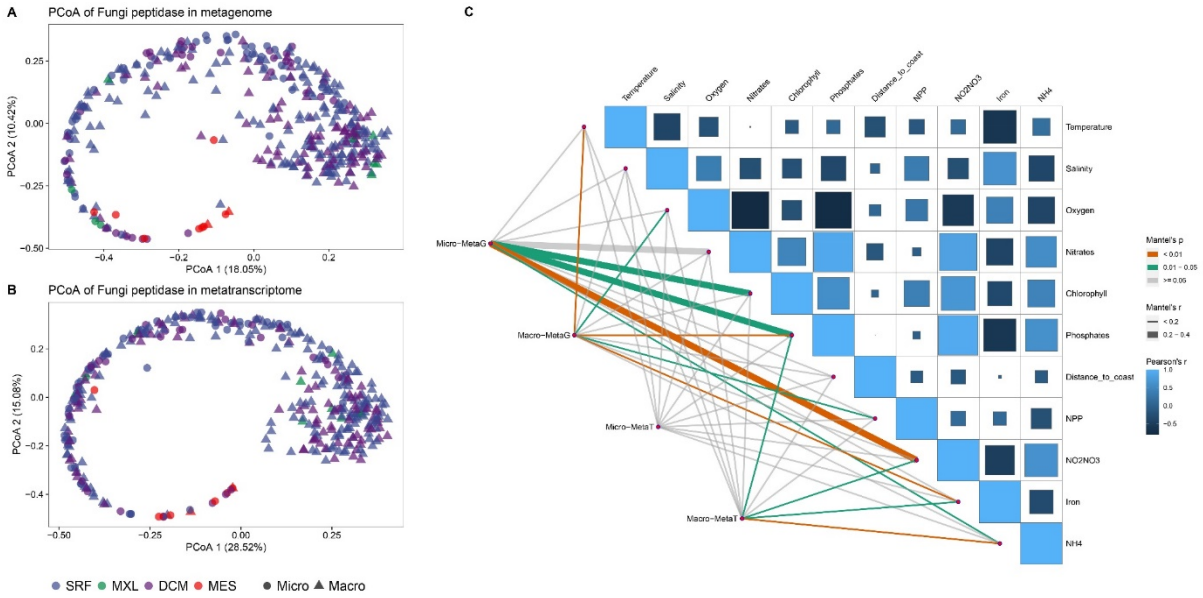

Figure 2-S1. Principal coordinate analysis of fungal peptidase fungal genes present in the metagenome (A) and in the metatranscriptome (B) and environmental drivers shaping fungal peptidase gene composition at both metagenomic and metatranscriptomic level (C). Micro, micro-mycobiome (0.8-5 µm); Macro, macro-mycobiome (5-2,000 µm). SRF, surface; MXL, mixed layer; DCM, deep chlorophyll maximum; MES, mesopelagic

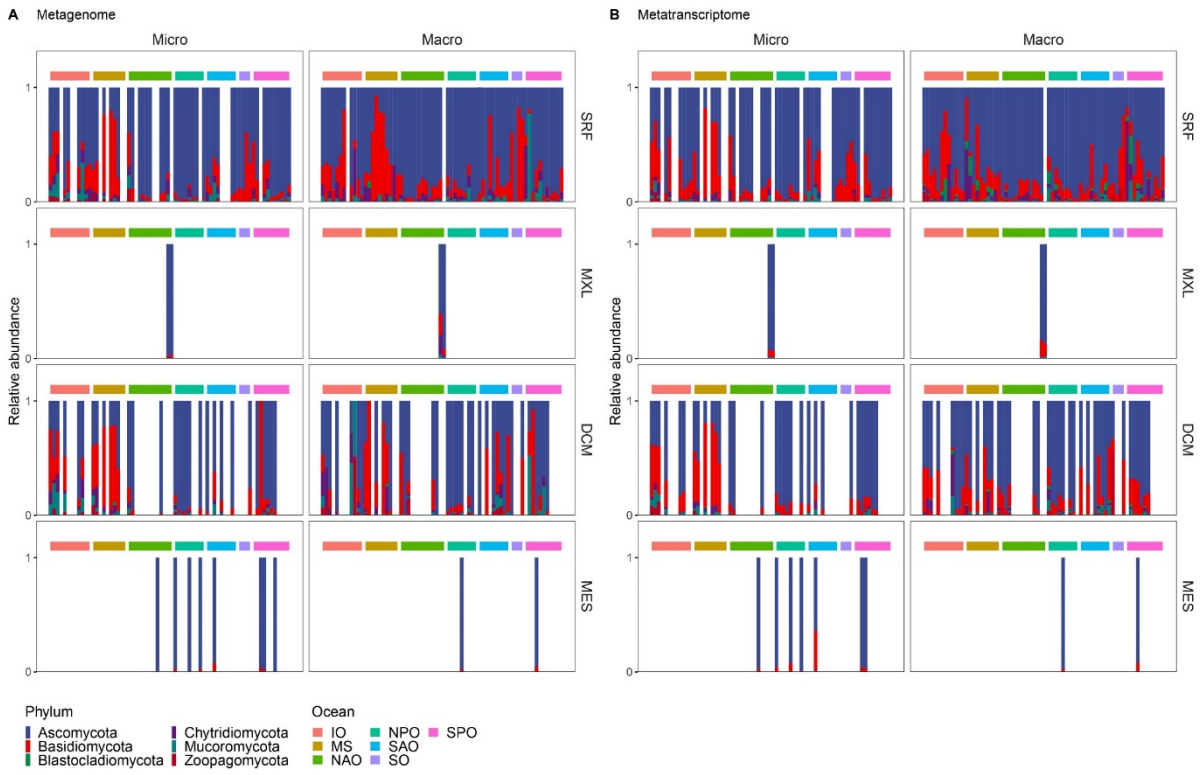

Figure 2-S2. Phylogenetic affiliation of genes (A) and transcripts (B) encoding fungal peptidases at the phylum level. Micro, micro-mycobiome (0.8-5 µm); Macro, macro-mycobiome (5-2000 µm). SRF, surface; MXL, mixed layer; DCM, deep chlorophyll maximum; MES, mesopelagic; IO, Indian Ocean; MS, Mediterranean Sea; NAO, North Atlantic Ocean; North Pacific Ocean; SAO, South Atlantic Ocean; SO, Southern Ocean; SPO, South Pacific Ocean

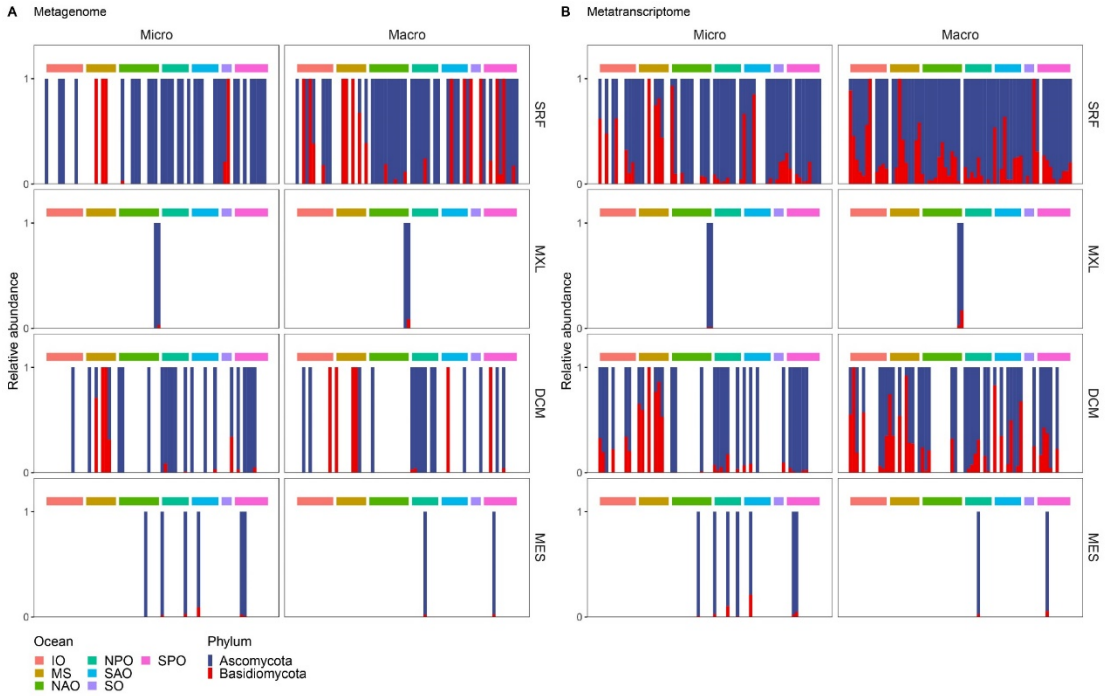

Figure 2-S3. Phylogenetic affiliation of genes (A) and transcripts (B) encoding secretory fungal peptidases at the phylum level. Micro, micro-mycobiome (0.8-5 µm); Macro, macro-mycobiome (5-2000 µm). SRF, surface; MXL, mixed layer; DCM, deep chlorophyll maximum; MES, mesopelagic; IO, Indian Ocean; MS, Mediterranean Sea; NAO, North Atlantic Ocean; North Pacific Ocean; SAO, South Atlantic Ocean; SO, Southern Ocean; SPO, South Pacific Ocean

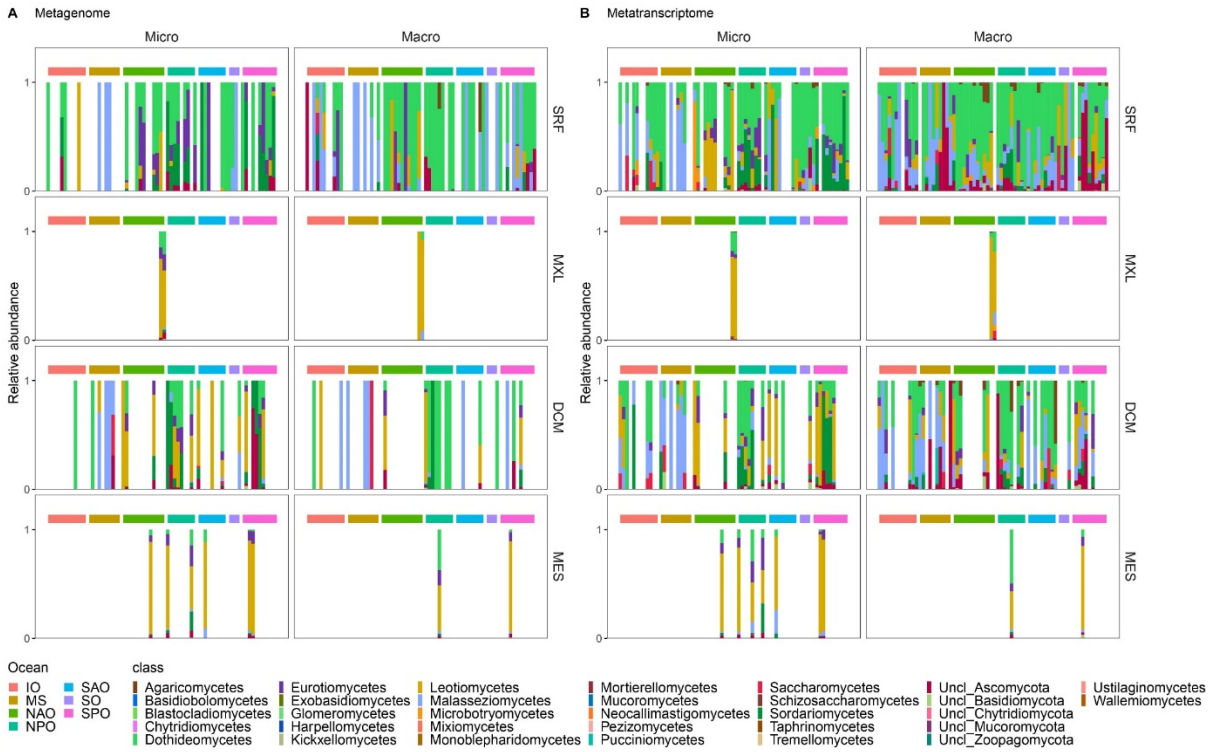

Figure 2-S4. Phylogenetic affiliation of genes (A) and transcripts (B) encoding secretory fungal peptidases at the class level. Micro, micro-mycobiome (0.8-5 µm); Macro, macro-mycobiome (5-2000 µm). SRF, surface; MXL, mixed layer; DCM, deep chlorophyll maximum; MES, mesopelagic; IO, Indian Ocean; MS, Mediterranean Sea; NAO, North Atlantic Ocean; North Pacific Ocean; SAO, South Atlantic Ocean; SO, Southern Ocean; SPO, South Pacific Ocean

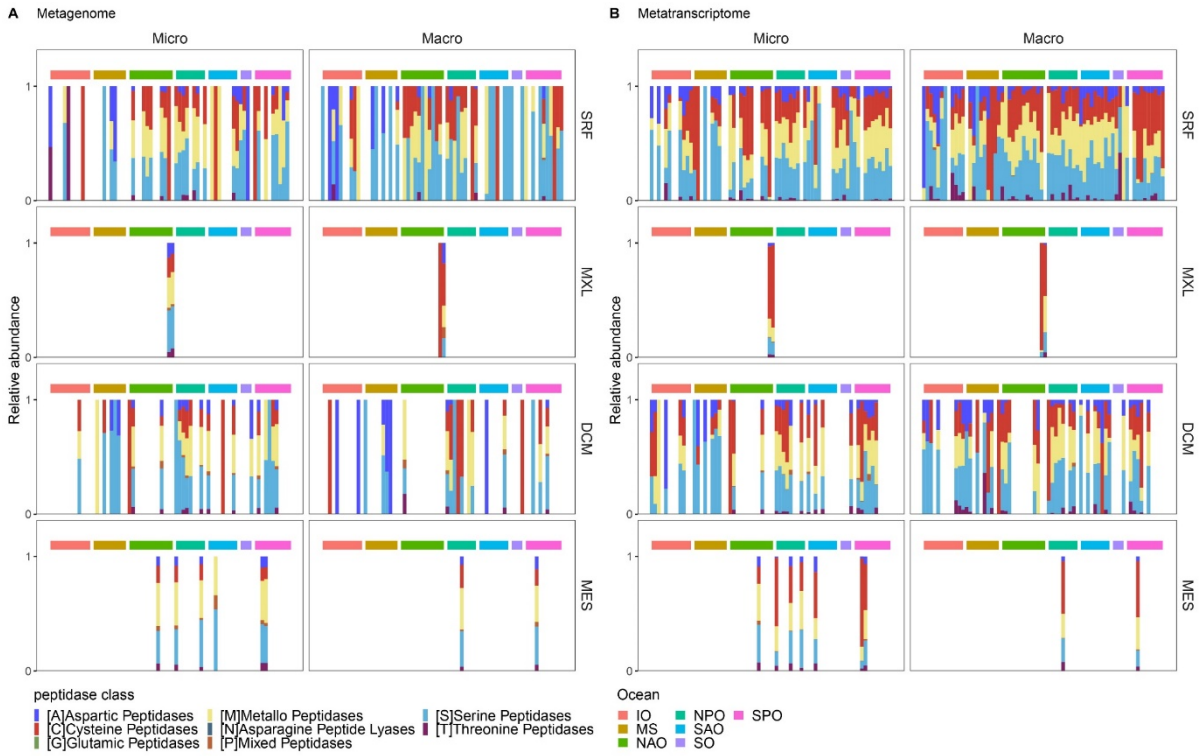

Figure 2-S5. Functional classification of genes (A) and transcripts (B) encoding secretory fungal peptidases. Micro, micro-mycobiome (0.8-5 µm); Macro, macro-mycobiome (5-2000 µm). SRF, surface; MXL, mixed layer; DCM, deep chlorophyll maximum; MES, mesopelagic; IO, Indian Ocean; MS, Mediterranean Sea; NAO, North Atlantic Ocean; North Pacific Ocean; SAO, South Atlantic Ocean; SO, Southern Ocean; SPO, South Pacific Ocean.

2.2. Additional online files

Additional large files can be found in the online published version of the manuscript: Breyer et al. Microbiome (2022) 10:143. https://doi.org/10.1186/s40168-022-01329-5:

- Table 2-S1: Families of proteases affiliated to Fungi, Bacteria and shared by both.
- Dataset 2-S1

3. Chapter 3: Supplementary Material

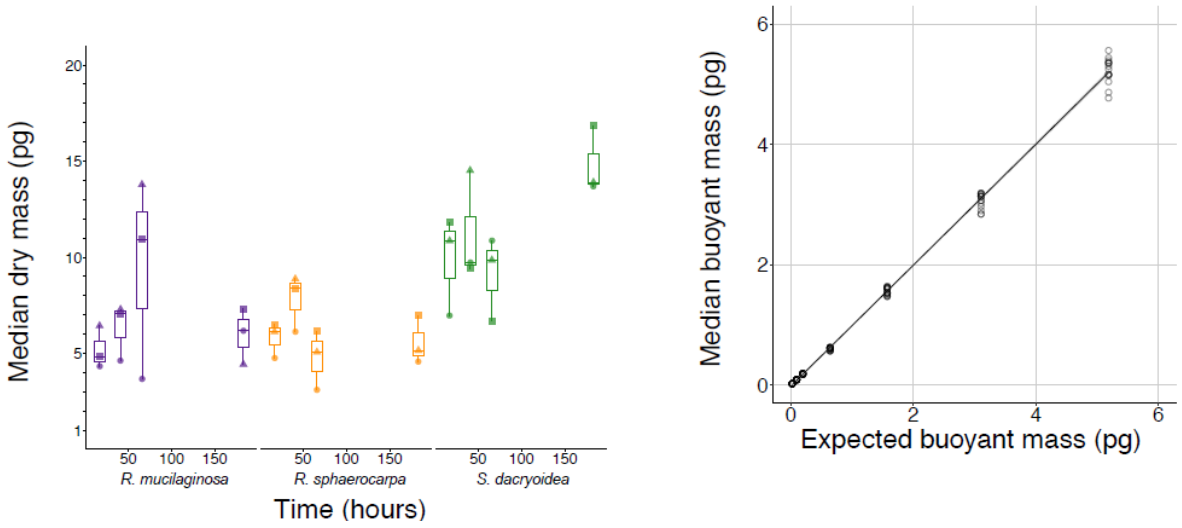

Figure 3-S1. Fungal cell dry mass. Left: Median cell dry mass derived from three marine pelagic fungal cultures in the exponential and early-, mid- and late stationary growth stage The box represents the interquartile range (IQR) containing the central 50% of the data, the line inside the box depicts the median of replicates, and whiskers extend to 1.5 times the IQR, with outliers plotted individually. Right: Calibration curve of buoyant mass.

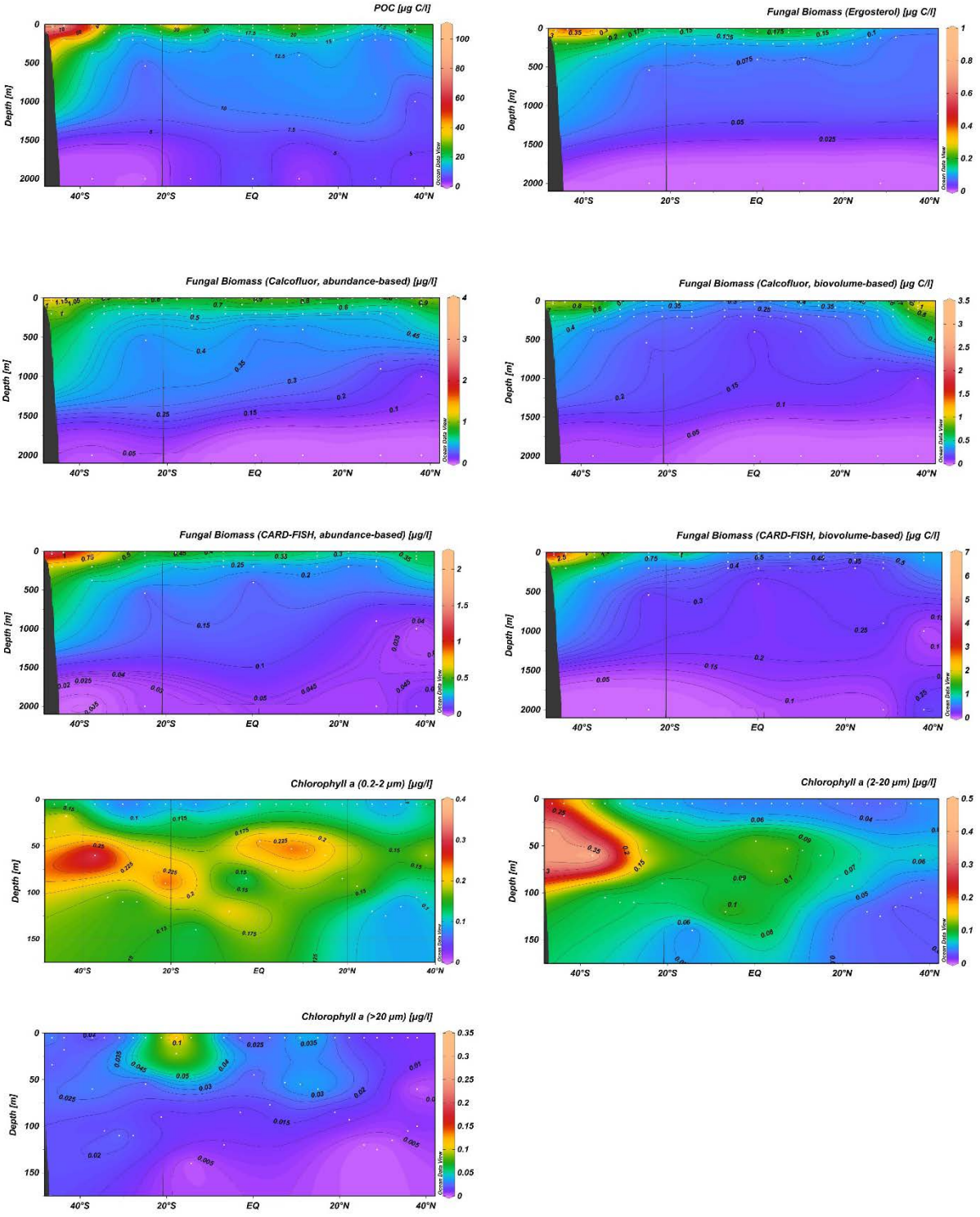

Figure 3-S2. Distribution of POC, size fractionated chlorophyll a and fungal biomass in the Atlantic Ocean. White points indicate sampling points during the ANTOM-1 Cruise. The first 2000 m in the water column are shown for POC and fungal biomass estimated with different quantification methods and the first 175 m in the water column for different chlorophyll a size fractions. The plots were generated with Ocean Data View (ODV).

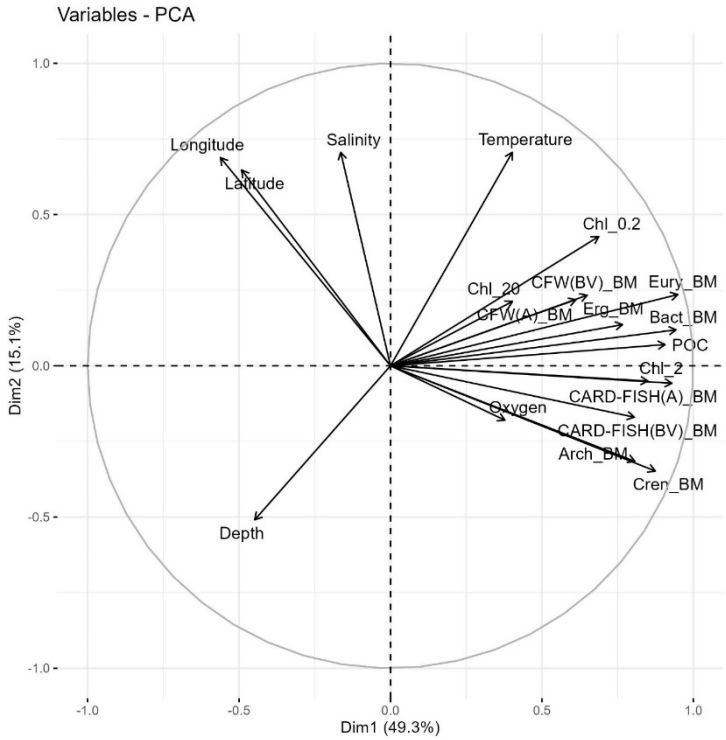

Figure 3-S3. Principal component analysis (PCA) of microbial biomass and environmental parameters in the Atlantic Ocean. PCA variable plot. Biomass (BM), biovolume-based measurements (BV), abundance-based measurements (A), Arch915 probe (Arch), Crenarchaeal 537/554 probes (Cren), Euryarchaeal 806 probe (Eury), ergosterol-derived fungal biomass (Erg), bacterial biomass (Bact).

Table 3-S1. Fungal cell dry mass of *R. mucilaginosa*, *R. sphaerocarpa* and *S. dacryoidea* in different growth stages quantified in a suspended microchannel resonator (SMR).

species	sample	growth stage	time_hrs	drymass_median	drymass_uq	drymass_lq	drydensity	N_H2O	N_D2O	replicate
R.mucilaginosa	E_rep1	exponential	17	4334.352077	4627.62516	3430.20304	1.6513078	7307	8919	1
R.mucilaginosa	E_rep2	exponential	17	6437.923554	11819.4843	4915.87985	1.35339144	4309	4518	2
R.mucilaginosa	E_rep3	exponential	17	4831.450745	7886.95108	3680.99103	1.47029811	4527	3778	3
R.mucilaginosa	S1_rep1	early stationary	41	4628.209648	8066.53009	3427.98366	1.52636925	3860	4414	1
R.mucilaginosa	S1_rep2	early stationary	41	7292.864881	13033.171	4006.604	1.30816172	6850	5971	2
R.mucilaginosa	S1_rep3	early stationary	41	7063.506394	12899.8262	4099.11336	1.3208109	8321	6060	3
R.mucilaginosa	S2_rep1	mid stationary	66	3676.844755	8335.66804	2675.23114	1.57853632	5784	13545	1
R.mucilaginosa	S2_rep2	mid stationary	66	13785.26443	27782.3282	7243.85384	1.20814516	5686	3486	2
R.mucilaginosa	S2_rep3	mid stationary	66	10944.49471	19386.7487	6298.55364	1.24539411	6114	3892	3
R.mucilaginosa	S3_rep1	late stationary	183	6181.867761	9393.17058	4131.86115	1.2229283	21884	7951	1
R.mucilaginosa	S3_rep2	late stationary	183	4431.90911	5979.95058	3027.05105	1.6274494	11957	9752	2
R.mucilaginosa	S3_rep3	late stationary	183	7312.8414	11901.2104	4718.56794	1.28348355	12491	7670	3
R.sphaerocarpa	E_rep1	exponential	17	4762.530303	6590.7581	3900.79804	1.55616973	2881	2007	1
R.sphaerocarpa	E_rep2	exponential	17	6127.802119	8479.35297	4864.84196	1.37835	6689	2361	2
R.sphaerocarpa	E_rep3	exponential	17	6500.830189	9914.9977	5061.42886	1.34409469	5953	1976	3
R.sphaerocarpa	S1_rep1	early stationary	41	6129.990292	9764.72341	3824.17908	1.42081153	6478	6715	1
R.sphaerocarpa	S1_rep2	early stationary	41	8877.851288	15801.8821	5662.18031	1.22272273	6927	1233	2

R.sphaerocarpa	S1_rep3	early stationary	41	8396.950655	13953.8617	5511.76177	1.2362777	6338	1826	3
R.sphaerocarpa	S2_rep1	mid stationary	66	3108.203094	3858.86848	2708.5846	1.84882497	6304	5296	1
R.sphaerocarpa	S2_rep2	mid stationary	66	5071.583017	6632.88793	3975.74921	1.43098785	9232	5612	2
R.sphaerocarpa	S2_rep3	mid stationary	66	6163.782378	8697.19404	4604.4568	1.33699337	8349	3534	3
R.sphaerocarpa	S3_rep1	late stationary	183	4575.830703	5928.46123	4001.59624	1.32853262	8592	2646	1
R.sphaerocarpa	S3_rep2	late stationary	183	5157.862307	7267.17728	4228.57008	1.28008924	5334	1477	2
R.sphaerocarpa	S3_rep3	late stationary	183	6986.370685	9514.68077	7840.2402	1.20862004	6862	947	3
S.dacryoidea	E_rep1	exponential	17	6971.605079	9987.03944	5148.6305	1.92474181	6184	4647	1
S.dacryoidea	E_rep2	exponential	17	10858.83004	16467.9085	7737.51395	1.40993675	5567	3722	2
S.dacryoidea	E_rep3	exponential	17	11823.5699	18578.5867	8493.34691	1.36784814	5536	3444	3
S.dacryoidea	S1_rep1	early stationary	41	9729.302742	15064.9045	6521.31851	1.72845654	8347	7871	1
S.dacryoidea	S1_rep2	early stationary	41	14516.28242	18543.8304	9599.37355	1.35356958	10421	3250	2
S.dacryoidea	S1_rep3	early stationary	41	9421.159818	12397.7601	7216.2281	1.57808616	9567	4926	3
S.dacryoidea	S2_rep1	mid stationary	66	10870.18853	20430.2298	5312.79685	1.95667752	7023	4874	1
S.dacryoidea	S2_rep2	mid stationary	66	9857.222764	18530.4785	4886.7062	1.94333266	3792	3434	2
S.dacryoidea	S2_rep3	mid stationary	66	6682.182808	12141.2862	3542.21372	2.9718158	2884	4737	3
S.dacryoidea	S3_rep1	late stationary	183	13689.17866	23819.9077	9928.27575	1.59891645	6448	3853	1
S.dacryoidea	S3_rep2	late stationary	183	13897.11408	22586.5599	10653.045	1.42982327	5084	2103	2

S.dacryoidea	S3_rep3	late stationary	183	16826.80126	20420.0985	14892.4422	1.3699203	3585	1871	3

Table 3-S2. Ergosterol to carbon conversion factors of *R. mucilaginosa, R. sphaerocarpa, S. dacryoidea, B. parvus* and *M. australis* in different growth stages (adaptation, exponential, stationary).

species	growth stage	mean ergosterol [mg/l]	standard deviation ergosterol	mean POC [mg/l]	standard deviation POC	mg ergosterol/ g carbon
S.dacryoidea	adaptation	0.01	0.00	5.39	0.65	1.87
S.dacryoidea	exponential	0.05	0.03	14.40	3.37	3.50
S.dacryoidea	stationary	0.21	0.14	46.65	7.78	4.40
R.mucilaginosa	adaptation	0.01	0.00	15.12	1.13	0.63
R.mucilaginosa	exponential	0.23	0.16	30.00	0.15	7.53
R.mucilaginosa	stationary	0.87	0.42	117.37	10.19	7.39
R.spherocarpa	adaptation	0.02	0.00	13.17	0.22	1.22
R.spherocarpa	exponential	0.25	0.16	38.08	0.24	6.53
R.spherocarpa	stationary	0.50	0.18	83.14	14.19	5.98
B.parvus	adaptation	0.01	0.01	6.26	1.05	2.31
B.parvus	exponential	0.42	0.18	62.65	3.24	6.78
B.parvus	stationary	0.41	0.17	34.79	15.68	11.90
M.australis	adaptation	0.01	0.01	16.94	0.60	0.75
M.australis	exponential	0.42	0.27	97.28	6.52	4.31
M.australis	stationary	0.93	0.43	150.66	26.10	6.16

Table 3-S3. Biovolume to carbon conversion factors of *R. mucilaginosa, R. sphaerocarpa, S. dacryoidea* and *M. australis* in different growth stages (adaptation, exponential, stationary) based on CFW staining.

M.australis			***R.sphaerocarpa***		
Adaptation			**Adaptation**		
Abundance [cells/l]	7.51E+07		**Abundance [cells/l]**	5.58E+07	
Average Biovolume [µm³/cell]	142		**Average Biovolume [µm³/cell]**	16	
POC [mg C/l]	16.94		**POC [mg C/l]**	13.17	
mg C per cell	2.25654E-07		**mg C per cell**	2.36185E-07	
mg C per µm³	1.58911E-09	1.59 pg/µm³	**mg C per µm³**	1.47616E-08	14.76 pg/µm³
Exponential			**Exponential**		
Abundance [cells/l]	1689976320		**Abundance [cells/l]**	7.63E+09	
Average Biovolume [µm³/cell]	35		**Average Biovolume [µm³/cell]**	15	
POC [mg C/l]	97.2838720 7		**POC [mg C/l]**	38.0808096 5	
mg C per cell	5.75652E-08		**mg C per cell**	4.99333E-09	
mg C per µm³	1.64472E-09	1.64 pg/µm³	**mg C per µm³**	3.32888E-10	0.33 pg/µm³
Stationary			**Stationary**		
Abundance [cells/l]	5168582400		**Abundance [cells/l]**	1.87E+10	
Average Biovolume [µm3/cell]	28		**Average Biovolume [µm³/cell]**	10	
POC [mg C/l]	150.66		**POC [mg C/l]**	83.14	
mg C per cell	2.9149E-08		**mg C per cell**	4.4508E-09	
mg C per µm³	1.04103E-09	1.04 pg/µm³	**mg C per µm³**	4.4508E-10	0.45 pg/µm³
Sakaguchia dacryoidea			***R. mucilaginosa***		
Adaption			**Adaptation**		
Abundance [cells/l]	1.93E+07		**Abundance [cells/l]**	6.43E+06	
Average Biovolume [µm³/cell]	35		**Average Biovolume [µm³/cell]**	47	
POC [mg C/l]	5.39		**POC [mg C/l]**	15.12	
mg C per cell	2.79069E-07		**mg C per cell**	2.35061E-06	
mg C per µm³	7.97341E-09	7.97 pg/µm³	**mg C per µm³**	5.00129E-08	50.01 pg/µm³
Exponential			**Exponential**		

Abundance [cells/l]	3.12E+09		**Abundance [cells/l]**	3.90E+09	
Average Biovolume [µm³/cell]	27		**Average Biovolume [µm³/cell]**	25	
POC [mg C/l]	14.40		**POC [mg C/l]**	30.00	
mg C per cell	4.60877E-09		**mg C per cell**	7.70038E-09	
mg C per µm³	1.70695E-10	0.17 pg/µm³	**mg C per µm³**	3.08015E-10	0.31 pg/µm³
Stationary Abundance [cells/l]	4.89E+09		**Stationary Abundance [cells/l]**	7.42E+09	
Average Biovolume [µm³/cell]	47		**Average Biovolume [µm³/cell]**	40	
POC [mg C/l]	46.65		**POC [mg C/l]**	117.37	
mg C per cell	9.54009E-09		**mg C per cell**	1.58239E-08	
mg C per µm³	2.02981E-10	0.20 pg/µm³	**mg C per µm³**	3.95598E-10	0.4 pg/µm³

Table 3-S4. CARD-FISH protocol for marine pelagic fungi.

Steps	Description	Note
1. Sample collection	Seawater is fixed with Formaldehyde to a final concentration of 4% for 0.5 to 2 hours at 4°C	
2. Sample filtration and fixation	Fixed seawater is filtered onto polycarbonate filter (25 mm, 0.22 µm) with support filter below (0.45 µm, nitrocellulose), maximum pressure 250 mbar	Filters can be stored in Eppendorf tubes at -20°C
3. Agarose Embedding	Filters are placed upside down onto 55 µl 0.1% Agarose and dried at 37°C in a hybridization oven for 15 minutes. Afterwards, 96% ethanol is poured over the filters to gently detach them followed by air drying	
4. Permeabilization of fungal cells	Filter pieces are incubated in tubes containing the Permeabilization Buffer for 1 hour at 30°C on a heat shaker at low speed. Afterwards, filters are washed 2x with MilliQ-water **Permeabilization Buffer Recipe:** 360 units Cellulase, 3.6 units Protease, 2 units Chitinase and 15 000 units Lyticase in PBS (1X) 1% SDS at pH 6.5.	Alternatively, tubes can be fixed on a rotor in an incubation oven.
5. Endogenous Peroxidase Inactivation	Filter pieces are incubated in 0.01M HCl for 15 minutes in the dark, afterwards washed 2x in MilliQ-water and subsequently dipped into 96% ethanol and air-dried	
5. Hybridization with the HRP-labelled probe	Filter pieces are placed into Eppendorf tube containing the Hybridization Buffer and the HRP-labelled probe (probe diluted 1:30 in Hybridization Buffer) and incubated for 3 hours at 46°C in the dark in a hybridization oven at slow rotation. **Hybridization Buffer Recipe:** 1800 µl 5M NaCl, 200 µl 1M Tris-HCl, 1 g Dextran Sulfate, 5 µl 100% Triton X100), 2 ml Formamide, 1 ml 10% Blocking reagent, 5 ml Sigma-Water. (The Formamide concentration depends on the probe used.)	For 6 small filter pieces (1/8 of a 25 mm filter) around 600 µl of Hybridization Buffer is necessary.
6. Washing	Filter pieces are placed into pre-heated Washing Buffer and washed for 15 minutes at 48°C in a water bath. Afterwards, filters are transferred into PBS (1X) and incubated for 15 minutes in the dark. **Washing Buffer Recipe**: 2150 µl 5M NaCl, 1000 µl 1M Tris-HCl, 500 µl 0.5M EDTA, 50 µl 10% SDS, 46.3 ml MilliQ-water.	
7. Amplification	Filter pieces are transferred into Eppendorf Tube containing 692 µl Amplification Buffer, 7 µl Solution A and 1 µl Alexa Tyramide. Incubate at 46°C for 45 minutes in a hybridization oven in the dark. Afterwards, filters are washed 3x in MilliQ-water, dipped into 96% Ethanol and air-dried. **Amplification Buffer Recipe:** 2g Dextran Sulfate, 8000 µl 5M NaCl, 200 µl 10% Blocking reagent, 11800 µl PBS (1X) **Solution A Recipe:** 200 µl Amplification Buffer with 1 µl 30% H_2O_2	Different fluorescence marked Tyramide can be used (e.g., Alexa Fluor™ 488, Thermo Fisher Scientific). After Amplification, filters can be counterstained with DAPI or CFW on a microscope slide.

Table 3-S5. Sampling locations of prokaryotic and archaeal biomass.

Station	Depth [m]	Prokaryotes	Bacteria	Archaea	Crenarchaeota	Euryarchaeota
1	5	✓				
1	60	✓				
1	100	✓				
1	1000	✓				
1	2000	✓				
2	5	✓				
2	105	✓				
3	5	✓				
3	115	✓				
4	5	✓	✓	✓	✓	✓
4	125	✓	✓	✓	✓	✓
4	200	✓	✓	✓	✓	✓
4	900	✓	✓	✓	✓	✓
4	2000	✓	✓	✓	✓	✓
5	5	✓				
5	120	✓				
6	5	✓				
7	5	✓				
7	85	✓				
8	5	✓	✓	✓	✓	✓
8	60	✓	✓	✓	✓	✓
9	5	✓				
9	55	✓				
9	2000	✓				
10	5	✓				
10	53	✓				
11	5	✓				
11	77	✓				
12	5	✓	✓	✓	✓	✓
12	45	✓	✓	✓	✓	✓
12	200	✓	✓	✓	✓	✓
12	400	✓	✓	✓	✓	✓
12	2000	✓	✓	✓	✓	✓
13	5	✓				
14	5	✓				
14	120	✓				
15	5	✓				
15	140	✓				
15	2000	✓				
16	5	✓				
16	22	✓				
17	5	✓				
17	90	✓				

18	5	✓				
18	55	✓				
18	2000	✓				
19	5	✓				
19	110	✓				
20	5	✓				
20	110	✓				
21	5	✓				
22	5	✓	✓	✓		
22	60	✓	✓	✓		
22	200	✓	✓	✓	✓	✓
22	375	✓	✓	✓	✓	✓
22	2000	✓	✓	✓	✓	✓
23	5	✓	✓	✓		
23	18	✓	✓	✓		
23	200	✓			✓	✓
24	5	✓	✓	✓		
24	34	✓	✓	✓		
24	200	✓	✓	✓	✓	✓